ISSN 0915-633X

NATIONAL INSTITUTE FOR FUSION SCIENCE

Statistical Properties of the Particle Radial Diffusion in a Radially Bounded Irregular Magnetic Field

A. Malǔckov, N. Nakajima, M. Okamoto, S. Murakami and R. Kanno

(Received - Sep. 25, 2001)

NIFS-715 Oct. 2001

RESEARCH REPORT
NIFS Series

TOKI, JAPAN

Statistical properties of the particle radial diffusion in a radially bounded irregular magnetic field

A Maluckov† , N Nakajima†‡ , M Okamoto†‡ , S Murakami †‡ and R Kanno†‡

† Department of Fusion Science, The Graduate University for Advanced Studies, Toki, Gifu, 509-5292, Japan

‡ National Institute for Fusion Science, Toki, Gifu, 509-5292, Japan

E-mail: sandra@nifs.ac.jp

Abstract.

Statistical properties of the particle radial diffusion are clarified in the various types of the radially bounded irregular magnetic field inside a torus plasma, where the collisional (statistical) stochasticity due to the Coulomb collision and the magnetic (deterministic) stochasticity due to a radially bounded perturbed field coexist. The former is initialized in the velocity space, and the latter is in the configuration space. Extensive numerical analyses are performed in the two dimensional parameter space $(s_b/s_{bc}, \nu/\nu_t)$, where s_b and ν are the strength of a magnetic field perturbation and the collision (deflection) frequency, respectively. The normalization parameter s_{bc} corresponds to the islands overlapping criterion, and ν_t is the characteristic frequency of the passing particle orbits in the corresponding regular magnetic field. In the absence of the Coulomb collision, as $s_b/s_{bc}(\geq 1)$ increases, the magnetic field stochasticity or the particle radial diffusion with only parallel drift motion comes to appear as a uniform mixing process reflecting the non-locality of orbits in a radially bounded stochastic region, which is a non-diffusive, uniform, statistically stationary, and Markov process after the exponentially fast relaxation of correlations. The Coulomb collisions interrupt the fast non-local radial displacement of particles along the stochastic magnetic field lines, however, the radial displacement is still non-local, so that the particle radial diffusion develops as a strange diffusive process in the long time limit: subdiffusive, neither uniform nor Gaussian, and statistically non-stationary process, in almost all $(s_b/s_{bc}, \nu/\nu_t)$ parameter space. When the collisions are fairly frequent $(\nu/\nu_t \gg 1)$ and uniformity of the magnetic field stochasticity is fairly lost $(s_b/s_{bc} \geq 1)$, the locality of the particle motion is recovered, leading to a Wiener process with normal diffusivity, Gaussianity, statistical non-stationarity, and Markovianity, as well as the neoclassical diffusion in the regular magnetic field. Non-locality of particle orbits due to magnetic stochasticity produces the various types of diffusion process under the influence of the Coulomb collisions.

PACS numbers: 52.20.Dq, 52.25. Fi

Submitted to: *Plasma Phys. Control. Fusion*

1. Introduction

The particle radial diffusion is a problem of great importance in the context of the transport in a magnetically confined torus plasma. The earliest theoretical approaches [1–6], being developed with premise to determine the constant diffusion coefficient, are based on the analogy between the diffusion process in an unbounded, homogeneous media and the Gaussian random walk or standard Brownian motion. Thus, the Gaussianity, Markovianity, and normal diffusivity of the collisional radial diffusion are assumed a priori. The usual diffusion constant is then evaluated from the long time limit of the second cumulant (mean square displacement) under a constraint that the diffusion is local. This constraint is necessary in order to treat a real bounded, inhomogeneous system as a unbounded and homogeneous one near a thermodynamical equilibrium. Note that the mean square displacement is taken as a fundamental quantity from the statistical viewpoint. In the regular magnetic field with topologically nested flux surfaces (domain of the neoclassical theory [1, 2]), the radial diffusion in the configuration space is completely determined by both the deterministic drift motion of particle guiding centers inherent in such a geometry and the stochasticity due to the Coulomb collisions in the velocity space. In such a case the locality constraint is ensured with respect to the smallness of the particle displacement which satisfies $\rho_p/a \ll 1$, where ρ_p is the particle poloidal gyroradius, and a is the minor radius.

However, experimentally obtained diffusion coefficients are usually much greater than the neoclassical ones. As one of the reasons, the destruction of the regular magnetic surfaces due to MHD instabilities and error fields is suggested. Even if the amplitude of the magnetic field perturbations is small, they can change the topology of the magnetic field structure due to the resonance at their mode rational surfaces, namely, the magnetic islands and stochastic region are created [7, 8]. Usually, many Fourier modes of the magnetic perturbation can be simultaneously excited, and so the radially extended magnetic stochastic region appears after the overlapping of the magnetic island chains, i.e. the global magnetic stochasticity is created as the amplitude of the magnetic perturbation increases [7, 8]. Thus, with the increase of the stochasticity level, the particle radial diffusion in the stochastic magnetic field region comes to be prescribed by the statistical properties of the stochastic magnetic field lines themselves.

In order to estimate the diffusion coefficient of the static highly stochastic magnetic field, the correlation of the radial component of the perturbed magnetic field between two different points (Eulerian correlation) is specified by two characteristic lengths of the stochastic magnetic field lines: the parallel $L_{||}$ and perpendicular length $L_\perp$ to the equilibrium magnetic field lines [3]. Moreover, the stochastic magnetic field is characterized by another characteristic length, radial Kolmogorov length L_K, which is associated with the fast exponential divergence of the stochastic magnetic field lines in the radial direction [8]. Depending on the relative magnitude of these three characteristic lengths: $L_{||}, L_\perp$ and L_K, the various types of diffusive regimes are defined. The most

famous one is the quasilinear regime, where the relation

$$L_{||} \ll L_K \ll L_\perp < L$$

holds, and L is the length of the stochastic region. In this limit, the constant diffusion coefficient of the stochastic magnetic field lines (the diffusion coefficient not depending on the length of the magnetic field lines in evaluation of the correlation) is derived by postulating that in a radially unbounded stochastic magnetic field region ($L \to \infty$), the magnetic field stochasticity appears as a radially homogeneous, Gaussian random process with $L_{||} \ll L_\perp \to \infty$. Note that the radial unboundedness of the homogeneous stochastic region is equivalent of the locality constraint in the neoclassical particle radial diffusion in the regular magnetic field configuration. In the quasilinear regime, the evaluation of the Lagrangian correlation, i.e. evaluation of the correlations along the magnetic field lines, is easily performed due to the feature of $L_\perp \to \infty$ [9]. When the perpendicular characteristic length $L_\perp$ is finite, the Corrsin approximation is used to evaluate the Lagrangian correlation [9]. However, this approximation is valid only for a homogeneous equilibrium magnetic field without a magnetic shear [10].

On the basis of the diffusion of the stochastic magnetic field lines, the diffusion coefficient of the radial heat (particle) transport is calculated under the influence of the Coulomb collisions. It is reasonably assumed that the particle displacements due to collisions appear as a standard (Gaussian) Brownian process with the mean free path λ_{mfp} as the characteristic length. Thus, depending on the relative magnitude of four characteristic lengths: $L_{||}, L_\perp, L_K$, and λ_{mfp}, several asymptotic diffusive regimes are obtained. In the pioneering paper [4], both the collisionless and collisional limits are considered in the quasilinear regime of the magnetic field stochasticity. For both of them, the time independent diffusion coefficient is found, which means that the particle radial diffusion is a normal diffusive process like a standard Brownian motion. However, the particle diffusion coefficient becomes time-dependent in the absence of any perpendicular motion to the stochastic magnetic field lines. This case corresponds to the subdiffusive process, where the diffusion coefficient decreases with time. The existence of subdiffusivity influenced extensive investigations of the particle radial diffusion in the highly stochastic magnetic field [11, 12, 13]. It is shown that the mean square displacement is not sufficient in order to understand statistical properties of the particle radial diffusion [12].

In these treatments of the particle radial diffusion in the highly stochastic magnetic field, it is worth to stress that the allowable analytical approaches are influenced to assume unboundedness and homogeneity of the highly stochastic magnetic field and to specify the statistical characteristics of the magnetic field perturbation. Thus, there are ambiguous points when such analytical results are applied to a realistic system as the ideal limits. Especially, the treatment of the statistical properties of the stochastic magnetic field in the radial direction leads to problems. In torus systems, generally, the equilibrium magnetic field is inhomogeneous in the radial direction due to the magnetic shear, and the magnetic stochastic region created by perturbed magnetic fields, e.g. due

to MHD instabilities or error fields, is usually bounded in the radial direction. It means that the Corrsin approximation is not valid and the perpendicular characteristic length $L_\perp$ can not be treated as infinity, but finite. From the technical point of view, due to the inhomogeneity and boundedness in the radial direction, the Fourier transformation is not applicable to the radial direction, which means that the approach to assume the Eulerian correlation function in the Fourier space may not be directly applicable to the systems with inhomogeneous and bounded stochastic region in the radial direction. Thus, in the realistic magnetic field configurations with radially bounded and inhomogeneous stochastic regions, the applicability of the previous analytical results is under question. As another aspect, it should be pointed out that the physical interpretation why the above mentioned subdiffusivity of the radial diffusion occurs is not so clear. Although the cause may not be unique depending on the situations investigated, as one of the reasons, the non-locality of the particle radial displacements is considered. Up to now, however the role of the non-locality has not been mentioned.

On the other hand in the case before overlapping, near overlapping, and moderate overlapping, the magnetic field inside the stochastic region is generally neither entirely regular nor entirely irregular, but a complicated mixture of regular and irregular regions. In the regular island like regions, the magnetic field lines lie on tori or KAM surfaces [7, 8], while in irregular domains the magnetic field lines are apparently stochastic, or chaotic indicating the deterministic stochasticity [7, 8]. With stress on the enhancement of the time-independent diffusion coefficient of the collisional radial diffusion by the magnetic field destruction, the series of research are developed [14, 15]. To ensure locality, i.e. not to allow large particle radial displacements from the initial flux surface, the value of the diffusion coefficient is evaluated in the interval of the order of several collisional times. In these cases, the statistical treatment of the particle radial diffusion inside the partially destroyed magnetic field region is missing.

To avoid problems coming from the applicability of the analytical results in an idealized situation to a realistic one, to clarify the relationship between expected various diffusion processes and non-locality of the particle radial displacements, and to clarify the statistical properties of the various types of irregular magnetic field themselves, in this paper, the statistical properties of the magnetic and particle radial diffusion have been examined for various values of the stochasticity parameter and the Coulomb collision frequency by using direct numerical calculations of the trajectories of magnetic field lines and Monte Carlo simulations of the particle radial diffusion. The adopted system consists of both an axisymmetric MHD equilibrium with perfect nested flux surfaces and a radially bounded irregular magnetic field created by superposing the three Fourier harmonics of a magnetic perturbation which resonate at their mode rational surfaces. By changing values of the strength of perturbation, which is treated as a stochasticity parameter, the level of stochasticity is controlled. Thus, four types of the radially bounded magnetic stochastic region are created: state with isolated island chains under the overlapping threshold, with weak overlapping of the magnetic islands, with moderate overlapping characterized by the mixture of regular

and irregular domains, and with highly irregular stochastic magnetic field lines. The statistical properties of the magnetic stochasticity, which realizes within the radially bounded stochastic region, are not assumed, but examined by numerically calculating the Liapunov exponent [8], the cumulant up to the fourth order [16, 17], and the autocorrelation coefficient [16, 18]. It is found that as the level of stochasticity increases, the magnetic field stochasticity inside the radially bounded perturbed magnetic field region tends to appear as a uniform mixing process characterized by non-diffusivity, radially uniform distribution, statistical stationarity, and Markovianity. The uniform mixing process, which stems from both the radial boundedness of the stochastic region and fast exponential divergence of the magnetic field lines in the radial direction, is firstly mentioned in the context of the particle radial diffusion in the stochastic magnetic field. Note that the radial diffusion of the guiding center particles tied to the stochastic magnetic field lines without both the perpendicular drifts and Coulomb collisions is equivalent to the radial diffusion of the magnetic field lines.

After clarifying the statistical properties of the magnetic field stochasticity within the radially bounded magnetic field region, the effects of the perpendicular drift of guiding centers and of the Coulomb collisions are investigated through the Monte Carlo technique. The perpendicular drifts qualitatively do not change the statistical properties of the particle radial diffusion, since the non-local radial displacement due to the fast parallel drift motions along the stochastic magnetic field lines is dominant compared with the local radial displacement due to the slow perpendicular drift motions. Thus, the statistical properties of the collisionless particle radial diffusion in the radially bounded stochastic magnetic field are prescribed by those of the stochastic magnetic field, and the particle radial diffusion is non-local. The Coulomb collisions interrupt the fast non-local motions along the stochastic magnetic field lines. As the stochasticity parameter increases and collision frequency decreases, the particle radial diffusion appears as a strange diffusive process characterized by subdiffusivity, neither uniform nor Gaussian profile, statistical non-stationarity, reflecting the statistical properties of the magnetic stochasticity. The radial diffusion is still non-local in this regime. In the opposite limit with small stochasticity parameter and a high collision frequency, the radial exponential divergence of the magnetic field lines is suppressed, and the frequent collisions recover the locality of the diffusion, so that the diffusion appears as the Wiener process which is previously recognized in the neoclassical radial diffusion in the regular magnetic field [19]. It is clarified that non-locality of the particle radial displacements leads to non-diffusivity or subdiffusivity in a radially bounded stochastic magnetic field region. The stochastic parameter is interpreted as the indicator of the non-locality of the particle radial displacements, and the Coulomb collision frequency is recognized as the scattering rate of such the non-local displacements. Thus, as a result of the superposition of these two effects, the degree of the non-locality of the particle radial displacements is determined, leading to various types of diffusion process.

The organization of this paper is as follows. In section 2, the basic equations of the guiding center electrons, the numerical Monte Carlo method, and magnetic field

configuration consisting of an axisymmetric MHD equilibrium and a radially bounded magnetic field region with irregularities are described. As the statistical measures the cumulant up to the fourth order, the diffusion coefficient and autocorrelation coefficient are defined in section 3. Additionally, the effective radial Liapunov exponent is introduced in connection with the magnetic stochasticity. By using these measures, the statistical analyses are performed in section 4 by comparing numerically obtained process with the fundamental diffusive process: the Wiener process in infinite domain; and the fundamental process from the viewpoint of the deterministic stochasticity: the uniform mixing in finite domain of configuration space. Section 4.1 is devoted to the statistical analysis of the magnetic field stochasticity which is meaningful in the region of so called global magnetic stochasticity initialized by the overlapping between two neighboring islands. One fitting equation is given for all mentioned stochastic levels in the region of global stochasticity, by which the saturated value of the effective radial Liapunov exponent is estimated. Additionally the number of the magnetic field lines with positive radial Liapunov exponent is taken as an indicator of the existence of the regular structures inside the stochastic region. In section 4.2, the effects of the perpendicular drift motions on the statistical properties of the radial diffusion in the radially bounded stochastic magnetic field region are presented. The statistical properties of the particle radial diffusion in the presence of both the magnetic field stochasticity inside the radially bounded perturbed magnetic field region and the collisional stochasticity due to the Coulomb collisions are investigated in section 4.3. The statistical properties are investigated in two-parameter space consisting of above mentioned four levels of stochasticity and for three collision frequencies corresponding to plateau, and Pfirsch-Schlüter regimes. In section 5, the characteristic lengths, the locality of diffusion, the second cumulant, and the ballistic phase in the highly stochastic magnetic field are discussed. It is shown that the present situation with radially bounded stochastic field is characterized by completely different ordering of the characteristic lengths from that in the quasilinear regime. Also, it is shown that the diffusion coefficient defined by the time derivative of the second cumulant has no clear physical meaning when the locality of the diffusion is not ensured. Moreover, the short time ballistic phase in the highly stochastic magnetic field is discussed associated with the dynamical relaxation to an equilibrium. Section 6 presents the conclusions.

2. Establishment of model

2.1. Model equations

The test particle diffusion in the presence of destroyed magnetic surfaces is evaluated by the solution of the linearized gyro-phase averaged Boltzmann equation

$$\frac{\partial f}{\partial t} + \mathbf{v} \cdot \nabla f = C(f), \tag{1}$$

where $f = f(t, \mathbf{r}, E, \mu)$ is the distribution function of guiding center particles, and $C(f)$ is the linearized pitch-angle scattering operator due to Coulomb collisions. The

background plasma is assumed to be uniform, the energy E of each guiding center particle is conserved, and only the magnetic moment μ is changed by the Coulomb collisions.

The stationary magnetic field $\mathbf{B}_t$ is assumed to be of the form

$$\mathbf{B}_t = \mathbf{B} + \delta\mathbf{B}, \tag{2}$$

where $\mathbf{B}$ is an equilibrium magnetic field, and $\delta\mathbf{B}$ is a small perturbation expressed as [14]

$$\delta\mathbf{B} = \nabla \times (b\mathbf{B}), \qquad (|\delta\mathbf{B}/\mathbf{B}| \ll 1) \tag{3}$$

Hence, the test particle drift velocity $\mathbf{v}$ is given by

$$\mathbf{v} = v_{||}\frac{\mathbf{B} + \nabla \times ((\rho_{||} + b)\mathbf{B})}{B + \hat{n} \cdot \nabla \times ((\rho_{||} + b)\mathbf{B})}, \tag{4}$$

where $v_{||}$ is the parallel velocity to the equilibrium magnetic field $\mathbf{B}$, $\rho_{||} = v_{||}/\Omega$ is the parallel gyro-radius, Ω is the gyrofrequency, and $\hat{n} = \mathbf{B}/B$.

Instead of solving equation (1) directly, the Monte Carlo technique is used [20]. Equations for each guiding center particle equivalent to equation (1) consist of two parts: orbit, and collision part. Without the Coulomb collisions the characteristic equations of equation (1) are obtained from [14]

$$\dot{\xi} \equiv \frac{d\xi}{dt} = \mathbf{v} \cdot \nabla\xi, \tag{5}$$

where $\xi = (\psi, \theta, \zeta, \rho_c)$. The variables ψ, θ, ζ are the Boozer coordinates: ψ is the label of a flux surface defined as the toroidal flux/2π, θ is the poloidal, and ζ is the toroidal angle. The forth variable is expressed as $\rho_c = \rho_{||} + b$. The equations of the guiding center in the Boozer coordinates become

$$\dot{\psi} = -\frac{1}{\gamma}\left[\delta\left(J\frac{\partial B}{\partial\theta} - I\frac{\partial B}{\partial\zeta}\right) - \frac{e^2B^2}{m}\rho_{||}\left(J\frac{\partial b}{\partial\theta} - I\frac{\partial b}{\partial\zeta}\right)\right], \tag{6}$$

$$\dot{\theta} = \frac{\delta}{\gamma}J\frac{\partial B}{\partial\psi} + \frac{e^2B^2}{\gamma m}\rho_{||}\left[\iota - \rho_c J' - J\frac{\partial b}{\partial\psi}\right], \tag{7}$$

$$\dot{\zeta} = -\frac{\delta}{\gamma}I\frac{\partial B}{\partial\psi} + \frac{e^2B^2}{\gamma m}\rho_{||}\left[1 + \rho_c I' + I\frac{\partial b}{\partial\psi}\right], \tag{8}$$

$$\begin{aligned}\dot{\rho}_c = &-\frac{\delta}{\gamma}\left[(\iota - \rho_c J')\frac{\partial B}{\partial\theta} + (1 + \rho_c I')\frac{\partial B}{\partial\zeta}\right] \\ &+ \frac{m\Omega^2\rho_{||}}{\gamma}\left[(\iota - \rho_c J')\frac{\partial b}{\partial\theta} + (1 + \rho_c I')\frac{\partial b}{\partial\zeta}\right],\end{aligned} \tag{9}$$

and

$$\gamma = e\left[J + \iota I + \rho_c(JI' - IJ')\right], \tag{10}$$

$$\delta = \mu + \frac{e^2B}{m}\rho_{||}^2, \tag{11}$$

where $2\pi J$ ($2\pi I$) are the poloidal (toroidal) current outside (inside) the flux surface.

Statistical properties of the particle radial diffusion

To investigate the structure of the magnetic field lines, similar equations are constructed as follows. By neglecting the particle drift motion, the equation (4) becomes

$$\mathbf{v} = v_{||}\frac{\mathbf{B}_t}{\mathbf{B}_t \cdot \hat{n}}. \tag{12}$$

Substituting equation (12) into equation (5) the equation of the magnetic field lines is obtained

$$\frac{d\psi}{\mathbf{B}_t \cdot \nabla\psi} = \frac{d\theta}{\mathbf{B}_t \cdot \nabla\theta} = \frac{d\zeta}{\mathbf{B}_t \cdot \nabla\zeta} = \frac{v_{||}dt}{\mathbf{B}_t \cdot \hat{n}}, \tag{13}$$

where the time t can be taken as an independent variable. Three equations on $\dot{\psi}, \dot{\theta}$, and $\dot{\zeta}$ obtained from equation (13) are expressed by equations (6), (7), and (8) by putting $\delta = 0$ and $\rho_c = b$, namely

$$\dot{\psi} = \frac{m\Omega^2\rho_{||}}{\gamma}\left(J\frac{\partial b}{\partial\theta} - I\frac{\partial b}{\partial\zeta}\right), \tag{14}$$

$$\dot{\theta} = \frac{m\Omega^2\rho_{||}}{\gamma}\left(\iota - \frac{\partial(Jb)}{\partial\psi}\right), \tag{15}$$

$$\dot{\zeta} = \frac{m\Omega^2\rho_{||}}{\gamma}\left(1 + \frac{\partial(Ib)}{\partial\psi}\right), \tag{16}$$

where

$$\gamma = e\left(J + \iota I + b(JI' - IJ')\right). \tag{17}$$

The equations (14)-(16) are solved under the condition that $v_{||} = const.$ and $\mu = 0$.

The pitch angle scattering in equation (1) is expressed as

$$\frac{\partial f}{\partial t} = C(f) = \frac{\nu}{2}\frac{\partial}{\partial\lambda}\left((1-\lambda^2)\frac{\partial f}{\partial\lambda}\right), \tag{18}$$

where the pitch angle $\lambda = v_{||}/v$ is used instead of μ, and ν is the deflection frequency [14]. Since a uniform background plasma is assumed, the deflection frequency is constant in both space and time. Knowing the solution of equation (18) with the initial condition $f(\lambda, t = 0) = \delta(\lambda - \lambda_0)$ a Langevin equation giving the same mean value of λ and standard deviation σ is constructed [20]

$$\frac{d\lambda}{dt} + \nu\lambda = F(t). \tag{19}$$

The white noise source $F(t)$ is characterized by

$$\langle F(t)\rangle = 0 \quad \text{and} \quad \langle F(t)F(t')\rangle = (1-\lambda_0^2)\nu\delta(t'-t) \tag{20}$$

From the solution (19), for a discrete time step Δt satisfying $\Delta t\nu \ll 1$, λ is changed as

$$\lambda(t_n) = \lambda(t_{n-1})(1-\nu\Delta t) \pm \sqrt{(1-\lambda^2(t_{n-1}))\nu\Delta t}, \tag{21}$$

for one step from $t_{n-1} = (n-1)\Delta t$ to $t_n = n\Delta t$. The symbol $\pm$ indicates that the sign is to be chosen randomly, but with equal probability for plus and minus.

The magnetic field stochasticity and pitch angle scattering due to Coulomb collisions introduce stochasticity in the system, so that the particle ensemble allows statistical treatment.

2.2. The structure of magnetic field

In the Boozer coordinates, the contravariant form of the equilibrium magnetic field $\mathbf{B}$ is expressed as

$$\mathbf{B} = \nabla\psi \times \nabla\theta - \iota\nabla\psi \times \nabla\zeta. \tag{22}$$

Hence, the topology of the equilibrium magnetic field $\mathbf{B}$ is torus consisting of nested toroidal flux surfaces. In the small perturbation given by equation (3), the function b, which has unit of length, is used to represent the structure of destroyed magnetic field $\mathbf{B}_\iota$, i.e. the islands and stochastic regions. Its Fourier representation is

$$b(\psi, \theta, \zeta) = \sum_{m,n} b_{mn}(\psi)\cos(m\theta - n\zeta + \zeta_{m,n}), \tag{23}$$

where $\zeta_{m,n}$ is the phase and $|b_{mn}|/a \ll 1$. The form of $b_{mn}(\psi)$ is assumed to be

$$\frac{b_{mn}(\psi)}{a} = s\exp\left(-\frac{(\psi - \psi_{mn})^2}{\Delta\psi^2}\right), \tag{24}$$

where parameter s indicates the strength of perturbation, so called a stochasticity parameter. The width of perturbation is controlled by the parameter $\Delta\psi$ which is chosen to be fixed.

The equations of the magnetic field lines are given by equation (13). Thus, by using equations (22), (3), and (23), the topological changes of the magnetic configuration are dominated by

$$\left|\frac{\delta\mathbf{B}\cdot\nabla\psi}{\mathbf{B}\cdot\nabla\zeta}\right| = \sum_{m,n}(mJ - nI)b_{mn}(\psi)\sin(m\theta - n\zeta + \zeta_{m,n}) \tag{25}$$

For the equilibrium field $\mathbf{B}$, the Poincare plot of the magnetic field lines satisfying $d\theta/d\zeta \equiv \iota = n/m$ corresponds to fixed points with period m [7, 8] in a poloidal cross section with $\zeta = const.$. In the presence of a small perturbation the resonances at $\iota(\psi) = n/m$ are origins for eventually topological changes in the system. According to the KAM theorem [8], some of the fixed points remain after the small perturbation is added, and the Poincare-Birkhoff theorem [8] proves that they are of elliptic and hyperbolic type: alternate appearance of elliptic and hyperbolic points is a generic property of the system at sufficiently small stochasticity parameter. Near every rational surface with $\iota(\psi) = n/m$, closed regular orbits appear encircling the m elliptic points, and forming a chain of m islands. The motion around hyperbolic points which are connected by separatrices is apparently irregular. The island width [8] is approximately given by

$$w_{m,n} = W_{m,n}\sqrt{s}, \qquad W_{m,n} = \left(4q\sqrt{\frac{aR}{q'}}\right)_{r=r_{m,n}}, \tag{26}$$

where $r_{m,n}$ is the radial position of the rational surface with $q = m/n$, $q' = dq/dr$, and a and R are minor and major radii, respectively. Most of irrational surfaces subsist as KAM barriers among the island chains. As the stochasticity parameter increases it reaches value at which the KAM curve changes its character from a continuous to

curve with holes. Thus, the KAM curve is transformed into so called cantory [7, 8]. Magnetic field lines, previously blocked by the KAM barriers, could chaotically wander through the formed holes. Different KAM barriers disappear at different value of the stochasticity parameter, and some occupy more and more area in phase space. Finally at a critical parameter the last KAM barrier is destroyed: overlapping is started. The value of the stochasticity parameter at which the overlapping starts is estimated from equalizing the distance between two selected neighboring rational surfaces Δr to the sum of the half widths of the corresponding islands:

$$\frac{w_{m,n} + w_{m',n'}}{2} = \frac{W_{m,n} + W_{m',n'}}{2}\sqrt{s}. \tag{27}$$

Thus, the threshold value for overlapping is

$$s_c \approx \left(\frac{2\Delta r}{W_{m,n} + W_{m',n'}}\right)^2. \tag{28}$$

However, there still remain regions bounded by islands which shrink as the stochasticity parameter increases. Thus, according to initial conditions and values of stochasticity parameter, orbits with different topology appear: cycles (which correspond to the elliptic points), invariant KAM curves (trapped orbits inside of island chains, and passing orbits on irrational KAM barriers), and chaotic orbits (in stochastic regions) whose intersection points densely fill a two dimensional region.

As an MHD equilibrium an axisymmetric FCT tokamak with regular nested flux surfaces is adopted. The boundary is circular, $B = 3T$, and major and minor radii are $R = 3\mathrm{m}$, and $a = 1.01\mathrm{m}$, respectively. The profile of the rotational transform is specified as

$$\iota = 0.9 - 0.5875\left(\frac{r}{a}\right)^2, \tag{29}$$

the aspect ratio is given by

$$\varepsilon = \frac{a}{R} = \frac{1}{3}, \tag{30}$$

and β =(kinetic pressure/magnetic pressure)= 0.

The Fourier harmonics of the magnetic field perturbation expressed by equation (23) are chosen to be

$$\frac{n}{m} = \frac{7}{10}, \frac{2}{3}, \frac{7}{11},$$

with $\zeta_{nm} \equiv 0$ and $\Delta\psi/\psi_a = 0.1$. The relative magnitude of the perturbation is given by $s_b \equiv |\delta\mathbf{B} \cdot \hat{r}|/B \approx ms/(r_{m,n}/a) = 4.8s$ for the Fourier mode with $(m, n) = (3, 2)$. Thus, according to equation (28), the critical value of s_b is

$$s_{bc} \approx 7 \times 10^{-5}. \tag{31}$$

2.3. Numerical model

The DCOM code [21] is used as well as in the neoclassical calculation [19]. The monoenergetic ($E = 3keV$) ensemble of $N = 10000$ guiding center electrons with randomly distributed λ is started from the same flux surface with $\iota = 2/3$ (rational surface) at $r/a = 0.63$, and with uniformly distributed poloidal and toroidal angles. Each of electrons evolutes independent of the others, and its motion is described by equations (6)-(9). The electron guiding center equations are solved using the 6th order Runge-Kutta method. Based on the equation (21), the pitch angle scattering due to Coulomb collisions is added at every particle orbit step.

In order to satisfy the energy conservation condition, the time orbit step size Δt of the numerical calculations is adopted to be $\Delta t = 0.5 \times 10^{-9}$s. The relative error of the energy conservation is tolerated up to $10^{-6}\%$ during the calculations.

When the magnetic field line diffusion is investigated (section 4.1) the test magnetic field line ensemble is initially loaded at $\iota = 2/3$ with randomly distributed θ, ζ. The magnetic field line is followed by numerically solving equations (14)-(16), with $\mu = 0$ and $E = 3$keV.

3. Establishment of the statistical approach

The particle radial diffusion is a realization of the collisional stochasticity (statistical stochasticity [7]), and the magnetic stochasticity (deterministic stochasticity [8, 11]).

As the statistical measures, the cumulant, diffusion and autocorrelation coefficients are calculated with respect to the radial particle displacement

$$\delta r(t) = r(t) - r(0),$$

adopting ensemble average:

$$\langle X \rangle = \frac{1}{N} \sum_{i=1}^{N} X_i, \tag{32}$$

where N is the number of particles.

The dimensionless n-th cumulant coefficient γ_n [16, 17] is given by

$$\gamma_n(t) \equiv \frac{C_n(t)}{C_2^{n/2}(t)}, \tag{33}$$

where $C_n(t)$ is n-th cumulant. The cumulants up to the 4th order are calculated as [17]

$$C_1(t) \equiv \langle \delta r(t) \rangle, \tag{34}$$

$$C_n(t) \equiv \langle (\delta r(t) - \langle \delta r(t) \rangle)^n \rangle, \qquad n = 2, 3 \tag{35}$$

$$C_4(t) \equiv \langle (\delta r(t) - \langle \delta r(t) \rangle)^4 \rangle - 3C_2^2(t). \tag{36}$$

The first cumulant is a measure of the advective effect or convective diffusion [17]. This advective effect is eliminated from the higher cumulants. The second cumulant, i.e. the mean square displacement, is the dispersion around $\langle \delta r(t) \rangle$, and a measure of the

conductive diffusion. Its time development determines the type of diffusivity [7]. The linear increasing in time corresponds to the normal diffusivity, slower, and faster than linear increasing in time are then associated with the subdiffusivity, and superdifusivity, respectively.

The effective diffusion coefficient is defined as

$$D(t) \equiv \frac{dC_2(t)}{2dt}, \tag{37}$$

and its power-law equivalent as

$$D_{pw}(t) \equiv \frac{C_2(t)}{2t}. \tag{38}$$

Note that both definitions have physical meaning, when the diffusion process is local. This point will be discussed in section 5. When the power-law behaviour of $C_2(t)$ is assumed as

$$C_2(t) \approx t^{\alpha}, \tag{39}$$

the value of the diffusion exponent denotes normal diffusive ($\alpha = 1$), subdiffusive ($\alpha < 1$), and superdiffusive ($\alpha > 1$) behaviour. Additionally, the relative difference of $D_{pw}(t)$ from $D(t)$ is calculated in order to evaluate how much the power-law behaviour of $C_2(t)$ given by equation (39) holds

$$\Delta D(\%) \equiv \frac{|D(t) - \alpha D_{pw}(t)|}{D(t)} \times 100. \tag{40}$$

When C_2 is well approximated by equation (39), $\Delta D(\%)$ vanishes.

It is proved [17] that the only physically acceptable random process with a finite number of nonvanishing cumulant coefficients is Gaussian with $\gamma_{n>2} = 0$. Therefore, the cumulant coefficients $\gamma_{n>2}$ generically carry information about non-Gaussianity [17] ‡. The degree of asymmetry around $\langle \delta r(t) \rangle$ and relative peakedness or flatness of a particle distribution compared with Gaussian, are characterized by γ_3 (skewness), and γ_4 (kurtosis), respectively. A positive (negative) value of skewness signifies a distribution with an asymmetric tail extending out towards $\delta r(t) > \langle \delta r(t) \rangle$ ($\delta r(t) < \langle \delta r(t) \rangle$). On the other hand, a positive (negative) value of kurtosis indicates more peaked (flatted) distribution than the Gaussian one, i.e. the importance of the tails of the distribution is enhanced (reduced), respectively.

The autocorrelation coefficient [16] is given by

$$A(t,t') \equiv \frac{\langle (\delta r(t) - \langle \delta r(t) \rangle)(\delta r(t') - \langle \delta r(t') \rangle) \rangle}{\sqrt{\langle (\delta r(t) - \langle \delta r(t) \rangle)^2 \rangle \langle (\delta r(t') - \langle \delta r(t') \rangle)^2 \rangle}}. \tag{41}$$

The statistical stationarity is ensured when the following relations are satisfied with arbitrary time T

$$C_{1,2}(t+T) = C_{1,2}(t), \tag{42}$$

$$\gamma_{3,4}(t+T) = \gamma_{3,4}(t), \tag{43}$$

$$A(t+T, t'+T) = A(t'-t). \tag{44}$$

‡ The non-Gaussianity is then related to the existence of the correlation effects in the treated diffusive process

In other words, when the cumulant, and autocorrelation coefficients are not affected by a shift in time, the stochastic process is statistically stationary. In this stationary process, corresponding α vanishes (non-diffusive behaviour), and the system of test particle (magnetic field line) ensemble is relaxed to an equilibrium state. Note that this definition of the statistical stationarity is more rigorous compared with that in [19], since more general types of diffusive processes are treated. In the following all the cumulants are normalized by the minor radius a.

In the context of the radial diffusion the degree of stochasticity of the magnetic field lines, or of the particle trajectories tied to magnetic field lines is additionally indicated by the effective radial Liapunov exponent. Generally, the Liapunov exponent of the i-th particle trajectory or i-th magnetic field line, for given initial conditions (position, and initial orientation of the infinitesimal displacement) indicates the exponential rate of divergence between it and initially neighboring trajectory

$$l_{ei}(t) \equiv \frac{1}{t}\ln\left(\frac{d_i(t)}{d_i(t=0)}\right), \tag{45}$$

where $d_i(t)$ is the distance at time t between two initially neighboring trajectories, which is usually evaluated in the tangential space of the trajectory [8]. The positive value of the Liapunov exponent $l_{ei} > 0$ denotes exponential separation of two initially neighboring trajectories. On the other hand, $l_{ei} < 0$ indicates that two initially neighboring trajectories are stuck to each other, and their distance does not change for $l_{ei} = 0$. Note that in N–dimensional system the Liapunov exponents can be defined with respect to any of the N directions [8]. The radial Liapunov exponent is expressed by the equation (45), by taking $d_i(t)$ as the radial distance. The effective radial Liapunov exponent is defined as the averaged radial Liapunov exponent over different initial conditions

$$\langle l_e(t)\rangle = \frac{1}{N}\sum_{i=1}^{N} l_{ei}(t), \tag{46}$$

where i denotes different initial conditions.

The radial diffusion due to collisional stochasticity (initialized in the velocity space) appears in the configuration space as a Wiener like process [19] in the presence of regular magnetic field. On the other hand, being of a deterministic type, the radial diffusion due to magnetic stochasticity inside the radially bounded irregular domains (initialized in the configuration space) is considered to be of a mixing type [22]. Hence, both the Wiener and the uniform mixing type process are used as references.

3.1. The Wiener process

The Wiener process in infinite domain [16, 18] is a Markov process described by the Langevin equation

$$\frac{\mathrm{d}x}{\mathrm{d}t} = F(t), \tag{47}$$

where $F(t)$ is the white noise characterized by

$$\langle F(t)\rangle = 0, \qquad \langle F(t)F(t')\rangle = \mathcal{D}\delta(t-t'),$$

with a constant $\mathcal{D}$. Note that the particle position $x(t)$ is expressed by the time integration of independent random events.

Corresponding Fokker-Plank equation [18] is

$$\frac{\partial}{\partial t} f_t(x,t|x_0,0) = \frac{\mathcal{D}}{2}\frac{\partial^2}{\partial x^2} f_t(x,t|x_0,0),$$

whose solution is the Gaussian conditional (transition) probability $f_t(x,t|x_0,0)$ with the initial condition $f_t(x,0|x_0,0) = \delta(x-x_0)$.

The Markov property of the Wiener process [16, 18] is expressed as the complete determination of the system by both the probability of any of its states (for example initial state , $f(x_0,0)$) and the transition probabilities $f_t(x,t|x_0,0)$ from the referent state to the i-th one

$$f(x_i,t_i) = f_t(x_i,t_i|x_0,0) f(x_0,0), \qquad \forall t_i.$$

In other words the successive transitions are statistically independent [18].

The cumulant coefficients, diffusion coefficient, diffusion exponent, and autocorrelation coefficient for $\delta x(t) = x(t) - x_0$ are

$$C_1 = 0,\ C_2 = \mathcal{D}t,\ \gamma_3 = 0,\ \gamma_4 = 0, \tag{48}$$
$$D(t) = D_{pw}(t) = \frac{\mathcal{D}}{2},\ \alpha = 1,\ A(t,t') = \sqrt{\frac{t}{t'}},\ t \le t'.$$

Thus, the Wiener process is a normal diffusive, Markov, Gaussian, and statistically non-stationary process [16, 18].

Here a criterion of the Wiener process on the numerically obtained processes, which will be used in section 4, is introduced. It is defined as

$$|\alpha_W - 1| \le 0.1, \quad |(\gamma_3)_W, (\gamma_4)_W| \le 0.1, \quad \text{good fitting to } A_W(t,t') = \sqrt{\frac{t}{t'}}. \tag{49}$$

3.2. Uniform mixing process

Following Krilov's determination of the mixing type systems [23], the mixing can be signed by a tendency of the points of an initially given phase-space region to be uniformly distributed over a bounded surface of the single-valued integrals of motion as time increases. Thus, the mixing is generically associated with the exponentially fast relaxation of distribution function to the uniform distribution:

$$\lim_{t>\tau_{corr}} f(x,t) = \langle f(x,t) \rangle, \tag{50}$$

where τ_{corr} is the correlation time, or the characteristic time of mixing, and with exponentially vanishing correlations :

$$\lim_{\tau=t'-t>\tau_{corr}} C(g_1(t), g_2(t')) \approx \mathrm{e}^{-(\tau/\tau_{corr})} \sim 0, \tag{51}$$

where $C(g_1(t), g_2(t'))$ denotes the correlation between arbitrary functions of the system's states, $g_1(t)$ and $g_2(t')$. One of the exponentially vanishing correlations among the states

of system may be expressed by the autocorrelation coefficients ($g_1(t) = g(t), g_2(t') = g(t')$) as

$$A(t,t') \approx A(\tau = t' - t) \approx \exp\left(-\frac{\tau}{\tau_{corr}}\right), \qquad t \leq t' \tag{52}$$

The weaker concept of mixing, which allows slower relaxation than exponential decay [23, 24], is suggested in the physical systems recently, so that the exponentially fast mixing is declared as the uniform mixing process. Note that the uniform mixing process shows the ergodic property [23] over the bounded region of phase space where mixing has been realized.

In uniform mixing-type systems trajectories starting from two points laying close to each other diverge rapidly following an exponential law [23]. This behaviour is described by the positive effective Liapunov exponent (section 3), and the positive Kolmogorov entropy [8]. Thus, the uniform mixing process in the configuration space is characterized by a time independent positive effective radial Liapunov exponent

$$\langle l_e \rangle = \lim_{t\to\infty} \langle l_e(t) \rangle \ (> 0) \tag{53}$$

The Kolmogorov entropy is estimated as a sum over all positive Liapunov exponents. In the absence of external forces, after the uniform mixing is established, the effective radial Liapunov exponent and then the Kolmogorov entropy saturate to finite positive value as a maximum entropy state.

The randomness with respect to the dynamical instability of motion, i.e. the exponential divergence of the close trajectories [8, 7], is called the deterministic stochasticity: the probability concept becomes applicable. Thus, neglecting the regular phase appearing in the growth of exponential instability, the Markov property is established [23].

The uniform mixing inside a bounded one-dimensional region $a \leq x \leq b$ is characterized by

$$C_1 = \frac{a+b}{2},\ C_2 = \frac{(b-a)^2}{12},\ \gamma_3 = 0,\ \gamma_4 = -\frac{6}{5},\ D(t) = 0,\ \alpha = 0, \tag{54}$$

and the autocorrelation coefficient given by equation (52) for $t > \tau_{corr}$. Hence, the uniform mixing process is a non-diffusive, Markov, uniform, and statistically stationary process for $t > \tau_{corr}$.

A criterion of the uniform mixing process on the numerically obtained processes is defined as

$$\begin{aligned} &\alpha_U \leq 0.1, \qquad C_2 \sim \frac{w_{st}^2}{12}, \quad |(\gamma_3)_U, (\gamma_4)_U + \frac{6}{5}| \leq 0.1, \\ &\text{good fitting to } \ A(t,t') = A_U(\tau = t' - t) = \mathrm{e}^{-\frac{\tau}{\tau_{corr}}}, \end{aligned} \tag{55}$$

where w_{st} is the radial width of the stochastic region.

3.3. Strange diffusive process

If the radial particle diffusion is neither the Wiener nor uniform mixing process, then the long-range correlations in space and time, and long tail effects are suggested [24].

In such a case, various relaxation processes may exist. In the context of the radial particle diffusion in the radially bounded stochastic magnetic field region, however, the diffusive process, which is neither the Wiener nor the uniform mixing process in the long time limit, is categorized as subdiffusive or non-diffusive, profile neither uniform nor Gaussian, statistically non-stationary, and (maybe) non-Markov process, which belongs to the domain of so called fractal Brownian motion [25]. Thus, when a numerically obtained radial diffusion does not satisfy the criteria given by equations (49) and (55), the radial diffusion is recognized as the strange diffusive process with above mentioned statistical properties.

4. Statistical properties of the particle radial diffusion

4.1. Statistical properties of the magnetic field stochasticity

To investigate the statistical properties of the magnetic field structure, namely the cumulant, diffusion coefficient, diffusion exponent, and autocorrelation coefficient, the equations of the magnetic field line given by (14)-(16) are solved under the condition of $\mu = 0, E = 3\text{keV}$, for various values of s_b in equation (24). In this treatment the time t is used as independent variable, so that the direct comparison of statistical quantities of the magnetic field structure with those of particles under Coulomb collision becomes possible. Moreover, obtained statistical properties are interpreted as those of guiding center particles without both perpendicular drift motion and Coulomb collisions. To create various types of magnetic field structure, s_b/s_{bc} is chosen as 0.33 (before overlapping), 1.3 (near overlapping), 3.3 (moderate overlapping), and 33 (highly overlapping), respectively. The critical value of s_b corresponding to the overlapping condition: s_{bc} is given by equation (31).

The magnetic field stochasticity appears in the configuration space through the growth of irregular domains. Thus, as long as the overlapping of neighboring islands (developing of the global magnetic stochasticity) has not been started, the irregularities are localized around the island separatrix regions, and the statistical treatment is meaningless. However, the values of the cumulant, and autocorrelation coefficients in the absence of the global magnetic stochasticity are mentioned because of comparison.

The magnetic field structures, for $s_b/s_{bc} = 0.33, 1.3, 3.3$, and 33, are the isolated island chain at $q = 3/2 (w_{3,2}/a = 0.024)$, overlapping among islands at $q = 3/2, 10/7, 11/7 (w_{st}/a \approx 0.14)$, stochastic sea ($w_{st}/a \approx 0.17$) with isolated island structures at $q = 10/7, 11/7 (w_{m,n}/w_{st} \approx 1/4)$, and stochastic sea without structures ($w_{st}/a \approx 0.25$). The $w_{m,n}$ and w_{st} are the width of the island and stochastic region, respectively. In figures 1a-1d, the corresponding Poincare plots at the poloidal cross section with $\zeta = 2.4\text{rad}$ are shown. The time interval for sequential plotting is $100 \times dt \equiv 10^{-7}\text{s}$, and the test magnetic field lines are followed during the time interval of $0 \leq t \leq 1.5 \times 10^{-4}\text{s}$ for $s_b/s_{bc} = 0.33, 3.3$, and 33, and the time interval of $1.3 \times 10^{-3}\text{s} \leq t \leq 1.5 \times 10^{-3}\text{s}$ for $s_b/s_{bc} = 1.3$.

Statistical properties of the particle radial diffusion

4.1.1. Effective Liapunov exponent The effective radial Liapunov exponent given by equation (46) provides a quantitative measure of the degree of stochasticity for magnetic field lines. Thus, the effective radial Liapunov exponent is calculated for a sample of $N = 1000$ magnetic field lines. The numerical approach of reference [26] is adopted for the magnetic field line described by equations (14)-(16), where the toroidal angle ζ is treated as an independent variable instead of time t by combining equations as $d\psi/d\zeta$ and $d\theta/d\zeta$. The transformation to time is done by $t \sim c\zeta$ with $c \approx R/v_{||}$, $v_{||} = \sqrt{2E/m}$, and $E = 3$keV.

Under the threshold for overlapping, $s_b/s_{bc} < 1$, although the effective radial Liapunov exponent $\langle l_e(t)\rangle$ increases almost monotonically in time, it is always negative during the calculation as is shown in figure 2a for $s_b/s_{bc} = 0.33$. The corresponding number of the magnetic field lines with positive Liapunov exponent $N_p(t)$ is very few as is indicated in figure 3a. On the other hand, in the region of the global magnetic stochasticity: $s_b/s_{bc} \geq 1$, the effective radial Liapunov exponent $\langle l_e(t)\rangle$ and the number of the magnetic field lines with positive Liapunov exponent $N_p(t)$ almost monotonically increase with time, as are shown in figures 2b (3b), 2c (3c), and 2d (3d) for $s_b/s_{bc} = 1.3, 3.3$, and 33, respectively. The $\langle l_e(t)\rangle$ changes from negative to positive values, asymptotically leading to saturation. The $N_p(t)$ also shows tendency to saturate as time increases, and it saturates faster than $\langle l_e(t)\rangle$. A characteristic time t_d is defined for $s_b/s_{bc} \geq 1$, as a time at which the effective radial Liapunov exponent becomes zero: $\langle l_e(t_d)\rangle = 0$. As is understood from figures 3b-3d, as s_b/s_{bc} increases, about half of the magnetic field lines come to have positive $l_{ei}(t)$ at $t = t_d$. After t_d, $N_p(t)$ still continuously increases, and $\langle l_e(t)\rangle$ becomes positive, which means that the divergence of the magnetic field lines starts in the sense of average. Thus, the time t_d is recognized as the decorrelation time of the stochastic magnetic field lines. Judging from figures 2b-2d, the simple analytical model expression of $\langle l_e(t)\rangle$ may be introduced as

$$\langle l_e(t)\rangle = \langle l_e\rangle \left(1 - \frac{t_d}{t}\right), \tag{56}$$

where $\langle l_e\rangle$ is the asymptotic value of $\langle l_e(t)\rangle$. By fitting the above expression to the numerically obtained one, the asymptotic value $\langle l_e\rangle$ is determined. The fitting curves are shown in figures 2b-2d by dotted lines, where good agreement between the numerical data and the model expression is seen. It may be concluded from this good fitting that the time independent effective radial Liapunov exponent is indeed asymptotically obtained, namely, in the infinite time limit, as is indicated by equation (53). Thus, it is useful to introduce such a finite time t_s that indicates how the system is near a final relaxed state. In the present case, such the time t_s is defined as $\langle l_e(t_s)\rangle/\langle l_e\rangle = 0.9$, namely, $t_s = 10 \times t_d$ from equation (56). Note that t_s depends only on t_d, once the ratio $\langle l_e(t)\rangle/\langle l_e\rangle$ is determined. The time t_s is also interpreted as an indicator of the relaxation of the effective radial Liapunov exponent. Times t_d and t_s, and the estimated $c\langle l_e\rangle$ are denoted in figures 2 and 3, and are summarized as

$$\begin{aligned} &t_d = 1.2 \times 10^{-4}\text{s}, t_s = 10 \times t_d, c\langle l_e\rangle = 5.4 \times 10^{-3}, \text{ for } s_b/s_{bc} = 1.3, \\ &t_d = 2.0 \times 10^{-5}\text{s}, t_s = 10 \times t_d, c\langle l_e\rangle = 3.7 \times 10^{-2}, \text{ for } s_b/s_{bc} = 3.3, \end{aligned} \tag{57}$$

$$t_d = 1.8 \times 10^{-6}\mathrm{s}, t_s = 10 \times t_d, c\langle l_e \rangle = 4.5 \times 10^{-1}, \text{ for } s_b/s_{bc} = 33,$$

Note that the larger s_b/s_{bc} is, the shorter t_d, t_s, $t_s - t_d$ become, and the larger $\langle l_e \rangle$ is. Moreover, by assuming $\langle \ln d(t) \rangle \approx \ln \langle d(t) \rangle$, from the equations (45), (46) and (56),

$$\langle d(t) \rangle \approx \langle d(0) \rangle e^{\langle l_e \rangle (t - t_d)}. \tag{58}$$

is obtained. This relation means that the averaged distance $\langle d(t) \rangle$ between two initially neighboring trajectories exponentially grows after $t = t_d$. As one of the measures of the uniformity, the dispersion of the effective radial Liapunov exponent around the mean value is defined as

$$\Delta l_e(t) = \frac{\sqrt{\langle l_e(t)^2 \rangle - \langle l_e(t) \rangle^2}}{\langle l_e(t) \rangle}. \tag{59}$$

The dispersion monotonically decreases with time after $t = t_d$. For $s_b/s_{bc} = 1.3$ and 3.3, $\Delta l_e(t)$ has a tendency to saturate to a finite value, namely, $\Delta l_e(t \approx t_s) = 0.99$ and 0.27, respectively. However, $\Delta l_e(t)$ tends to become zero for $s_b/s_{bc} = 33$, and $\Delta l_e(t \approx t_s) = 0.093$. This tendency leads to interpretation that the uniform exponential divergence of magnetic field lines is obtained as s_b/s_{bc} increases.

On the other hand, as is shown in figures 3a-3d, approximately $0\%, 82\%, 98\%$, and 100% of magnetic field lines have a positive radial Liapunov exponent for $s_b/s_{bc} = 0.33, 1.3, 3.3$, and 33, respectively. The existence of magnetic field lines with a non-positive Liapunov exponent for $s_b/s_{bc} = 0.33, 1.3$, and 3.3 is related to regular structures in the destroyed magnetic field region. As long as the test magnetic field lines are stuck to the regular structures (e.g. island like structures) or around them (e.g. separatrix regions), freely wandering of the magnetic field lines, which is a characteristic of magnetic field lines in the irregular regions, is prohibited, leading to the negative or zero radial Liapunov exponent. For example, the mentioned very slow increase of $\langle l_e(t) \rangle$ and $N_p(t)$ with time in the region of overlapping threshold, $s_b/s_{bc} = 1.3$, can be associated with the fact that approximately 20% of magnetic field lines are prevented from wandering by sticking to regular structures at $t > t_d$. Additional confirmation is obtained from the Poincare sections. Roughly, the part of magnetic field lines, which is started from flux surface with $q = 3/2$ and is stuck to island like structure around $q = 3/2$ for $t < t_d$, can wander into the region around $q = 11/7$ after $t \approx t_d$, and at $t \approx t_s$ wandering into the region $q = 10/7$ starts. Thus, being temporary stuck to regular structures, the magnetic field lines need long time to experience all allowable bounded destroyed region, and the tendency of $\langle l_e(t) \rangle$ and $N_p(t)$ to saturate becomes slow.

As it is clear from the above argument, even if the overlapping condition of magnetic islands is satisfied ($s_b/s_{bc} \geq 1$), the statistical treatment of the magnetic field stochasticity is meaningless before $t = t_d$. From figures 3a-3d it is seen that the number of the magnetic field lines with positive Liapunov exponent becomes constant before $t = t_s (> t_d)$ for $s_b/s_{bc} = 3.3$, and 33, and almost constant for $s_b/s_{bc} = 1.3$. Since the magnetic field lines with positive Liapunov exponent have similar expanding properties, once the number of magnetic field lines with positive Liapunov exponent becomes nearly

constant, the statistical properties of the magnetic field stochasticity are considered not to change, but to become uniquely clear at least qualitatively. Hence, the statistical properties of the magnetic field stochasticity are mainly examined after the number of the magnetic field lines with positive Liapunov exponent becomes constant, namely after $t = t_s$, in order to save the computational time. In the following calculations, this condition is satisfied for $s_b/s_{bc} = 3.3$, and 33, and it is weakly satisfied for $s_b/s_{bc} = 1.3$.

4.1.2. Type of diffusive behaviour The case with isolated magnetic field irregularities ($s_b/s_{bc} = 0.33$) is characterized by the oscillatory behaviour of the second cumulant $C_2(t)$ around 2×10^{-5} and the diffusion exponent α around 0. Those oscillatory behaviours come from regular motions.

In figure 4 the time developments of the second cumulant in the region of global stochasticity ($s_b/s_{bc} \geq 1$) are shown for $s_b/s_{bc} = 1.3$ (solid line), for $s_b/s_{bc} = 3.3$ (dashed line), and for $s_b/s_{bc} = 33$ (dotted line), respectively. Note that C_2 for $s_b/s_{bc} = 1.3$ is enlarged by the factor 4. After the transient phase ($t > t_d = t_s/10$), the second cumulants gradually increase. This behaviour is completely different from that of the Wiener process shown in figure 2 in [19]. The corresponding diffusion exponent α, two types of diffusion coefficient $D(t), D_{pw}(t)$, and the relative difference $\Delta D(\%)$ in the long time limit ($t > t_s$) are shown in tables 1 and 2 (the corresponding row is indicated by $\nu/\nu_t = 0 (v_{d\perp} = 0)$). In the case of $s_b/s_{bc} = 1.3$ with regular structures in the stochastic region, the diffusion exponent α is fairly less than unity, but finite. Thus, it is understood that the radial magnetic field diffusion behaves as subdiffusive. In this case, the relative difference $\Delta D(\%)$ given by equation (40) between $D(t)$ given by equation (37) and $D_{pw}(t)$ given by equation (38) is not so large. The power-law approximation of the diffusion coefficient is not so wrong. However, as s_b/s_{bc} increases, e.g., $s_b/s_{bc} = 3.3$ or 33, this difference becomes quite large, and the diffusion exponent becomes significantly small. Thus, the radial magnetic field diffusion is considered to be non-diffusive.

After the overlapping of the magnetic islands, as s_b/s_{bc} increases, the type of diffusive behaviour changes from subdiffusivity to non-diffusivity in the long time limit. This tendency is natural in the considered magnetic field. The stochastic magnetic field considered here is bounded in the radial direction, namely outside of the stochastic region KAM surfaces exist. Thus, the maximum relative radial displacement $|\delta r(t) - \langle \delta r(t) \rangle|_{max}$ in the duration of the calculation is bounded by $w_{st}/2$ for each field line. Moreover, as s_b/s_{bc} increases, the magnitude of the average Liapunov exponent $\langle l_e \rangle$ rapidly increases as is shown in figure 2, so that majority of magnetic field lines reach the boundary of the stochastic region in a short time. Hence $C_2(t)$ rapidly increases up to the order of the bounded value $(w_{st})^2/12$, which means the non-diffusive behaviour in the long time limit. Indeed as is shown in figure 4, $C_2(t)$ for $s_b/s_{bc} = 3.3$ and 33 is of the order of $(w_{st})^2/12$ after $t = t_d$. In the long time limit, $C_2 \approx (w_{st})^2/16$ for $s_b/s_{bc} = 3.3$ and $C_2 \approx (w_{st})^2/12$ for $s_b/s_{bc} = 33$. Note that the non-locality of the trajectories leads to sub- or non-diffusivity. The situation of the radial particle diffusion in the regular magnetic field

investigated in [19] is completely different. Although the system is bounded by the minor radius a, the relative radial displacement $\delta r(t) - \langle \delta r(t) \rangle$ is significantly small compared with a because of the quite small radial drift width, so that the particles never reach the plasma boundary in the observation duration, or the particles can not recognize the existence of the boundary. Therefore, the locality of particle diffusion is ensured and the relative radial displacement can act as $\delta r(t) - \langle \delta r(t) \rangle \sim \sqrt{\nu t} c$ (c is positive constant) by the collisional effect, leading to the normal diffusion.

4.1.3. Autocorrelation coefficient The oscillatory behaviour of $A(t, \tau)$ with respect to τ is one of characteristics of the dynamical motions in the region of isolated island chain with $s_b/s_{bc} = 0.33$.

In figure 5, the autocorrelation coefficients $A(t, \tau = t' - t)$ vs τ/t_s are plotted at $t = 0.56\, t_s$ for $s_b/s_{bc} = 1.3$ (solid line), for $s_b/s_{bc} = 3.3$ (dashed line), and for $s_b/s_{bc} = 33$ (dotted line), respectively. The reminiscent oscillatory pattern on the power-law like envelope for $s_b/s_{bc} = 1.3$ (where overlapping between islands has just been started (figure 1b)) is the indication of the relative importance of the regular motion inside the stochastic region. It is indicated by P_{osc} in table 3. As s_b/s_{bc} increases, this oscillatory behaviour of $A(t, t')$ vanishes, and a stationary power-law like behaviour appears. For $s_b/s_{bc} = 3.3$, this stationary power-law like behaviour can be fitted as

$$A(t, t') \approx A(\tau) \approx \tau^{-0.87}, \tag{60}$$

for large τ (figure 5, dashed line), and is indicated by P_{st} in table 3.

In the presence of stochastic sea without structures ($s_b/s_{bc} = 33$), the exponentially fast vanishing autocorrelation coefficient (denoted by E in table 3) is obtained (figure 5, dotted curve). Note that τ is normalized by t_s. Since the autocorrelation coefficient has been found to be independent of the starting time t, it may be expressed as

$$A(t, t') \approx A(\tau) \approx \exp\left(-\frac{\tau}{\tau_{corr}}\right), \tag{61}$$

where τ_{corr} is the autocorrelation time. The numerically evaluated τ_{corr} is around 2.4×10^{-6}s. This time corresponds to t_d given by equation (57).

According to figure 5 and the above discussion, as s_b/s_{bc} increases, the time correlations are lost faster, and the tendency of $A(t, t')$ to be stationary becomes stronger. For $s_b/s_{bc} \geq 1$, as it is shown in figure 3, some of magnetic field lines have a negative Liapunov exponent, which means that those field lines stick on the regular structures inside the stochastic region as mentioned in section 4.1.1. This sticking may be related with the slow power-law like decay of $A(t, t')$ without the autocorrelation time. As s_b/s_{bc} increases more ($s_b/s_{bc} \gg 1$), regular structures disappear, so that all of the magnetic field lines have a positive Liapunov exponent as is shown in figure 3d and the effective radial Liapunov exponent has an almost time independent positive value in the long time limit with $t \geq t_s$. Since relative dispersion of the effective radial Liapunov exponent is small: $\Delta l_e(t) \approx 0.093$, all magnetic field lines have time-independent similar magnitude of the Liapunov exponent in the average sense. In other words, it is connected

with ergodicity of the magnetic field lines. Hence, the autocorrelation coefficient $A(t,t')$ may become independent of time, namely stationary: $A(t,t') = A(\tau = t' - t)$, and shows an exponentially fast decay with the autocorrelation time $\tau_{corr} \sim t_d$, after which the time correlation vanishes,

4.1.4. Cumulant coefficients Although the first cumulants C_1 show complicate temporal behaviours depending on s_b/s_{bc}, the magnitude normalized by the minor radius is always quite small independent on s_b/s_{bc}, as is indicated in table 4 for the long time limit.

Before island overlapping with $s_b/s_{bc} < 1$, as well as C_1 and C_2, both the skewness γ_3 and kurtosis γ_4 show oscillatory behaviours in time around $\gamma_3 \sim 0$ and $\gamma_4 \sim -0.4$, reflecting the regular motions in the magnetic islands.

After the overlapping with $s_b/s_{bc} \geq 1$, such oscillatory behaviours in time disappear, and the radial distribution of the stochastic magnetic field lines or particles strongly tied to them is completely different between the state near island overlapping threshold with $s_b/s_{bc} \sim 1$ and the more stochastic state with $s_b/s_{bc} > 1$. Near the threshold of island overlapping, both the skewness γ_3 and kurtosis γ_4 rapidly increase in the ballistic phase corresponding to the time $t < t_d$, and gradually decrease keeping the values positive, as is indicated in figures 6 and 7 by solid lines. Thus, the radial distribution is a peaked profile compared with Gaussian, and also the distribution has an asymmetric tail extending out towards $\delta r > \langle \delta r \rangle$, which is consistent to the Poincare plot shown in figure 1b.

In the moderate overlapping case with $s_b/s_{bc} > 1$, sticking of the magnetic field lines to O-points and around X-points of the magnetic island chain near the flux surface, from which magnetic field lines are started, is fairly released as is shown in figure 1c. Thus, except for such sticking regions and inside of the magnetic islands with different helicity, the Poincare plots of the field lines are almost uniform. Reflecting the results of the Poincare plots, the kurtosis γ_4 has a tendency to reach the values similar to the uniform mixing process: $\gamma_4 = -6/5$, as is shown in figure 7 by the dashed line. As s_b/s_{bc} increases more, the uniformity of the Poincare plots becomes stronger as is shown in figure 1d, so that within the ballistic phase ($t < t_d$), the kurtosis γ_4 almost reaches the value of the uniform mixing process, as is indicated in figure 7 by the dotted line. The skewness γ_3 of the moderate or highly overlapping case takes a small negative value within ballistic phase, and keeps the sign and the magnitude unchanged after $t = t_d$, as is shown in figure 6 by dashed and dotted lines. Thus, in these cases, the radial distribution of the stochastic magnetic field or particles strongly tied to them is fairly or almost the uniform distribution with a small asymmetric tail towards $\delta r < \langle \delta r \rangle$.

4.1.5. Type of statistical process Judging from the criteria given by equations (49) and (55), in the partially destroyed magnetic field structure with mixture of regular and irregular regions ($s_b/s_{bc} \geq 1$), the magnetic field stochasticity appears in the long time limit with $t > t_s$ or $t \gg t_d$ as a strange diffusive process: subdiffusive or non-

diffusive, profile neither Gaussian nor uniform, and statistically non-stationary or almost stationary process. This strange diffusive process is symbolized by S in table 7. As s_b/s_{bc} increases, the autocorrelation coefficient changes from oscillatory for $s_b/s_{bc} = 1.3$ to stationary power-law like behaviour given by equation (60) for $s_b/s_{bc} = 3.3$. Thus, in order to distinguish these properties, S_{osc} and S_{st} are used in table 7, respectively.

When $s_b/s_{bc} \gg 1$, the magnetic stochasticity in the long time limit with $t \gg \tau_{corr} \approx t_d$ appears as a uniform mixing process (equation 55): non-diffusive, uniform, Markov, statistically stationary process with exponentially vanishing autocorrelation coefficient. It is denoted by symbol U in table 7. Note that the criterion of the skewness γ_3 is violated for uniform mixing process: $\gamma_3 = -0.13 < (-0.1)$ in table 5. This deviation of γ_3 from the uniform mixing process comes from inhomogeneity of the system: the asymmetry of the system due to a fairly wide ($w_{st}/a \approx 0.24$) stochastic region in the circular bounded cross section and a not so small equilibrium magnetic shear. However, this asymmetry indicated by γ_3 looks like not affecting other statistical properties, thus the highly overlapping case with $s_b/s_{bc} = 33$ is treated as a uniform mixing process.

The question about Markovianity remains open. The Markovian approximation is justified whenever the correlations are rapidly lost during the relaxation of the system [7, 24]. In the present case, the Markov approximation is applicable only to the case with highly developed magnetic field stochasticity ($s_b/s_{bc} \gg 1$) in the long time limit. In the partially destroyed magnetic field structure with mixture of regular and irregular domains ($s_b/s_{bc} \geq 1$), however, the non-uniform particle distribution, and power-law like or oscillatory like behaviour of the autocorrelation coefficient indicate that the space-time correlations remain in the long time limit $t > t_s$. Thus, from the statistical point of view, it is considered that obstruction of the uniform mixing by sticking of test magnetic field lines to the local regular structures or around them leads to non-Markovianity.

4.2. Collisionless drift decorrelation

In section 4.1, the statistical properties of the magnetic field are examined from the view point of the radial displacement. As is mentioned in section 4.1, those properties are interpreted as the statistical properties of the radial particle diffusion without both the perpendicular drift motion and Coulomb collision. In this section, the influences of the perpendicular drift motion on the statistical properties of the radial particle diffusion without Coulomb collision are investigated. For such purposes, equations (6)-(9) are solved in the stochastic magnetic field considered in section 4.1 without Coulomb collision, under the initial conditions mentioned in section 2.3.

Even if the Coulomb collision does not exist, the particle can move from one magnetic field line to another due to the perpendicular drift motion. This effect is called the collisionless drift decorrelation from the magnetic field line. However, since the drift velocity perpendicular to the magnetic field lines is much smaller than the parallel velocity, effects due to drift motion across magnetic field lines on the statistical properties are considered to be small. Indeed, although quantitative

differences exist as shown in tables (1)-(7), qualitative differences are not seen except for the autocorrelation coefficient for $s_b/s_{bc} = 33 \gg 1$. In figure 8, the autocorrelation coefficients $A(t, \tau = t' - t)$ vs time interval τ/t_s are drawn for several starting times t: $t = (2.7 \times 10^{-3}, 0.74 \text{ and } 3.3)t_s$. Although the autocorrelation coefficients exponentially vanish independent of the starting time, a finite correlation $A(t, t') \approx 0.05$ is recovered after the correlation time $\tau > \tau_{corr}$, when the starting times are taken as large as $t > \tau_{corr}$. It is denoted by E_{corr} in table 3 and U_{corr} in table 7. Due to the perpendicular drift, the particles are redistributed compared with case without drift. However, the physical reason of the finite correlations is not clear.

As summary, although quantitative differences (and qualitative differences in the limited range of parameter s_b/s_{bc}) exist, the statistical properties of the radial diffusion without Coulomb collision are determined by those of the stochastic magnetic field.

4.3. Particle radial diffusion in the presence of both magnetic and collisional stochasticity

The statistical properties of the particle radial diffusion in the presence of the magnetic field stochasticity without Coulomb collisions have been examined in 4.1 (without perpendicular drift motion) and 4.2 (with them), respectively. In this section the statistical properties of the radial particle diffusion in the presence of both magnetic field and collisional stochasticities are considered. The same magnetic configurations as in sections 4.1 and 4.2 are used. Three cases of collisionality are chosen to be $\nu/\nu_t = 0.45, 4.5$, and 45, where $\nu_t = 2.21 \times 10^6 \text{s}^{-1}$ is the transit frequency of passing particles defined in the equilibrium magnetic field [19]. Thus, $\nu/\nu_t = 0.45$ corresponds to plateau collisionality regime, and $\nu/\nu_t = 4.5$, and 45 correspond to Pfirsch-Schlüter collisionality regime, respectively.

When the global magnetic stochasticity has not been developed ($s_b/s_{bc} < 1$), the particle radial diffusion is governed by the collisional stochasticity. In the collisionless limit the test particles started inside the islands are prevented from escaping there into the regular KAM regions. Thus, the trapped particles inside islands execute periodic motion as long as they are tied to the magnetic field line. The characteristic time of this motion around O-point is estimated to be $t_b \approx 2\tau_t \approx 8.7 \times 10^{-7}$s, where $\tau_t = \nu_t^{-1} = 4.35 \times 10^{-7}$s is the characteristic time of passing particle motion [19]. Thus, the long time limit in the presence of collisions is determined by

$$t \gg \max(\tau_c, \langle t_b \rangle), \tag{62}$$

where $\tau_c = \nu^{-1}$ is the collisional characteristic time and $\langle t_b \rangle = 1.8 t_b = 1.6 \times 10^{-6}$s is the averaged time of t_b, which is obtained by simple approximation of the motions in the magnetic islands as one dimensional pendulum. The ratios of $\langle t_b \rangle$ to τ_c are shown in table 8 for $s_b/s_{bc} = 0.33$. Since $\langle t_b \rangle > \tau_c$, the long time limit for $s_b/s_{bc} = 0.33$ is defined as $t \gg \langle t_b \rangle$.

In the region of global magnetic stochasticity with $s_b/s_{bc} \geq 1$ the relaxation time of the effective radial Liapunov exponent, t_s (section 4.1.1) is compared with the collisional

characteristic time, and the long time limit is defined as

$$t \gg \max(\tau_c, t_s) \tag{63}$$

The ratios of t_d to τ_c are shown in table 8 for $s_b/s_{bc} = 1.3, 3.3$, and 33, respectively. Because of $t_s > t_d > \tau_c$, the long time limit for these cases is defined as $t \gg t_s$. However as well as the magnetic field structure in 4.1, once $t > t_s$ is satisfied, the statistical properties do not change qualitatively. Thus, to save computational time, the long time limit is treated as $t > t_s$.

4.3.1. Type of diffusive behaviour The collisional effects on the second cumulant (the mean square displacement) $C_2(t)$ are shown in figure 9, (a) for $s_b/s_{bc} = 0.33$, (b) for $s_b/s_{bc} = 1.3$, (c) for $s_b/s_{bc} = 3.3$, and (d) for $s_b/s_{bc} = 33$, respectively. Before the island overlapping ($s_b/s_{bc} = 0.33$), $\langle l_e(t) \rangle$ is always negative as is discussed in 4.1. When the collisions are absent , $C_2(t)$ shows a superdiffusive phase due to the ballistic motion in the early time ($t < t_d$), where the maximum of C_2 becomes of the order of that in the corresponding uniform mixing process: $C_2^{uniform} = (w_{2,3})^2/12 \sim 4.8 \times 10^{-5}$. After such the superdiffusive phase, $C_2(t)$ decreases and oscillates around a constant value, because of stickness to the regular structures inside of the magnetic islands ($\langle l_e(t) \rangle$ is always negative). When the collisions are introduced, such the superdiffusive phase and oscillatory behaviour are suppressed because of $\tau_c < \langle t_b \rangle$ as is shown in table 8, and C_2 comes to monotonically increase in time. As the collision frequency increases, the diffusive behaviour in the long time limit changes from subdiffusive for $\nu/\nu_t = 0.45$ to normal diffusive for $\nu/\nu_t = 4.5$ and 45 as is shown in table 1, and the magnitude of the diffusion coefficient decreases up to the level of the neoclassical diffusion in the regular magnetic field, independent of the definition of the diffusion coefficient, as is indicated in table 2. The magnetic structure before overlapping considered here has both magnetic islands with small widths and quite tiny stochastic region around the separatrix. Thus, when the Coulomb collisions are fairly frequent ($\tau_c \ll \langle t_b \rangle$), particle orbits scattered by the collisions can not follow the magnetic field lines inside of small magnetic islands and of tiny stochastic region, leading to the normal diffusion with the magnitude similar to that in the neoclassical diffusion. As the collision frequency decreases ($\tau_c < \langle t_b \rangle$), particles can trace the magnetic field lines, which may lead to the subdiffusivity reflecting magnetic field structures. Note that the change of the magnitude of C_2 with respect to ν/ν_t is not monotonic. Since this behaviour becomes more clear for $s_b/s_{bc} = 1.3$, the reason is considered there.

Near the threshold of the island overlapping ($s_b/s_{bc} = 1.3$), the behaviour of C_2, and so, the behaviour of the diffusion exponent and the diffusion coefficient, are qualitatively similar to those before the island overlapping ($s_b/s_{bc} = 0.33$), as are shown in figure 9(b), and tables 1 and 2, namely with increasing in the collision frequency, type of diffusivity changes from the subdiffusive for $\nu/\nu_t = 0.45$ to the normal diffusivity for $\nu/\nu_t = 4.5$ and 45. As is similar to the case before overlapping, the change of the magnitude of C_2 with respect to ν/ν_t is not monotonic. In the absence of the Coulomb collision, a

superdiffusive phase due to ballistic motion exists in the early time ($t < t_d$) as well as before overlapping, where $\langle l_e(t)\rangle$ is negative and the maximum of C_2 becomes the order of that in the corresponding uniform mixing process: $C_2^{uniform} = (w_{st})^2/12 \sim 6.6 \times 10^{-4}$. After decreasing, $C_2(t)$ increases in time with oscillatory behaviour because $\langle l_e(t)\rangle$ becomes positive and the number of field lines with positive radial Liapunov exponent $N_p(t)$ increases with time as is seen in figures 2 and 3. When weak collisions with $\nu/\nu_t = 0.45$ are introduced, such the superdiffusive phase and oscillatory behaviour disappear according to $\tau_c < t_d$ as shown in table 8, and the magnitude of $C_2(t)$ decreases. This phenomenon is due to the interruption of the parallel free streaming by the pitch angle scattering. Since the mean free path is still long ($\lambda_{mfp} = v_{||}\tau_c \sim 32$m), however, the subdiffusivity due to the magnetic field is still strong. As the collision frequency increases more ($\nu/\nu_t = 4.5$), according to the reduction of the mean free path ($\lambda_{mfp} \sim 3.2$m), the subdiffusive properties and the magnitude of $C_2(t)$ are more reduced. When the collision frequency becomes extremely large ($\nu/\nu_t = 45$), the mean free path becomes considerably short ($\lambda_{mfp} \sim 0.32$m), so that the diffusion due to the stochastic magnetic field is lost and the normal diffusion due to the pitch angle scattering appear. This collisional effect is understood in terms of the Kolmogorov length defined as $L_K = v_{||}/\langle l_e\rangle$. From this equation, the relative average radial displacement of the stochastic magnetic field lines Δd in the duration of the collision time τ_c after $t = t_d$ is expressed as

$$\Delta d \equiv \frac{\langle d(t+\tau_c)\rangle - \langle d(t)\rangle}{\langle d(t)\rangle} \sim \mathrm{e}^{\lambda_{mfp}/L_K} - 1. \tag{64}$$

In the case with $s_b/s_{bc} = 1.3$, as is shown in figure 2b, $\langle l_e\rangle c$ is the order of 5.4×10^{-3}, so that $\Delta d \sim \lambda_{mfp}/L_K \ll 1$, namely the relative average radial displacement of the stochastic magnetic field lines in the duration of the collision time is too small in the range of the collision frequency considered here, and the radial displacements due to collisions themselves become significant as ν increases. In the weak stochastic magnetic field with $s_b/s_{bc} \leq 1$, infrequent collisions reduce the mean square displacement C_2, however, frequent collisions enhance it in the long time limit.

In the moderate overlapping case with $s_b/s_{bc} = 3.3$, when the collision is absent, the mean square displacement C_2 becomes as large as the corresponding uniform mixing level in the early superdiffusive phase: $C_2^{uniform} = (w_{st})^2/12 \sim 2.4 \times 10^{-3}$. After that, C_2 does not decreases so much, but hold the level in the interval of $t < t_d$, where the effective radial Liapunov exponent $\langle l_e\rangle$ is still negative. Since the magnetic field is considerably stochastic compared with those for $s_b/s_{bc} \leq 1$, field lines or particles with only parallel drift spreading in the superdiffusive phase are considered not to return near the original position. After $t = t_d$, the effective radial Liapunov exponent becomes positive, and both $\langle l_e\rangle$ and the number of field lines with $\langle l_e\rangle > 0$ increase, so that C_2 gradually increases keep the level of the uniform mixing process. Weak collisions with $\nu/\nu_t = 0.45$ do not disturb so much the radial diffusion due to magnetic field stochasticity, because $\langle l_e\rangle c$ is larger than that for $s_b/s_{bc} = 1.3$ by one order of magnitude as is understood from figure 2, so that the relative average radial displacement of the stochastic magnetic field lines

in the duration of the collision time is fairly large, e.g., $\Delta d \sim 0.45$ for $\langle l_e \rangle c = 3.7 \times 10^{-2}$. Hence, subdiffusivity stemming from the magnetic field stochasticity remains, and the level C_2 is in the range of the uniform mixing process. When the collision frequency increases as $\nu/\nu_t = 4.5$ and 45, Δd decreases and the property of subdiffusivity is gradually lost, and finally the normal diffusivity appears, as is shown in table 1. In the range of the collision frequency considered here, the magnitude of C_2 monotonically decreases as the collision frequency increases.

In the highly overlapped case with $s_b/s_{bc} = 33$, as well as the moderate overlapping, the mean square displacement C_2 becomes as large as the uniform mixing level in the early superdiffusive phase: $C_2^{uniform} = (w_{st})^2/12 \sim 5.2 \times 10^{-3}$. Since the stochastic magnetic field has no regular structures, t_d is quite small, and all of magnetic field lines have positive Liapunov exponent in a short time as is seen in figure 2, then C_2 becomes almost constant with the level of uniform mixing process except for the small oscillatory behaviour. The relative average radial displacement of the stochastic magnetic field lines in the duration of the collision time Δd is 89., 0.58, and 4.7×10^{-2} for $\nu/\nu_t = 0.45, 4.5$, and 45, respectively. Thus, the collisional effects are so weak that the process always shows subdiffusivity due to the magnetic field stochasticity in the range of the collision frequency considered here, and the magnitude of C_2 monotonically decreases as the collision frequency increases.

4.3.2. Autocorrelation coefficients The effect of collisions on the autocorrelation coefficient $A(t, t')$ is shown in figures 10a-d: (a) for $s_b/s_{bc} = 0.33$, (b) for $s_b/s_{bc} = 1.3$, (c) for $s_b/s_{bc} = 3.3$, and (d) for $s_b/s_{bc} = 33$, respectively. In each figure, the autocorrelation coefficients $A(t, t') = A(t, \tau = t' - t)$ are plotted as the functions of the normalized time interval between the ending time t' and the starting time t: $\tau = (t' - t)/\langle t_b \rangle$ for $s_b/s_{bc} = 0.33$ and τ/t_s for $s_b/s_{bc} = 1.3, 3.3$, and 33, respectively. Two starting times $t = t_1$ and $t = t_2$ are specified. The starting time $t \equiv t_1$ corresponds to the early time: $t = 3.1 \times 10^{-3} \langle t_b \rangle$ for $s_b/s_{bc} = 0.33$, $t = 8.3 \times 10^{-4} t_s$ for $s_b/s_{bc} = 1.3$, $t = 2.5 \times 10^{-4} t_s$ for $s_b/s_{bc} = 3.3$, and $t = 2.8 \times 10^{-3} t_s$ for $s_b/s_{bc} = 33$; and the starting time $t = t_2$ corresponds to the late time: $t = 41. \langle t_b \rangle$ for $s_b/s_{bc} = 0.33$, $t = 0.56\, t_s$ for $s_b/s_{bc} = 1.3$, $t = 0.56\, t_s$ for $s_b/s_{bc} = 3.3$, and $t = 1.51 t_s$ for $s_b/s_{bc} = 33$. The dashed, dot-dashed, and dotted curves correspond to $\nu/\nu_t = 0.45, 4.5$, and 45, respectively and the corresponding Wiener cases are drown by solid curves. As the collision frequency ν/ν_t increases, independent of s_b/s_{bc}, the autocorrelation coefficient $A(t, \tau)$ has a tendency to become non-stationary power law like, whose values for a fixed t and τ are smaller than those of the corresponding Wiener process in the range of the collision frequency considered here. When the collision frequency ν/ν_t increases and s_b/s_{bc} decreases, $A(t, \tau)$ finally becomes Wiener like. In table 3, the types of the behaviour of $A(t, \tau)$ as a function of t and τ are indicated, where P_W means that the behaviour of $A(t, \tau)$ is well approximated by the Wiener process in the whole starting time or in the long time limit, and P_f indicates the above mentioned power-law like behaviour. These properties are understood as follows.

Statistical properties of the particle radial diffusion

The numerator of the autocorrelation coefficient $A(t,t')$ is expressed as

$$\begin{aligned}&\langle(\delta r(t)-\langle\delta r(t)\rangle)(\delta r(t')-\langle\delta r(t')\rangle)\rangle \sim \langle\delta r(t)\delta r(t')\rangle \\ &= \langle\delta r(t)^2\rangle + \langle(\delta r(t')-\delta r(t))\delta r(t)\rangle, \quad \text{for} \quad t'>t, \end{aligned} \tag{65}$$

where the first cumulant $C_1(t) = \langle\delta r(t)\rangle$ is neglected, because it is quite small as indicated in table 4. Thus, the starting time t appearing in $A(t,\tau)$ is interpreted as the common time interval between two trajectories $\delta r(t)$ and $\delta r(t')$ for $t' > t$. In the case of the Wiener process, as is understood from equation (47), the radial displacement is a superposition (time integration) of completely independent events created by the white noise. In this context, the pitch-angle scattering acts as the white noise (although both the pitch-angle scattering frequency and the width of perpendicular particle drifts determine the magnitude of the correlation of the white noise). Therefore, the correlation without common time interval vanishes, namely, $\langle(\delta r(t')-\delta r(t))\delta r(t)\rangle = 0$ in the above equation. In other words, the correlation is created within the common time interval t. For a fixed τ, the longer such the common time interval t becomes, the more the correlation persists. This property of the Wiener process is one of the characteristics of the particle radial diffusion by the Coulomb collision in the regular magnetic field [19], and is closely related to the locality of the particle orbits and particle diffusion in the radial direction. Partially because the drift width is quite small compared with the system size, and partially because the accumulation of small pitch-angle scatterings created in the velocity space gradually change the particle radial drift motions, the locality of the radial diffusion is ensured. Thus,the correlation indicating that the constituents of the particle ensemble stays near each other between two different times is increased, as the common time interval t or the starting time of $A(t,\tau)$ increases for a fixed τ.

On the other hand, the stochastic magnetic field in the radially bounded region shows the uniform mixing properties when $s_b/s_{bc}(\geq 1)$ increases, as discussed in 4.1. In these cases, the stochasticity of the magnetic field lines is characterized by the positive radial effective Liapunov exponent $\langle l_e\rangle(>0)$, namely the ensemble of field lines or particles tied to the magnetic field lines have a tendency to exponentially spread in the radial direction. Thus, the knowledge that the field lines or particles stay near to each other is easily lost even if the common time interval t is large, so that the correlation between stochastic field lines or particle trajectories, comes to be rapidly lost independent of the common time interval or starting time t. As $s_b/s_{bc}(\geq 1)$ increases, the autocorrelation coefficient has a tendency to be reduced faster with stationary form: $A(t,\tau) \sim A(\tau)$. Note that the parallel motion of particles along stochastic magnetic field lines leads to the decorrelation in the radial direction. In other words, the non-locality of the radial displacements due to the stochastic magnetic field lines makes fast loss of the correlations or fast decorrelation in the radial direction.

When the collisions are introduced to the particle radial diffusion in the stochastic magnetic field, the fast radial spreading of the particles along the perturbed field lines is interrupted. As a result, particles can stay nearer compared with the case

without collisions, which means that the fast loss of the correlations by the stochastic magnetic field is suppressed by the Coulomb collisions. The fact that the Coulomb collisions suppress the decorrelation due to the magnetic field stochasticity appears as the non-stationary power-law like behaviour of the autocorrelation coefficient. As s_b/s_{bc} increases, such the collisional suppression of the decorrelation is reduced, since $\langle l_e \rangle \tau_c = \lambda_{mfp}/L_K$ increases, where $\lambda_{mfp} = v_{||}\tau_c$ and $L_K = v_{||}/\langle l_e \rangle$ are the mean free path and the Kolmogorov length, respectively. Note that the Coulomb collisions themselves do not make the correlation, but suppress the decorrelation by the stochastic magnetic field. In the case of the neoclassical particle radial diffusion, perpendicular particle drifts are decorrelated by the Coulomb collisions, and superposion of such random events leads to the Wiener process according to the central limit theorem [22]. In contrast with it, in the particle diffusion in the highly stochastic magnetic field, parallel particle drift along stochastic magnetic field lines leads to the decorrelation in the radial direction, and Coulomb collisions suppress such the decorrelation through the scattering of the parallel particle drift.

In figures 11a,b, $A(t,\tau)$ vs τ/t_s for $s_b/s_{bc} = 3.3$ is plotted by solid curve with respect to various starting times: (a) for $\nu/\nu_t = 0.45$, and (b) for $\nu/\nu_t = 45$, respectively. The corresponding $A(t,\tau)$ of the Wiener process is also drawn by dashed curve. The starting time is chosen as $t = (2.5 \times 10^{-4}, 6.2 \times 10^{-2}, ..., 0.56)\, t_s$. It is quite clear that the $A(t,\tau)$ becomes that of the Wiener process, as ν/ν_t increases.

4.3.3. Cumulant coefficients As is shown in table 4, the convective effect indicated by C_1 is quite weak independent of both s_b/s_{bc} and ν/ν_t. Although the values of C_1 are larger that those in the neoclassical cases in [19], they are still too small compared with the minor radius a (C_1 is normalized by a).

As is mentioned in section 2, the both non-vanishing skewness γ_3 and kurtosis γ_4 indicate the deviation of the particle distribution from a Gaussian profile, and $\gamma_4 = -6/5$ corresponds to the uniform mixing process.

Before the island overlapping with $s_b/s_{bc} < 1$, the oscillatory behaviours coming from the particle regular motions, observed in the case without Coulomb collisions, are suppressed by the Coulomb collisions. Since the particle radial displacements stemming from the isolated magnetic island chain are quite small (particles are initially loaded at the corresponding rational surface), the radial displacements are mainly governed by the Coulomb collisions, leading to the distribution with vanishing both γ_3 and γ_4 (tables 5 and 6). Note that the vanishing of the skewness and kurtosis together with the previously mentioned normal diffusivity (section 4.3.1) and the Wiener like autocorrelation coefficient (section 4.3.2) for $\nu/\nu_t = 4.5$ and 45 means that the particle distribution is Gaussian according to the criterion given by equation (49).

In the highly overlapping case with $s_b/s_{bc} \gg 1$, the scattering due to the Coulomb collision of the parallel particle motion along the stochastic magnetic field lines is so weak that the particle radial distribution is similar to the corresponding uniform profile with $\gamma_4 = -6/5$, as is shown in table 6. As is mentioned in section 3, inhomogeneity of

the equilibrium magnetic field due to the magnetic shear creates the finite skewness γ_3, but the values of γ_3 are similar to the cases without collisions.

The behaviour of γ_3 and γ_4 in the case near the island overlapping threshold and the moderate overlapping are fairly complicated. The reason may be due to the regular structures inside the stochastic sea, to or around which particles stick. The Coulomb collisions scatter particle motions: they sometimes scatter the particle from the stochastic field line to the particle stuck by regular structure and vice versa. The change of the temporal behaviours of γ_4 due to the Coulomb collisions is shown in figure 12 for $s_b/s_{bc} = 3.3$, where the change of the radial profile in the long time limit from a broad profile ($\gamma_4 < 0$) to a peaked one ($\gamma_4 > 0$) is understood as ν/ν_t increases.

4.3.4. Type of statistical process The type of statistical process is summarized in table 7, being based on the results presented in 4.3.1-4.3.3, where U and W indicate the uniform mixing and Wiener process, respectively, and the symbol S denotes the strange diffusive process.

In the absence of the Coulomb collision, as $s_b/s_{bc}(\geq 1)$ increases, the magnetic field stochasticity or the particle radial diffusion with only parallel drift motion comes to appear as a uniform mixing process reflecting non-locality of orbits, which is a non-diffusive, uniform, statistically stationary, and Markov process after the exponentially fast relaxation during the time interval $t \sim \tau_{corr} \approx t_d$. The Coulomb collisions interrupts the fast non-local radial displacement of particles along the stochastic magnetic field lines. When the collision frequency is not so frequent ($\nu/\nu_t < 1$), however, the locality is not established. Thus, the particle radial diffusion develops as a strange diffusive process in the long time limit: subdiffusive, profile neither uniform nor Gaussian, and statistically non-stationary process, in almost all $(s_b/s_{bc}, \nu/\nu_t)$ parameter space. The Markovianity in the strange diffusive process is still open question, which will be considered in future. When the collisions are fairly frequent ($\nu/\nu_t \gg 1$) and uniformity of the magnetic field stochasticity is fairly lost ($s_b/s_{bc} \geq 1$), the locality of the particle motion is recovered. Then the particle radial diffusion is governed as the Wiener process with normal diffusivity, Gaussianity, statistical non-stationarity, and Markovianity, as well as the neoclassical diffusion in the regular magnetic field.

The process corresponding to $s_b/s_{bc} = 3.3$ and $\nu/\nu_t = 45$ is similar to the Wiener process. However, only the kurtosis γ_4 does not satisfy the criterion given by equation (49), and so this process is expressed by W_P in table 7. As is understood from this example and other cases recognized as the strange diffusive process in table 7, the various types of the strange diffusive process exist, e.g., even if the process shows a normal diffusivity: $\alpha \sim 0.92$ for $s_b/s_{bc} = 1.3$ and $\nu/\nu_t = 4.5$, the radial profile is broader than a Gaussian and the autocorrelation is not Wiener like. The significant point is not the detail differences in the diffusive process, but the overall tendency in two-parameter space $(s_b/s_{bc}, \nu/\nu_t)$. Table 7 shows that the change in the type of diffusive process is prescribed by the Coulomb collisional suppression of the non-locality of radial particle displacements due to the stochastic magnetic field.

5. Discussion

Here, following several points are discussed.

5.1. Characteristic lengths of magnetic field lines

In this work, the several types of radially bounded stochastic magnetic field region are treated. On the contrary, in the most of previous works the statistical properties of the magnetic stochasticity are given a priori, mainly as a static, homogeneous Gaussian process which develops in the radially unbounded magnetic field region [3, 4, 5, 6, 9]. In other words, all these cases correspond to the parametric domain $s_b/s_{bc} \gg 1$ in actual model. In order to clarify the effects of the boundedness, three characteristic lengths associated with the magnetic field stochasticity are examined: the perpendicular correlation length $L_\perp$, the parallel correlation length $L_{||}$, and the Kolmogorov length L_K. The most significant difference in the present context is connected with the perpendicular correlation length $L_\perp$. For example, in the quasi-linear approximation [4, 5, 6, 9, 11], in order to obtain a constant diffusion coefficient of the magnetic field lines, a radially unbounded, homogeneous stochastic region is used, where the perpendicular correlation length may be treated as infinity: $L_\perp \to \infty$. However, in present situation, $L_\perp$ is limited, namely, $L_\perp < w_{st}$, where w_{st} is radial width of the stochastic region. According to the discussion in 4.1.1, the parallel correlation length $L_{||}$ is recognized as a length which corresponds to the decorrelation time of the stochastic magnetic field lines t_d: $L_{||} = t_d v_{||}$. Indeed, such the decorrelation time is similar to the correlation time τ_{corr} of the autocorrelation coefficient in the highly stochastic case with $s_b/s_{bc} \gg 1$. The Kolmogorov length is obtained from the asymptotic value of the effective radial Liapunov exponent $\langle l_e \rangle$ as $L_K = v_{||}/\langle l_e \rangle$. Substituting the corresponding values to the three characteristic lengths, the following ordering is obtained for $s_b/s_{bc} \geq 1$:

$$L_\perp \ll L_K \ll L_{||}. \tag{66}$$

Note that ordering in the radially bounded stochastic magnetic field is completely different from other situations, especially from the quasi-linear approximation [4, 5, 6].

The ordering between the collisional mean free path λ_{mfp} and the characteristic lengths of the stochastic magnetic field lines for $s_b/s_{bc} \geq 1$ is summarized in table 9. As ν/ν_t decreases, and as s_b/s_{bc} increases, the collisional mean free path λ_{mfp} becomes comparable to the Kolmogorov length L_K, and finally larger than L_K and comparable to the parallel correlation length $L_{||}$. Thus, it is understood that the collisional effects becomes more significant as the level of stochasticity of the magnetic perturbation decreases or s_b/s_{bc} decreases. Moreover, it will be expected that in more collisionless cases with $L_{||} \ll \lambda_{mfp}$, whose condition will be established for banana collisionality regime, the statistical properties of the particle radial diffusion become closer to those of the magnetic field stochasticity. In order to obtain the proper statistical properties in the parameter space considered here, all of calculations have been performed up to $z \gg L_{||}$ or $t \sim t_s = 10 \times t_d \gg t_d$. In the case before overlapping with $s_b/s_{bc} < 1$,

the ensemble averaged Liapunov exponent is always negative. Thus, L_K and $L_{||}$ are interpreted as infinity, so that the ordering $L_\perp \ll \lambda_{mfp} \ll L_K$, $L_{||} \to \infty$ holds, where $L_\perp$ is recognized as the width of the magnetic islands at $q = m/n = 3/2$: $w_{2,3}$. Note that the characteristic lengths and orderings discussed here have not strict sense in the inhomogeneous magnetic field stochastic region: the mixture of regular and irregular structures. In such a case, the stickness of the magnetic field lines to or around regular structures, indicated by the presence of magnetic field lines with a negative Liapunov exponent in the long time limit $t > t_s$ means the existence of many different scales [25]. To investigate more precise properties of the radial diffusion in such a case, the method of the continuous time random walk [12] may be suggested. However, in order to understand the general and global tendencies of the particle radial diffusion, the concept of characteristic lengths is useful for all $s_b/s_{bc} \geq 1$ cases, because both L_K and $L_{||}$ are definitely determined by the effective radial Liapunov exponent $\langle l_e(t) \rangle$ in average sense without ambiguity.

5.2. Locality of the radial diffusion

In this section the relation between locality of the diffusion and the constant diffusion coefficient is investigated. In the standard theory of Brownian motion, according to the Gaussian central limit theorem [24], the spreading of the Gaussian is described by the diffusion coefficient given by

$$D \equiv \lim_{t\to\infty} D(t) = \lim_{t\to\infty} \frac{dC_2(t)}{2dt}. \tag{67}$$

Such a diffusion coefficient is analogy of that in the standard random walk [18]

$$D = \frac{(\Delta x)^2}{\Delta t}, \tag{68}$$

where Δx, and Δt are the characteristic space and time steps of random walker, respectively. Following these developments, in the classical diffusion theory [7], the diffusion process in an unbounded, homogeneous media is characterized by the diffusion coefficient. In the context of the confinement physics, it is ensured by the demand for locality of diffusion. In order to understand the meaning of the locality, the standard neoclassical radial diffusion treated in [19] is reconsidered. By integrating the linearized gyro-phase averaged Boltzmann equation given by equation (1) in the velocity space (in the present case, the energy E is a parameter , so that integration is done only over the magnetic moment μ), and by taking the flux surface average, the equation of continuity in the radial direction is obtained

$$\frac{\partial \langle n \rangle_F}{\partial t} = -\frac{1}{V'} \frac{\partial}{\partial r} \left(V' \langle \vec{\Gamma} \cdot \nabla r \rangle_F \right), \tag{69}$$

where $\langle Q(\vec{r},t) \rangle_F$ is the flux surface average of $Q(\vec{r},t)$, and $\langle Q(\vec{r},t) \rangle_F$ becomes a function with respect to r and t. Also, $\langle n \rangle_F$ is the flux surface averaged density, $\vec{\Gamma} = n(\vec{r},t)\vec{v}(\vec{r},t)$ is the particle flux, and $V' \equiv dV/dr$ with the volume V surrounded by the flux surface

specified by an appropriate radial coordinate r. The diffusion coefficient D is introduced through the phenomenological Fick's law in the radial direction given by

$$\vec{\Gamma} \cdot \nabla r = -D(\vec{r}, t) \frac{\partial n(\vec{r}, t)}{\partial r}. \tag{70}$$

Since the radial diffusion is concerned, by assuming a weak poloidal and toroidal dependence (this is usually ensured by the strong magnetic field and the rotational transform), the flux surface averaged Fick's law becomes

$$\langle \vec{\Gamma} \cdot \nabla r \rangle_F = -\langle D \frac{\partial n}{\partial r} \rangle_F \sim -D(r, t) \frac{\partial \langle n \rangle_F}{\partial r} \tag{71}$$

where $D(r, t) \equiv \langle D \rangle_F$. As is clear from the form of the above equation, the standard Fick's law is based on the locality of the diffusion, since the particle flux at a position r is completely determined only by the diffusion coefficient D and the gradient of $\langle n \rangle_F$ at the same position r. By using the Fick's law, and defining the probability $f(r, t) \equiv \langle n(r, t) \rangle_F / N$ where N is the total number of the particles, the diffusion equation of the particles is obtained

$$\frac{\partial f(r, t)}{\partial t} = \frac{1}{V'} \frac{\partial}{\partial r} \left(V' D(r, t) \frac{\partial f(r, t)}{\partial r} \right). \tag{72}$$

Here, how to obtain the diffusion coefficient $D(r, t)$ by the Monte Carlo method is considered [20]. In the Monte Carlo method, the particles are initially loaded on a flux surface as $f(r, 0) = \delta(r - r_0)$. Putting $\delta r = r - r_0$, from the equation (72),

$$\frac{dC_1}{dt} = \frac{d}{dt} \langle \delta r \rangle = \left\langle \frac{1}{V'} \frac{\partial}{\partial r} (V' D) \right\rangle, \tag{73}$$

where two partial integrations in r are done, assuming $f = \partial f / \partial r = 0$ at $r = 0$ and a. Similarly,

$$\frac{dC_2}{dt} = \frac{d}{dt} \langle (\delta r - \langle \delta r \rangle)^2 \rangle = 2 \langle D \rangle + 2 \left\langle \frac{\delta r - \langle \delta r \rangle}{V'} \frac{\partial}{\partial r} (V' D) \right\rangle, \tag{74}$$

is obtained. Thus, when the particle distribution f does not spread so much in the radial direction (in this case the above boundary conditions are satisfied), namely the locality of the radial diffusion is ensured: $|\delta r| / L \ll 1$, where L is scale length of the equilibrium (in this case $L \sim a$),

$$D(r_0, t) = \frac{1}{2} \frac{dC_2}{dt}, \tag{75}$$

is obtained, partially because the second term in the right-hand side of the equation (74) is neglected due to $|\delta r - \langle \delta r \rangle| / L \ll 1$, where $L \equiv |1/D \cdot \partial D / \partial r|^{-1}$ (note that the diffusion coefficient is determined by the equilibrium quantities), and partially because $\langle D \rangle \sim D(r_0, t)$ by the condition $|\langle \delta r \rangle| / L \ll 1$. The equation (75) means that the local diffusion coefficient at the position where particles are initially loaded is obtained, when the locality of the diffusion is ensured.

From above consideration, it is known that

Statistical properties of the particle radial diffusion

(a) The definition of the diffusion coefficient through the second cumulant given by the equation (37) has meaning, when the locality of the diffusion is satisfied. Note that the validity of this definition of the diffusion coefficient is not directly related to the time-dependence of the diffusion coefficient.

(b) The more significant point is that the concept of the diffusion process itself using the diffusion coefficient assumes the locality of the diffusion process as is seen in the standard Fick's law.

In the present parameter space $(\nu/\nu_t, s_b/s_{bc})$, except for the Wiener domain, the locality of the diffusion process does not hold, where the diffusion coefficient defined by equation (37) does not have clear meaning, and moreover, the standard local Fick's law may not hold. In such strange diffusive processes and a uniform mixing process, the diffusion coefficient defined by the equation (37) have to be understood as the time derivative of the second cumulant itself, and the particle radial transport must be treated as a non-local transport.

5.3. The second cumulant

As is discussed in section 5.2, the diffusion coefficient, introduced through the local Fick's law, have no clear physical meaning in the diffusive process without locality like a strange diffusive process and uniform mixing process. On the contrary, the second cumulant itself always has a clear physical meaning as the mean square displacement [11, 16]. The time dependence of the second cumulant $C_2(t)$ indicates how fast the radial dispersion of particles spread out as time increases. Thus, when the systems with time-dependent diffusion coefficient are compared in order to evaluate how long or how much particles are confined near their initial position, the temporal behaviour of C_2 must be evaluated instead of the diffusion coefficient.

5.4. Ballistic phase of uniform mixing process

The uniform mixing process and the strange diffusive process strongly affected by the fast exponential divergence of magnetic field lines in the radial direction, are observed in the highly stochastic magnetic field with $s_b/s_{bc} \gg 1$. As is understood from figure 9d, as the collision frequency decreases, the magnitude of C_2 almost reaches the final state within the short ballistic phase $(t < t_d)$, which indicates that the process for particle to spread in the radial direction up to the level of the fast exponential divergence, is not regarded as a diffusive process, but as a dynamical relaxation process. After such a ballistic phase or dynamical relaxation process $(t > t_d)$, the uniform mixing properties of the magnetic field lines mainly make the particle radial motions diffusive process. In contrast with it, in the case of Wiener process, although the ballistic phase exists in the early time, such a phase does not influence the time evolution of the system after that, or it does not prescribe the final state of the system, because of the locality of the particle orbits. Thus, the time evolution of the system showing the Wiener behaviour is treated

as a diffusive process in almost all time. However, in the uniform mixing process and the strange diffusive process similar to that, created by the non-local particle motions, the ballistic phase almost prescribes the final state of the system. Hence, the time evolution of such non-local fast processes should be treated in the framework of a fast dynamical relaxation process of a system to an equilibrium.

6. Conclusion

In the present paper, the statistical properties of the electron radial diffusion are investigated in a radially bounded stochastic magnetic field region existing in the axisymmetric torus MHD equilibrium. In order to take account of the practical situation that magnetic field perturbations usually create a radially bounded stochastic region in the axisymmetric torus equilibria and to avoid the assumptions related to the statistical properties of the stochastic magnetic field, a radially bounded stochastic magnetic field is created by superposing three Fourier harmonics of the perturbed magnetic field which resonate at their mode rational surfaces in an axisymmetric MHD equilibrium. Due to the radial boundedness, the statistical properties of such a stochastic magnetic field are completely different from those used in the previous works [4, 5, 6, 9, 7, 12]. Especially, the radially bounded stochastic magnetic field has a finite correlation length in the radial direction. It is opposite to the quasi-linear approximation [4, 5, 6] where usually the radial (perpendicular) correlation length is treated as infinity by assuming radially infinite homogeneous stochastic field.

By changing the amplitude of the perturbed magnetic field, several types of stochastic field structure are created: state before overlapping ($s_b/s_{bc} < 1$), state near the overlapping threshold ($s_b/s_{bc} \sim 1$), moderate overlapping ($s_b/s_{bc} > 1$), and state of highly overlapping ($s_b/s_{bc} \gg 1$). The stochasticity parameter s_b corresponds to the amplitude of the perturbation (strength of perturbation), and s_{bc} is the value of stochasticity parameter at the overlapping threshold. These four types of stochastic magnetic field region correspond to the Poincare plots in the poloidal cross section with the isolated magnetic island chains ($s_b/s_{bc} < 1$), the overlapping of island chains ($s_b/s_{bc} \sim 1$), stochastic sea with regular structures ($s_b/s_{bc} > 1$), and stochastic sea without regular structures ($s_b/s_{bc} \gg 1$), respectively. One aspect of the stochasticity of the resonantly perturbed magnetic field is understood from the temporal behaviour of the effective radial Liapunov exponent $\langle l_e(t) \rangle$ and the number of the magnetic field lines with the positive Liapunov exponent $N_p(t)$, where time t is used as the independent variable. The conversion into the length along the equilibrium field direction is performed as $z \sim R\zeta \sim v_{||}t$ with the major radius R and the parallel velocity of particle $v_{||}$ tied to the magnetic field line. Before overlapping with $s_b/s_{bc} < 1$, the number of the magnetic field lines with the positive Liapunov exponent $N_p(t)$ is zero or quite a few, and the effective radial Liapunov exponent $\langle l_e(t) \rangle$ is always negative. After overlapping with $s_b/s_{bc} \geq 1$, N_p almost monotonically increases with time, finally leading to the saturation. As $s_b/s_{bc}(\geq 1)$ increases, the saturated value of N_p increases,

i.e. from $N_p < N$ for $s_b/s_{bc} \geq 1$ to $N_p = N$ for $s_b/s_{bc} \gg 1$, where N is the total number of observed field lines. The existence of the magnetic field lines with the negative Liapunov exponent for $s_b/s_{bc} \geq 1$ indicates the existence of sticking of the magnetic field lines to regular structures inside the stochastic region. Associated with the variation of $N_p(t)$, $\langle l_e(t) \rangle$ almost monotonically increases from negative to positive value, finally leading to asymptotic saturation, as time t increases. In spite of the various stochasticity levels depending on s_b/s_{bc}, after overlapping, the effective radial Liapunov exponent has such a common feature that the time dependence is $\langle l_e(t) \rangle = \langle l_e \rangle (1 - t_d/t)$, where t_d is the decorrelation time of the magnetic field lines satisfying $\langle l_e(t_d) \rangle = 0$, and $\langle l_e \rangle$ is the saturated value of $\langle l_e(t) \rangle$. In other words, the effective radial Liapunov exponent is characterized by two independent quantities t_d and $\langle l_e \rangle$. Recognizing $t_d v_{||}$ as the parallel correlation length of the magnetic field lines: $L_{||} \equiv t_d v_{||}$, and defining the Kolmogorov length $L_K \equiv v_{||}/\langle l_e \rangle$,it is seen that both the parallel correlation length $L_{||}$ and the Kolmogorov length L_K decrease as $s_b/s_{bc}(\geq 1)$ increases. Since the perpendicular (radial) correlation length of the magnetic field lines $L_\perp \approx w_{st}$, where w_{st} is the radial width of the stochastic region, $L_\perp \ll L_K \ll L_{||}$ holds independent of $s_b/s_{bc}(\geq 1)$ in the considered cases. Note that this ordering is different from that of the usual quasi-linear approximation. To obtain the statistically meaningful results, the calculations are performed up to $z \gg L_{||}$ or $t \sim t_s = 10 \times t_d \gg t_d$, where t_s is defined as a time satisfying $\langle l_e(t_s) \rangle / \langle l_e \rangle = 0.9$. The evaluation in the long time limit is done at $t > t_s$ for $s_b/s_{bc} \geq 1$ or at $t \gg \langle t_b \rangle$ for $s_b/s_{bc} < 1$, where $\langle t_b \rangle$ is a typical time of particle motion trapped by the islands. As $s_b/s_{bc}(\geq 1)$ increases, the dispersion of the effective radial Liapunov exponent Δl_e decreases, which means that all the magnetic field lines have a tendency to radially spread with almost same exponential divergence rate.

The statistical properties of the magnetic field stochasticity are examined by evaluating the cumulant coefficients up to the fourth order, the effective diffusion coefficient, the diffusion exponent α, and autocorrelation coefficient $A(t, t')$ between two different times t and t'. Due to the above mentioned fast exponential divergence of the magnetic field lines in a radially bounded stochastic magnetic field region, the radial diffusion of magnetic field stochasticity or particles tied to magnetic field lines without the perpendicular drift and Coulomb collisions has a tendency to become a uniform mixing process, as $s_b/s_{bc}(\geq 1)$ increases. Namely, the stochastic process is characterized by non-diffusivity ($\alpha \sim 0$), uniform distribution, statistical stationarity, and Markovianity after the correlation time $\tau_{corr} \approx t_d$, which is estimated from the exponentially vanishing autocorrelation coefficient: $A(t, t') \sim A(\tau = t' - t) \sim \exp(-t/\tau_{corr})$. A clear uniform mixing process is obtained for $s_b/s_{bc} \gg 1$. When the regular structures exist inside stochastic sea ($s_b/s_{bc} \geq 1$), the magnetic field stochasticity in the long time limit appears as one of strange diffusive processes characterized by non-diffusivity, uniform like broad distribution, almost statistical stationarity and power-law autocorrelation coefficient: $A(t, t') \sim A(\tau = t' - t) \sim \tau^{-c}$ with a positive constant c. Near the overlapping threshold with $s_b/s_{bc} \sim 1$, the process in the long time limit more deviate from the uniform mixing process. The magnetic field stochasticity appears as

a strange diffusive process with subdiffusivity ($\alpha < 1$), distribution far from uniform and Gaussian, statistical non-stationarity. Sticking of the magnetic field lines to or around regular structures inside the stochastic region leads to the space and time correlations compared with uniform mixing process, so that in these strange processes non-Markovianity may be suggested.

The uniform mixing process and the strange processes are related to the non-locality of particle radial motions. Particles tied to the stochastic magnetic field lines easily spread out in the radial direction and reach up to the boundary, so that the radial displacement δr is prescribed by the radial width of the stochastic region w_{st} : $\delta r \sim w_{st}$, leading to the non-locality of the radial diffusion where $\delta r/a \leq 1$ with the minor radius a as the scale length of the system. In contrast with it, the particle radial diffusion in the regular nested flux surfaces, namely, the neoclassical radial diffusion has different property [19]. In such a case, collisionless particle motions are regular periodic motions, whose drift width δr is at most the poloidal gyroradius ρ_p in the axisymmetric systems, hence $\delta r \sim \rho_p \ll a$. The pitch-angle scattering created in the $\lambda(= v_{||}/v)$ velocity space as a uniform mixing process acts as the white noise on the perpendicular drift motions (although the magnitude of the correlation of the white noise is determined by both the pitch-angle scattering and the drift width). Thus, due to the radial locality of the collisionless particle motion: $\delta r/a \ll 1$ and the accumulation effect of the small pitch-angle scattering acting as a white noise, the locality of the particle radial diffusion is ensured and the radial diffusion appears as a Wiener process with normal diffusivity, Gaussian distribution, statistical non-stationarity and Markovianity.

The deviation of the particle orbits by the collisionless perpendicular drift motion from the stochastic magnetic field qualitatively do not change the above mentioned statistical properties of the radial diffusion of particles tied to stochastic magnetic field lines, except for generation of the small correlation of $A(t, t')$ after τ_{corr} for $s_b/s_{bc} \gg 1$. Hence, it is concluded that the stochastic properties of the collisionless particle radial diffusion are almost all determined by those of the stochastic magnetic field lines. The reason is due to the fact that the parallel drift velocity of particles along the stochastic magnetic field is quite larger than the perpendicular drift velocity. The fast parallel drift motions along the stochastic magnetic field themselves make the stochastic radial displacement quite larger than that due to the slow perpendicular drift motions.

In the presence of the Coulomb collisions, the Coulomb collisions interrupts the fast non-local motions along the stochastic magnetic field lines. The range of the collision frequency considered here is from the neoclassical plateau regime with $\nu/\nu_t < 1$, to Pfirsch-Schlüter regime with $\nu/\nu_t > 1$ and $\nu/\nu_t \gg 1$, where ν_t is the transit frequency of particles in the regular magnetic field. Since $\tau_c < \langle t_b \rangle$ and $\tau_c < t_s$ hold, the long time limit is defined as $t > \max(t_s, \tau_c) = t_s$ for $s_b/s_{bc} \geq 1$, and as $t \gg \max(\langle t_b \rangle, \tau_c) = \langle t_b \rangle$ for $s_b/s_{bc} < 1$, where τ_c is the collision characteristic time defined as $\tau_c = 1/\nu$. As $s_b/s_{bc}(\geq 1)$ increases, both the Kolmogorov length L_K and the parallel correlation length $L_{||}$ become shorter with keeping the inequality $L_\perp \ll L_K \ll L_{||}$. The significance of collisional scattering of parallel drift motions for $s_b/s_{bc} \geq 1$ is qualitatively determined

by the relative magnitude of the mean free path λ_{mfp} to characteristic lengths of the stochastic magnetic field lines: $L_\perp, L_K$, and $L_{||}$, especially the relative magnitude between λ_{mfp} and L_K is important. When $\lambda_{mfp} \ll L_K$, the collisional interruption of the non-local parallel drift along the stochastic magnetic field lines becomes significant. In contrast, when $\lambda_{mfp} \gg L_K$ particles spread out in the radial direction along the stochastic magnetic field lines before they suffer significant scattering due to collisions. Thus, the collisions become significant as s_b/s_{bc} decreases for a fixed ν/ν_t or as ν/ν_t increases for a fixed s_b/s_{bc}. Before overlapping with $s_b/s_{bc} < 1$, $\langle l_e(t) \rangle$ is always negative, thus the collisional scattering are more significant than that after overlapping with $s_b/s_{bc} \geq 1$. So, as ν/ν_t decreases and as s_b/s_{bc} increases, the particle radial diffusion reflects the statistical properties of the magnetic field stochasticity, and behaves as a strange diffusive process with subdiffusivity, profile neither uniform nor Gaussian, statistical non-stationarity. The autocorrelation coefficient shows power-law like, non-stationary decay, $A(t,t') \equiv A(t,\tau = t'-t)$, and non-locality of the stochastic process still remains by reflecting fast non-local motion along the stochastic magnetic field lines. The Markovianity is still open question. In opposite limit, namely, in the region with $\nu/\nu_t \gg 1$ and $s_b/s_{bc} \leq 1$, the collisional scattering of parallel drift motions becomes so significant that the stochastic radial particle displacements are created not by non-local drift motions along the stochastic field lines, but by the collisional scattering of the local perpendicular drift motions, leading to Wiener process through recovering the locality of the particle displacements. Note that the non-locality of the particle radial displacements caused by the radially bounded stochastic magnetic field creates various types of diffusion process under the influence of the Coulomb collision.

The normal diffusivity with time independent diffusion coefficient is obtained only in the Wiener domain, where locality of the diffusion is ensured. In other processes, namely, a strange or uniform mixing process, time dependent or vanishing diffusion coefficient is obtained, where the locality of the diffusion process is not ensured. In the present situations with radially bounded stochastic magnetic region, the subdiffusivity and non-diffusivity appear associated with the non-locality of the stochastic process. In such a non-local process, the diffusion coefficient defined by the time derivative of the second cumulant does not have the clear physical meaning, or rather the second cumulant itself is a better indicator of the process compared with the diffusion coefficient. Note that the diffusion coefficient is introduced through standard phenomenological Fick's law based on the locality of the diffusion process, hence if the locality is not ensured, then such a Fick's law does not hold as it is. Associated with such a doubt about applicability of the Fick's law, it should be pointed out that the role of the ballistic phase ($t < t_d$) becomes more significant, as the level of the magnetic field stochasticity increases and the collision frequency decreases. Within the ballistic phase, the mean square displacement, i.e., C_2 almost reaches the level of the uniform mixing process. In other words, the system almost reaches the final state within the ballistic phase. The fast process in the ballistic phase is closely related to the non-locality of the particle radial displacements, because in the Wiener process, the ballistic phase does not prescribe

the final state of the system. Thus, in such the non-local process, the radial particle diffusion should be reconsidered from the viewpoint of the dynamical relaxation process of the system. The consideration about non-locality of the particle displacements, the dynamical relaxation process in the ballistic phase, and their relation will be persued.

References

[1] Hinton F L and Hazeltine R D 1976 *Rev. Mod. Physics* **48** 309 309
[2] Hirshman S P and Sigmar V D 1981 *Nuclear Fusion* **21** 1079
[3] Kadomtsev B B and Pogutse O P 1979 *Plasma Physics and Controlled Nuclear Fusion Research* 1 649
[4] Rechester A B and Rosenbluth M N 1978 *Phys. Rev. Lett.* **40** 38
[5] Kromers J A, Oberman C and Kleva R G 1983 *Journal of Plasma Physics* **30** 11
[6] Ishichenko M B 1991 *Plasma Physics and Controlled Fusion* **33** No.7 795
[7] Balescu R 1997 *Matter out of Equilibrium* (Imperial Collage Press)
[8] Lihtenberg A J and Lieberman M A 1992 *Regular and Chaotic Dynamics* (Springer-Verlag)
[9] Wang H-D, Vlad M, Vanden E E, Spineanu F, Misquich J H and Balescu R 1995 *Phys. Rev. E* **51** 4844
[10] Vanden E E and Balescu R 1995 *Phys. Plasmas* **3** NO.3 815
[11] Balescu R, Wang H-D and Misquich J H 1994 *Phys. Plasmas* 1 3826
[12] Balescu R 1995 *Phys. Rev. E* **51** No.5 4807
[13] Rax J M and White R B 1992 *Phys. Rev. Lett.***68** 1523
[14] Boozer A H and White R B 1982 *Phys. Rev. Lett.* **49** No.11 786
[15] White R B 1984 *Statistical Physics and Chaos in Fusion Plasma* (John Wiley)
[16] Van-Kampen N G 1981 *Stochastic Processes in Physics and Chemistry* (North-Holland)
[17] Dubkov A A and Malakhov A N 1977 *Radiophys. Quantum Electron.* **19** 833
[18] Gardiner C W 1983 *Handbook of Stochastic Methods for Physics and the Natural Sciences* (Springler-Verlag)
[19] Maluckov A, Nakajima N, Okamoto M, Murakami S and Kanno R 2001 *Plasma Physics and Controlled Fusion* in press
[20] Boozer A H and Kuo-Petravic G 1981 *Phys. Fluids* **24** 851
[21] Wakasa A, Murakami S, Maassberg H, Beider C D, Nakajima N, Watanabe K, Yamada H, Okamoto M, Oikawa S and Itegaki M 2001 *JPFR Series*
[22] MacKay R S, Meiss J D and Percival I C 1984 *Physica* **13D** 55
[23] Krilov N S 1979 *The Foundations of Statistical Physics* (Princeton University Press, Guildford, Surrey)
[24] Bouchand J-P and Georges A 1990 *Physics Reports* **195** No.4-5 127-293
[25] Shlesinger M F, Zaslavsky G M and Klafer J 1993 *Nature* **31** 363
[26] Benettin G, Galgani L and Strelcyn J-M 1976 *Physical Review A* **14** No.6 2338

Tables and table captions

Table 1. The values of the diffusion exponent α in the long time limit in the parameter space (s_b/s_{bc}, ν/ν_t).

$\nu/\nu_t \backslash s_b/s_{bc}$	0.33	1.3	3.3	33
0 ($v_{d\perp} = 0$)	osc.$\sim$ 0.0	0.40	0.01	0.02
0 ($v_{d\perp} \neq 0$)	osc.$\sim$ 0.0	0.29	0.01	0.02
0.45	0.73	0.63	0.30	0.07
4.5	0.97	0.92	0.52	0.12
45	1.07	1.00	1.04	0.22

Table 2. The values of the effective diffusion coefficient $D(t)$, D_{pw} and $\Delta D(\%) = |D(t) - \alpha D_{pw}(t)|100/D(t)$ in the long time limit in (s_b/s_{bc},ν/ν_t) parametric space. In the circumstances when ΔD becomes enormously high (e.g. $\geq$ 100%) the system behaviour is noted as the exponentially like. Note that in the presence of collisions $D(t)$ and D_{pw} are normalized by the corresponding neoclassical value of diffusion coefficient D_{nc}.

$\nu/\nu_t \backslash s_b/s_{bc}$	0.33	1.3	3.3	33
0 ($v_{d\perp} = 0$)	osc.	0.079	0.26	0.60
	osc.	0.18	3.3	100
		(1%)	**(exp)**	**(exp.)**
0 ($v_{d\perp} \neq 0$)	osc.	0.042	0.26	0.62
	osc.	0.13	3.3	80.0
		(10%)	**(exp.)**	**(exp.)**
0.45	4.08	4.7	67.1	93.0
	5.2	7.7	190	1170
	(7.5%)	(6.5%)	(15%)	(11%)
4.5	1.2	2.2	14.	38.1
	1.2	2.5	25.	270
	(0.6%)	(2.7%)	(7.2%)	(5%)
45	1.01	1.10	1.85	4.53
	0.96	1.10	1.8	20.
	(2%)	(0.0%)	(0.1%)	(3%)

Table 3. The time behaviour of the autocorrelation coefficient in the parametric space $(s_b/s_{bc}, \nu/\nu_t)$.

$\nu/\nu_t \backslash s_b/s_{bc}$	0	0.33	1.3	3.3	33
$0\,(v_{d\perp}=0)$		osc.	P_{osc}	P_{st}	E
$0\,(v_{d\perp}\neq 0)$		osc.	P_{osc}	P_{st}	E_{corr}
0.45	P_W	P_f	P_f	P_f	P_f
4.5	P_W	P_W	P_f	P_f	P_f
45	P_W	P_W	P_W	P_W	P_f

Table 4. The values of the first cumulant $C_1(t)$ in the long time limit in the parameter space $(s_b/s_{bc}, \nu/\nu_t)$.

$\nu/\nu_t \backslash s_b/s_{bc}$	0.33	1.3	3.3	33
$0\,(v_{d\perp}=0)$	1.5×10^{-4}	5.7×10^{-3}	-5×10^{-3}	-6×10^{-3}
$0\,(v_{d\perp}\neq 0)$	2.0×10^{-4}	6.2×10^{-3}	-6.5×10^{-3}	-5×10^{-3}
0.45	2.0×10^{-5}	1.4×10^{-3}	2.0×10^{-4}	-6×10^{-3}
4.5	-3.0×10^{-5}	1.1×10^{-3}	2.0×10^{-4}	-4×10^{-3}
45	3.0×10^{-4}	2.9×10^{-3}	1.1×10^{-3}	-1×10^{-3}

Table 5. The values of the third cumulant, γ_3 in the long time limit in the parameter space $(s_b/s_{bc}, \nu/\nu_t)$.

$\nu/\nu_t \backslash s_b/s_{bc}$	0.33	1.3	3.3	33
$0\,(v_{d\perp}=0)$	osc.	0.60	-0.08	-0.13
$0\,(v_{d\perp}\neq 0)$	osc.	0.60	-0.02	-0.18
0.45	0.0	0.70	-0.20	-0.11
4.5	0.05	0.25	-0.15	-0.15
45	0.045	0.10	0.02	-0.17

Table 6. The values of the forth cumulant, γ_4 in the long time limit in the parameter space $(s_b/s_{bc}, \nu/\nu_t)$.

$\nu/\nu_t \backslash s_b/s_{bc}$	0.33	1.3	3.3	33
$0\,(v_{d\perp}=0)$	osc.	1.8	-0.95	-1.15
$0\,(v_{d\perp}\neq 0)$	osc.	1.7	-0.95	-0.85
0.45	-0.05	3.0	-0.15	-1.1
4.5	-0.05	1.7	1.4	-1.0
45	-0.10	0.02	0.6	-0.8

Table 7. The type of diffusion process in the parametric space $(s_b/s_{bc}, \nu/\nu_t)$.

$\nu/\nu_t \backslash s_b/s_{bc}$	0	0.33	1.3	3.3	33
$0\,(v_{d\perp}=0)$			S_{osc}	S_{st}	U
$0\,(v_{d\perp}\neq 0)$			S_{osc}	S_{st}	U_{corr}
0.45	W	S	S	S	S
4.5	W	W	S	S	S
45	W	W	W	W_P	S

Table 8. The relation of characteristic times in $(s_b/s_{bc}, \nu/\nu_t)$ parametric space: $\langle t_b\rangle/\tau_c$ for $s_b/s_{bc} = 0.33$, and t_d/τ_c for $s_b/s_{bc} > 1$. The time $\langle t_b\rangle$ is the characteristic time for trapping by the island, τ_c is the collisional characteristic time, and t_d is the decorrelation time of the effective radial Liapunov exponent. Note that $t_d/\tau_c = L_{||}/\lambda_{mfp}$ (see table 9).

$\nu/\nu_t \backslash s_b/s_{bc}$	0.33	1.3	3.3	33
0.45	1.6	120	20	1.8
4.5	16	1200	200	18
45	160	12000	2000	180

Table 9. The ordering of the characteristic lengths: $L_{||}$ the parallel characteristic length, $L_\perp$ the perpendicular characteristic length, L_K the Kolmogorov length, and λ_{mfp} the mean free path; with respect to $s_b/s_{bc} \geq 1$ and $\nu/\nu_t > 0$ parameter space.

$\nu/\nu_t \backslash s_b/s_{bc}$	1.3	3.3	33
0.45	$L_\perp \ll \lambda_{mfp} \ll L_K \ll L_{||}$	$L_\perp \ll \lambda_{mfp} < L_K \ll L_{||}$	$L_\perp \ll L_K \ll \lambda_{mfp} < L_{||}$
4.5	$L_\perp \ll \lambda_{mfp} \ll L_K \ll L_{||}$	$L_\perp \ll \lambda_{mfp} \ll L_K \ll L_{||}$	$L_\perp \ll \lambda_{mfp} < L_K \ll L_{||}$
45	$L_\perp < \lambda_{mfp} \ll L_K \ll L_{||}$	$L_\perp < \lambda_{mfp} \ll L_K \ll L_{||}$	$L_\perp < \lambda_{mfp} \ll L_K \ll L_{||}$

Figure captions

Figure 1. The Poincare plots of the test magnetic field line ensemble in (r, θ) plane at $\zeta = 2.4$: (a) $s_b/s_{bc} = 0.33$, (b) $s_b/s_{bc} = 1.3$, (c) $s_b/s_{bc} = 3.3$, and (d) $s_b/s_{bc} = 33$. The arrows show positions of the rational surfaces, $q = 10/7, 3/2$, and $11/7$.

Figure 2. The time behaviour of the effective radial Liapunov exponent $\langle l_e(t)\rangle c$ vs t for $s_b/s_{bc} = 0.33, 1.3, 3.3$, and 33 is plotted in figures (a), (b), (c), and (d), respectively. The asymptotic value of the effective Liapunov exponent, $\langle l_e\rangle$, multiplied with conversion factor c is given by dotted line, and values of t_d and t_s indicated by arrows.

Figure 3. The number of magnetic field lines N_p with positive radial Liapunov exponent vs time t for $s_b/s_{bc} = 0.33, 1.3, 3.3$, and 33 is plotted in figures (a), (b), (c), and (d), respectively. The arrows show the values of t_d and t_s.

Figure 4. The 2nd cumulant time behaviour in the region of the global magnetic stochasticity: $s_b/s_{bc} = 1.3$ ($C_2(t) \times 4$) (solid curve), $s_b/s_{bc} = 3.3$ (dashed curve), and $s_b/s_{bc} = 33$ (dotted curve). Time is normalized with t_s.

Figure 5. The autocorrelation coefficient, $A(t, t') = A(\tau = t' - t)$, in the long time limit, $t = 0.56t_s$, with respect to τ/t_s. The solid line corresponds to the value: $s_b/s_{bc} = 1.3$; the dashed line to: $s_b/s_{bc} = 3.3$; the dotted line to: $s_b/s_{bc} = 33$, respectively.

Figure 6. The time development of the third cumulant, γ_3, with respect to the strength of the magnetic perturbation. The solid, dashed, and dotted curve correspond to $s_b/s_{bc} = 1.3, 3.3$, and 33, respectively. Time is normalized with t_s.

Figure 7. Kurtosis, γ_4, is the measure of the narrowness of the magnetic field line distribution function. The positive value of kurtosis for $s_b/s_{bc} = 1.3$ (solid curve) indicates more peaked distribution function than Gaussian. On the other hand, the values of γ_4 in the stochastic sea with, $s_b/s_{bc} = 3.3$, (dashed curve), and without structures, $s_b/s_{bc} = 33$ (dotted curve) show more flatted distribution than the Gaussian, and uniform distribution, respectively. On axis the values t/t_s are plotted.

Figure 8. The autocorrelation coefficients $A(t,t')$ vs $\tau/t_s = (t'-t)/t_s$ for the stochastic sea without structures in the presence of the drift decorrelation. The curves are calculated at starting time t: $t/t_s = 2.7 \times 10^{-3}, 0.74$, and $t/t_s = 3.3$.

Figure 9. The second cumulant vs time for $s_b/s_{bc} = 0.33, 1.3, 3.3$, and 33 is drawn in figures (a), (b), (c), and (d), respectively. On each figure the solid curve presents the case with $\nu/\nu_t = 0$ (only magnetic field stochasticity exists); dashed curve presents case with $\nu/\nu_t = 0.45$; dot-dashed curve presents case with $\nu/\nu_t = 4.5$; and dotted curve presents case $\nu/\nu_t = 45$. Time is normalized with t_s.

Figure 10. The autocorrelation coefficient versus $\tau/t_s = (t'-t)/t_s$ for the starting times $t = t_1 = 3.1 \times 10^{-3}\langle t_b\rangle, t = t_2 = 41.\langle t_b\rangle$ for $s_b/s_{bc} = 0.33$ (a); $t_1 \approx 8.3 \times 10^{-4} t_s, t_2 \approx 0.56\, t_s$ for $s_b/s_{bc} = 1.3$ (b); $t_1 \approx 2.5 \times 10^{-4} t_s, t_2 \approx 0.56\, t_s$ for $s_b/s_{bc} = 3.3$ (c) and $t_1 = 2.8 \times 10^{-3} t_s$, $t_2 = 1.51\, t_s$ for $s_b/s_{bc} = 33$ (d), respectively. The solid, dashed, dot-dashed, and dotted line correspond to the Wiener curve, and $\nu/\nu_t = 0.45, 4.5$, and 45, respectively.

Figure 11. The autocorrelation coefficient versus $\tau = t' - t$ for (a) $\nu/\nu_t = 0.45$, and (b) 45 at fixed value of parameter $s_b/s_{bc} = 3.3$. Different curves correspond to the starting time $t = (2.5 \times 10^{-4}, 6.2 \times 10^{-2}, ..., 0.56)t_s$ (arrow in figure is in direction of increasing t). Because of comparison the Wiener curves (equation (48)) are shown by the dashed curves. Time τ is normalized with respect to t_s.

Figure 12. The qualitative change from broader than Gaussian distribution, $\gamma_4 < 0$, for $s_b/s_{bc} = 3.3, \nu/\nu_t = 0$ (solid curve), $\nu/\nu_t = 0.45$ (dashed curve), to the peaked compared with Gaussian distribution, $\gamma_4 > 0$, for $\nu/\nu_t = 4.5$ (dot- dashed curve), and $s_b/s_{bc} = 1.3, \nu/\nu_t = 45$ (dotted curve).

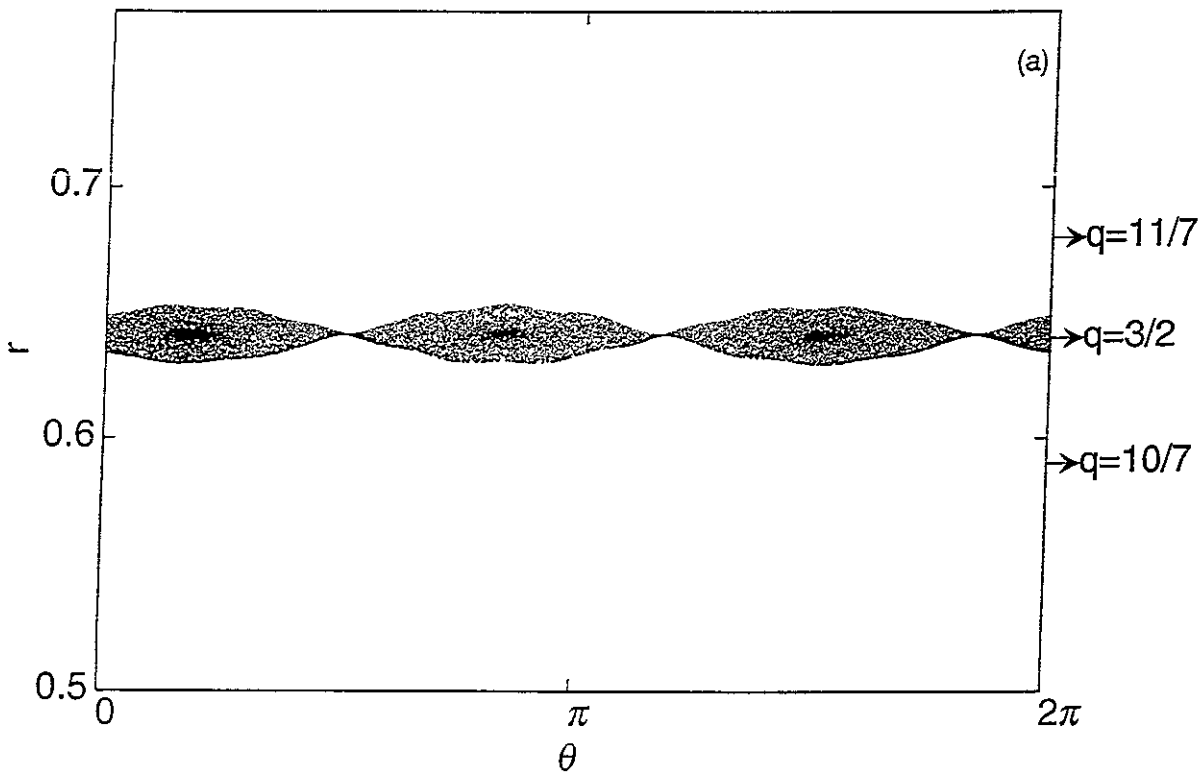

Fig.1a

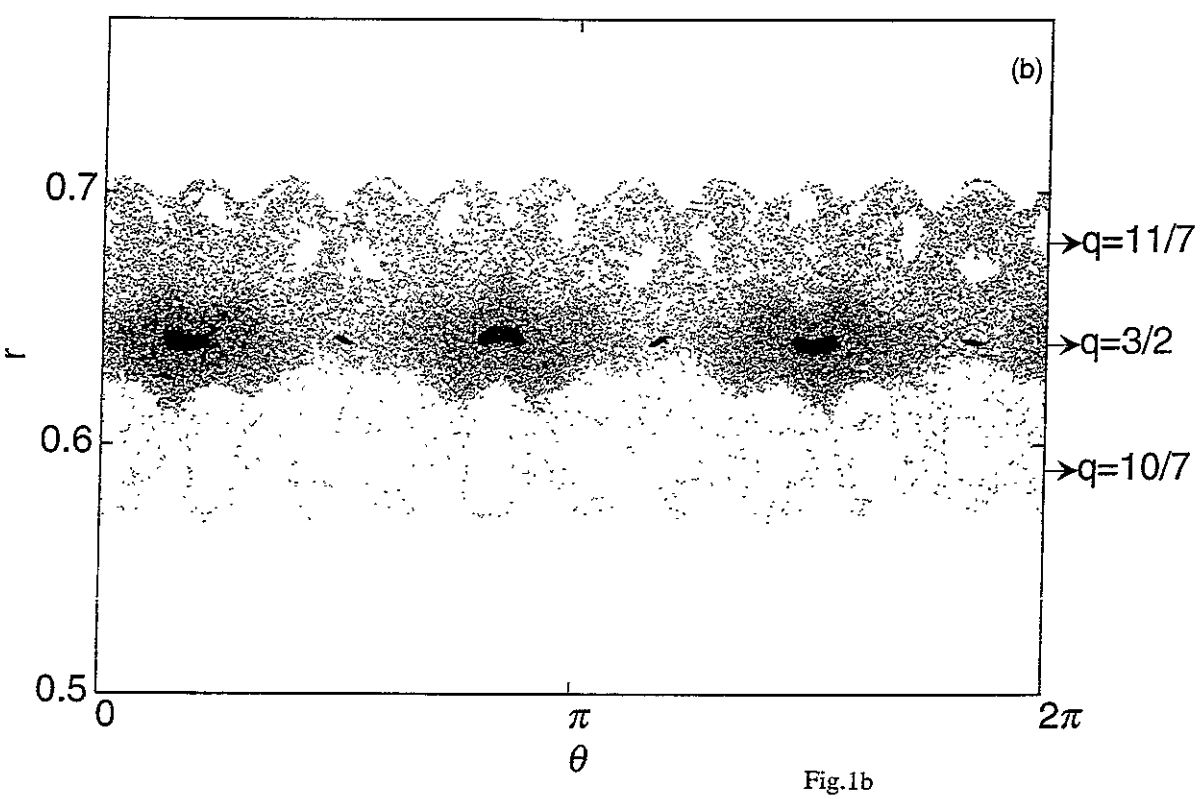

Fig.1b

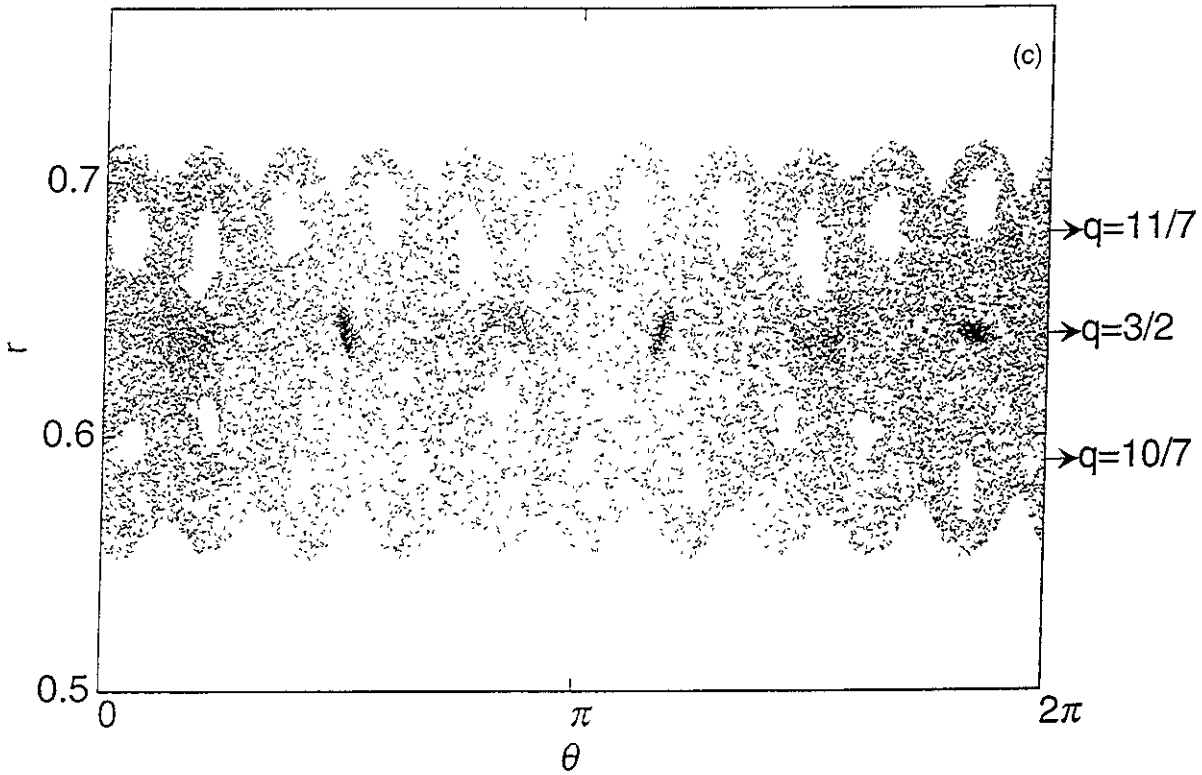

Fig.1c

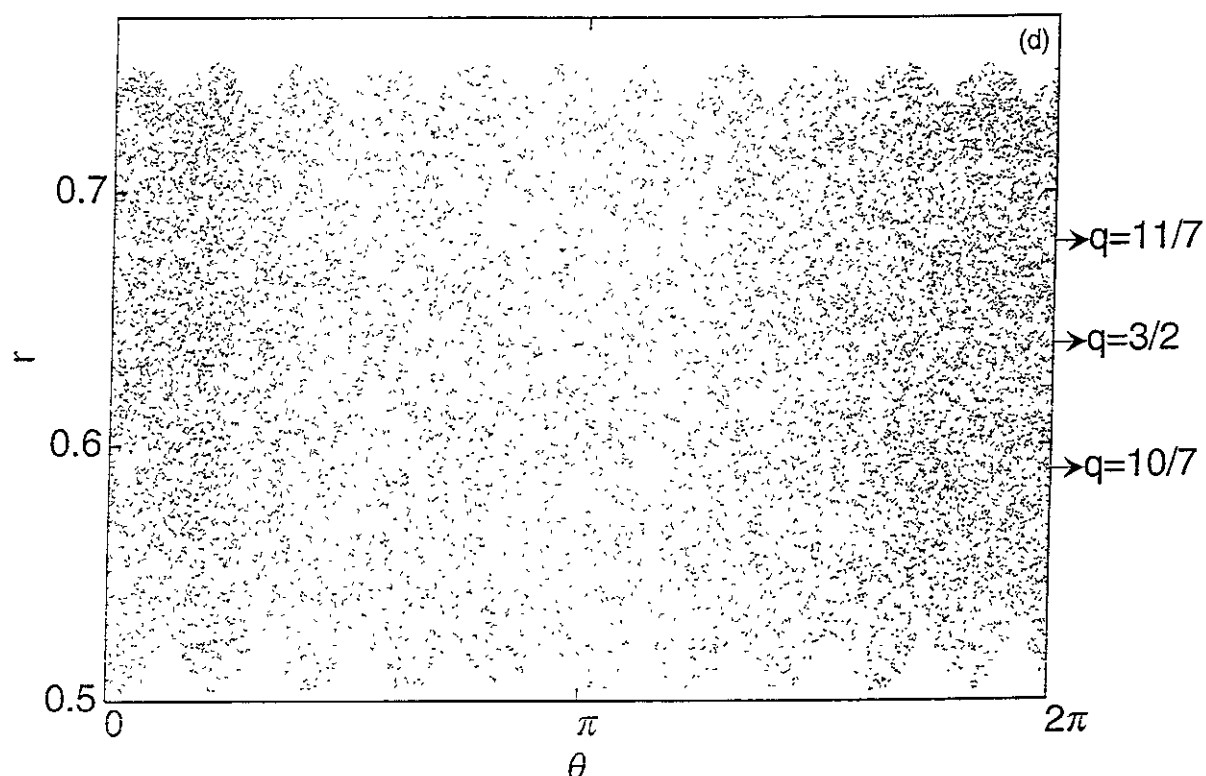

Fig.1d

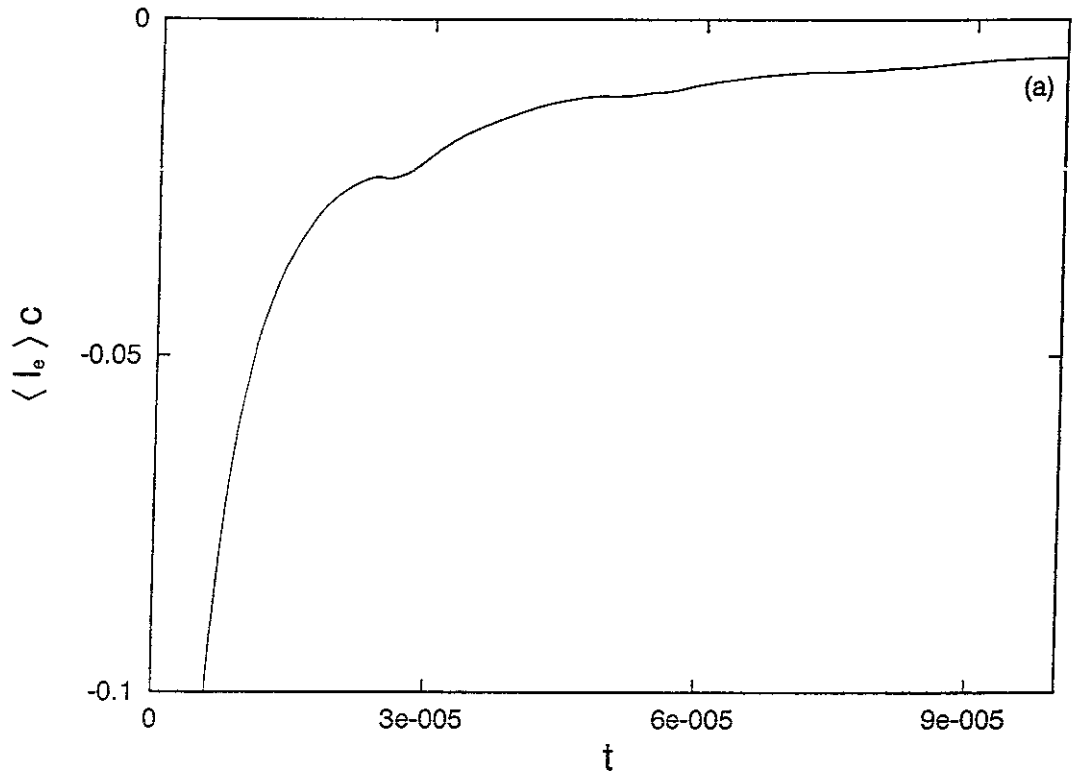
0
-0.05
-0.1
0
3e-005
6e-005
9e-005
t
⟨ I_e ⟩ c
(a)

Fig.2a

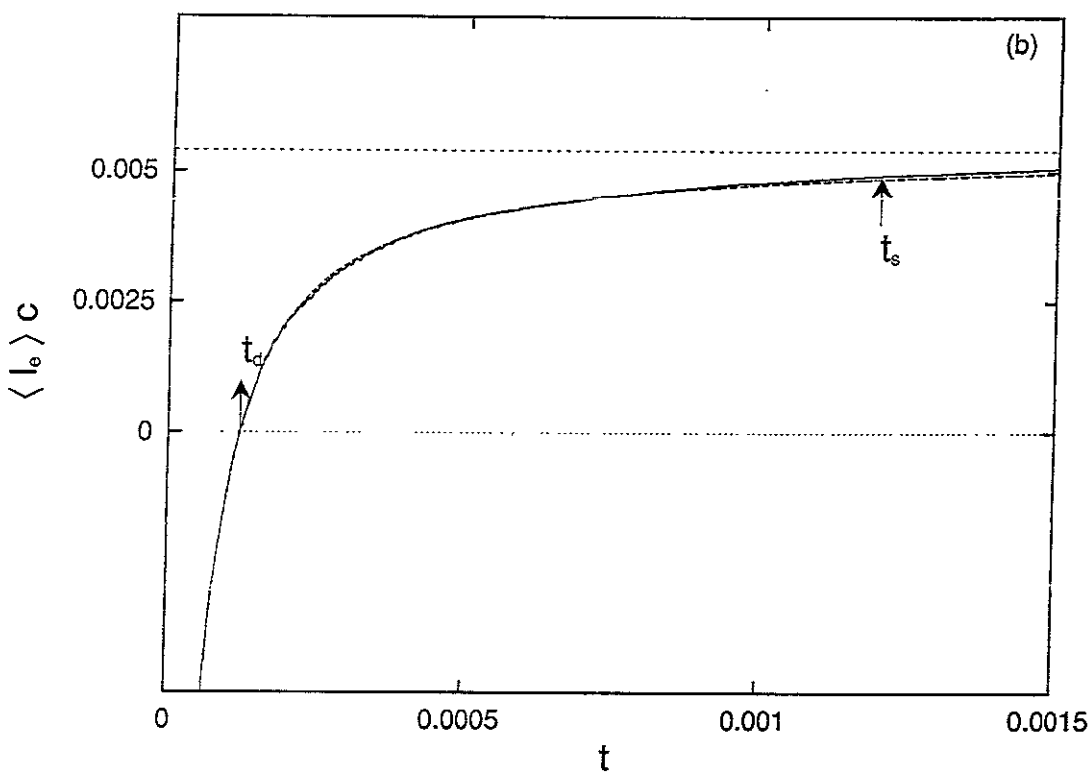
0.005
0.0025
0
0
0.0005
0.001
0.0015
t
⟨ I_e ⟩ c
t_d
t_s
(b)

Fig.2b

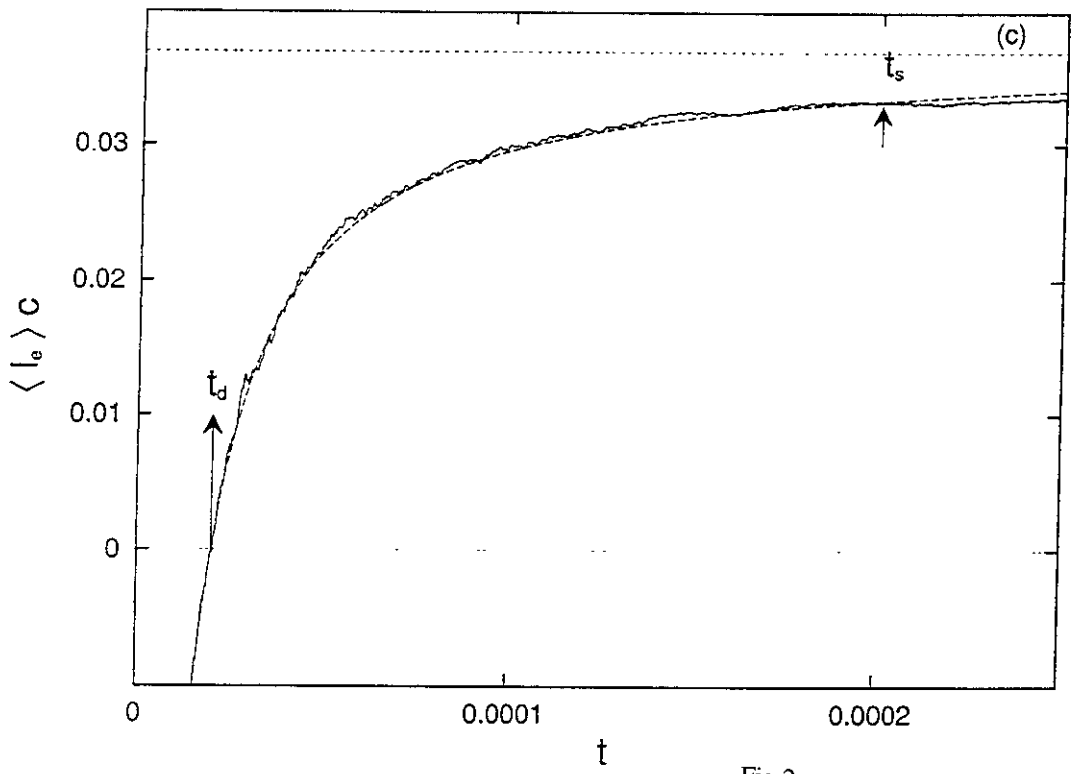
(c)
t_s
t_d
0.03
0.02
0.01
0
$\langle I_e \rangle c$
0
0.0001
0.0002
t

Fig.2c

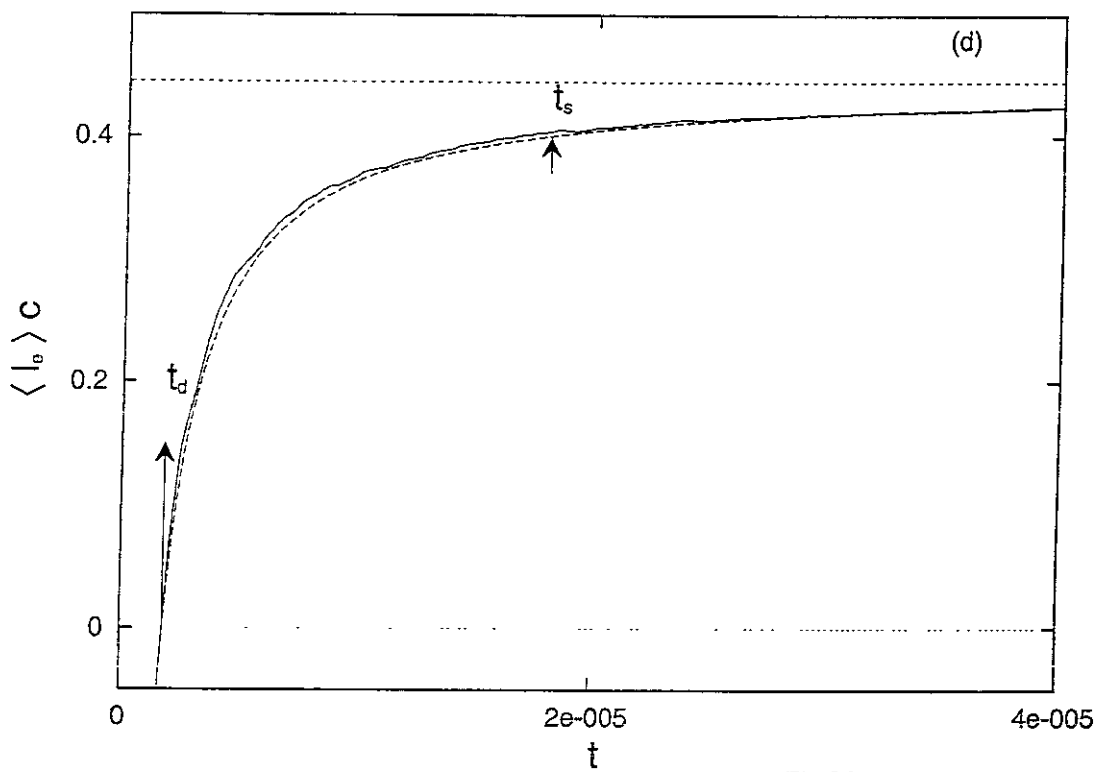
(d)
t_s
t_d
0.4
0.2
0
$\langle I_e \rangle c$
0
2e-005
4e-005
t

Fig.2d

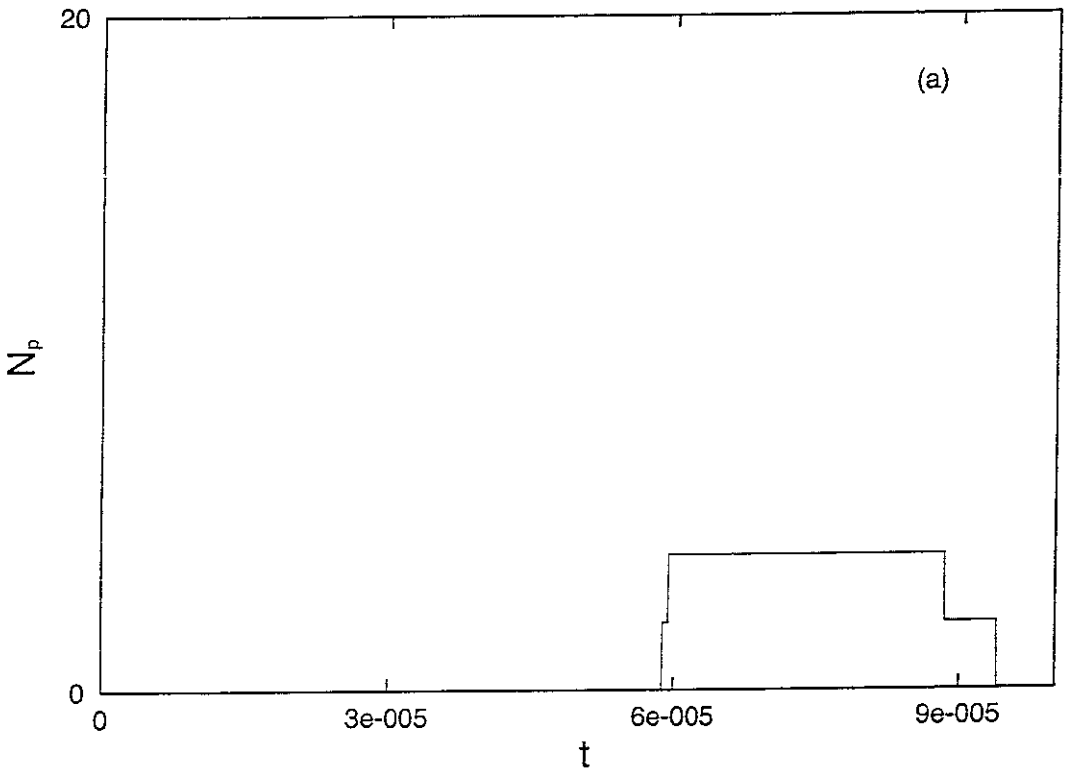
20
(a)
N_p
0
0
3e-005
6e-005
9e-005
t

Fig.3a

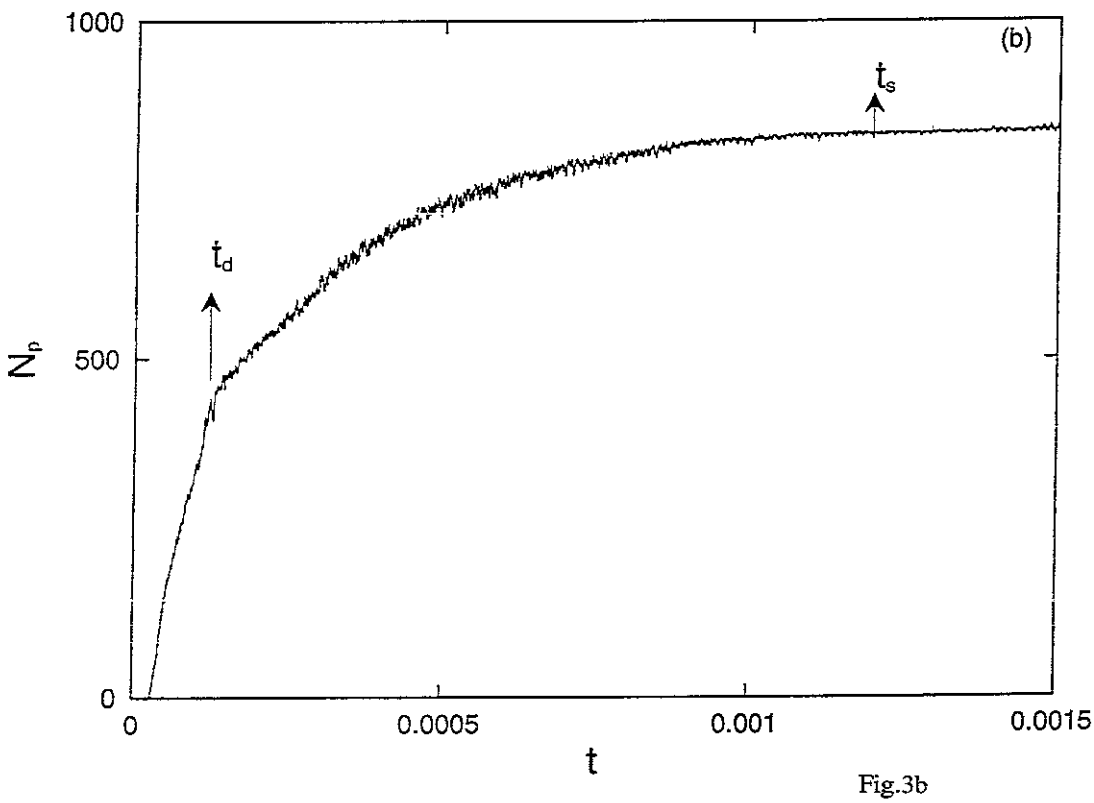
1000
(b)
t_s
t_d
N_p
500
0
0
0.0005
0.001
0.0015
t

Fig.3b

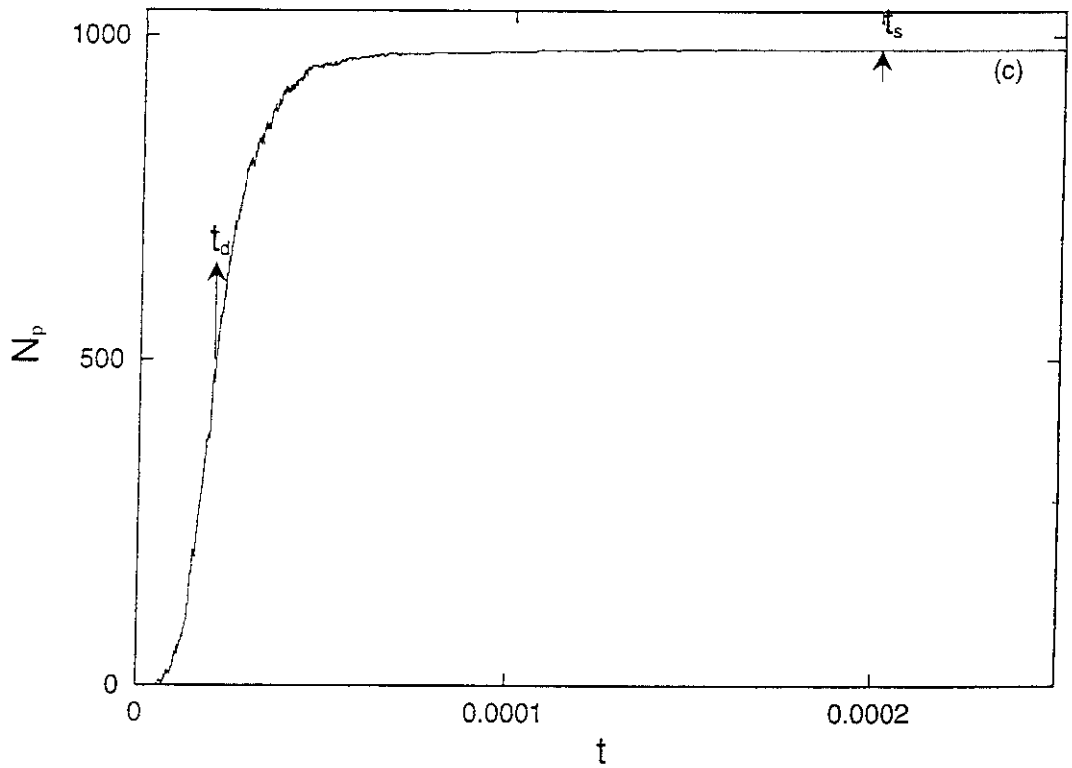
1000
500
0
N_p
t_s
(c)
t_d
0
0.0001
0.0002
t

Fig.3c

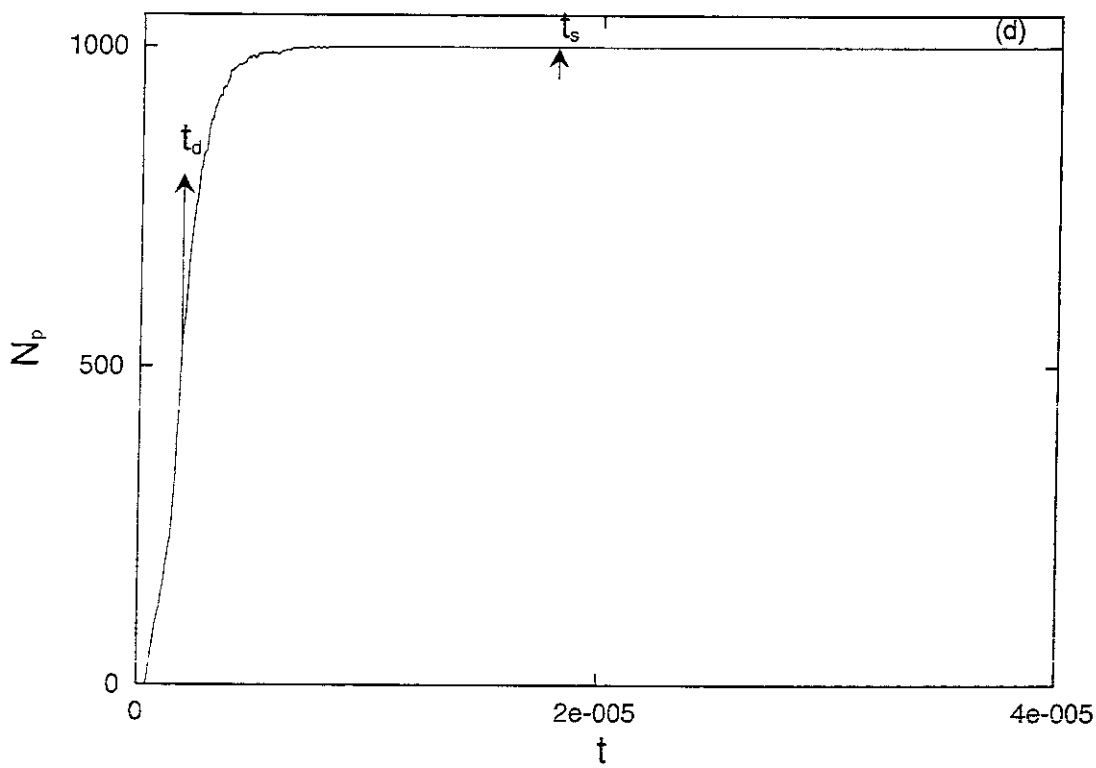
1000
500
0
N_p
t_s
(d)
t_d
0
2e-005
4e-005
t

Fig.3d

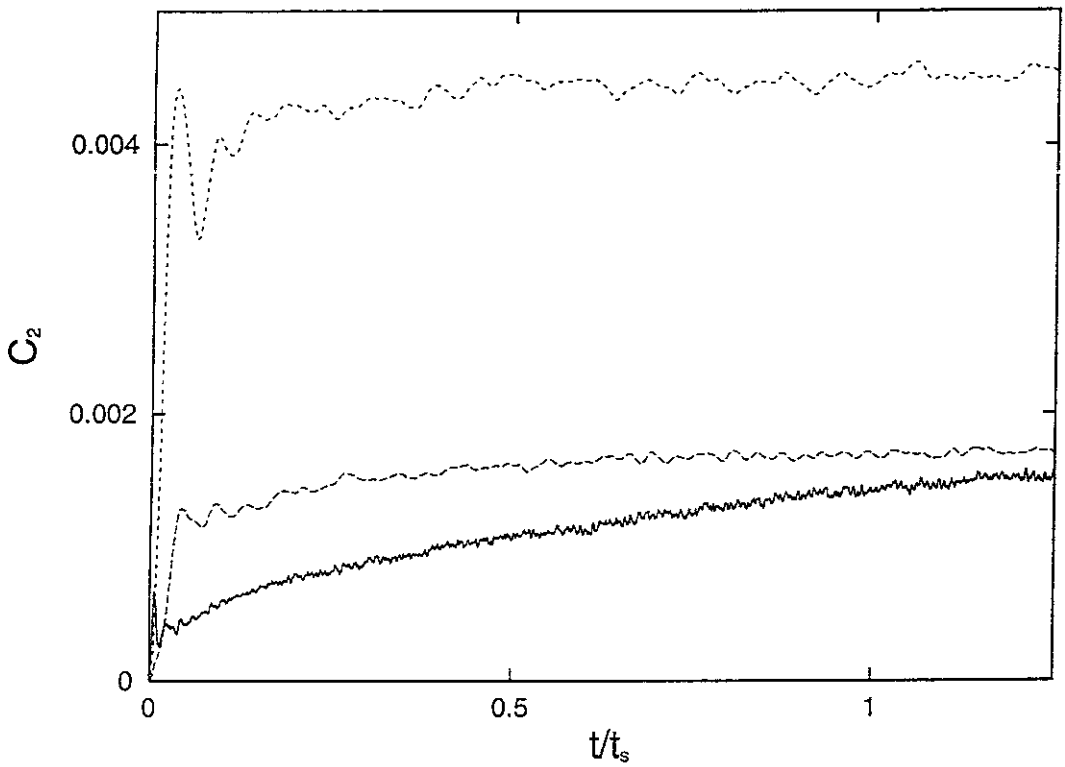

Fig.4

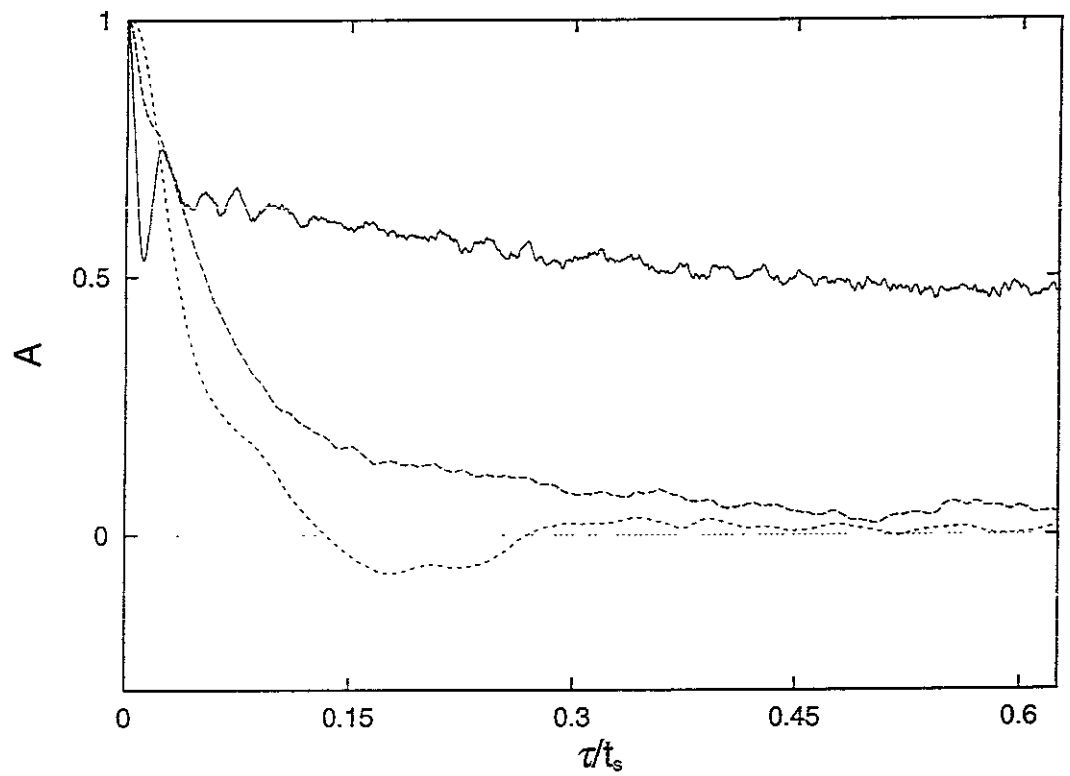

Fig.5

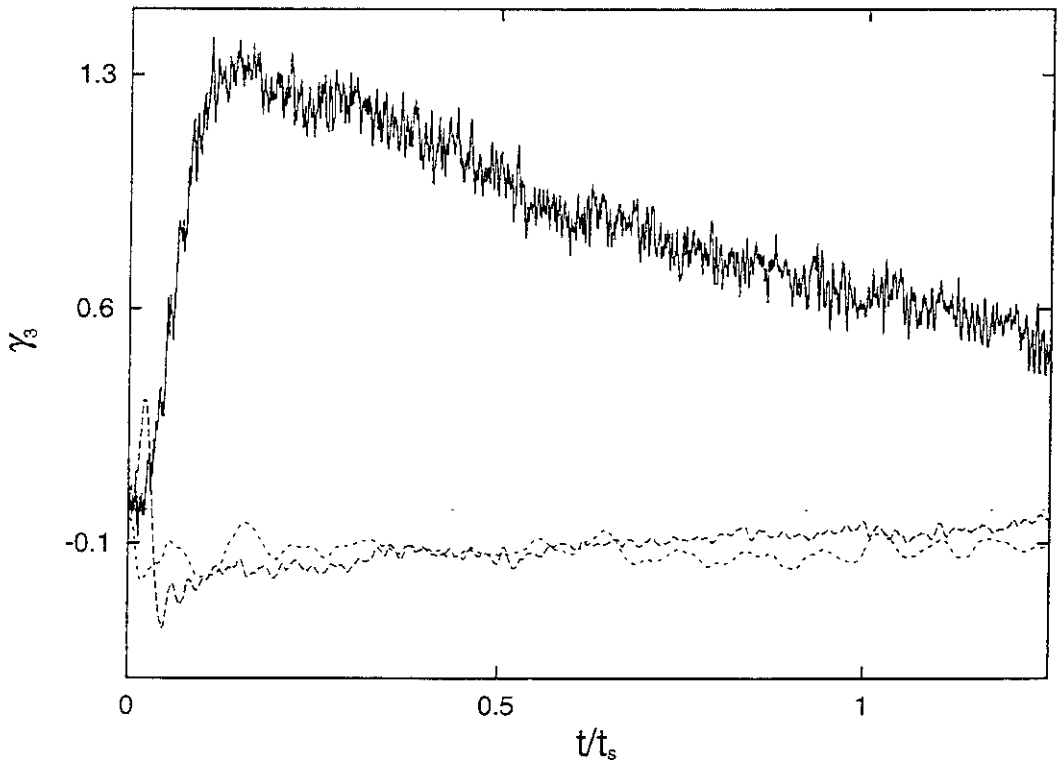

Fig.6

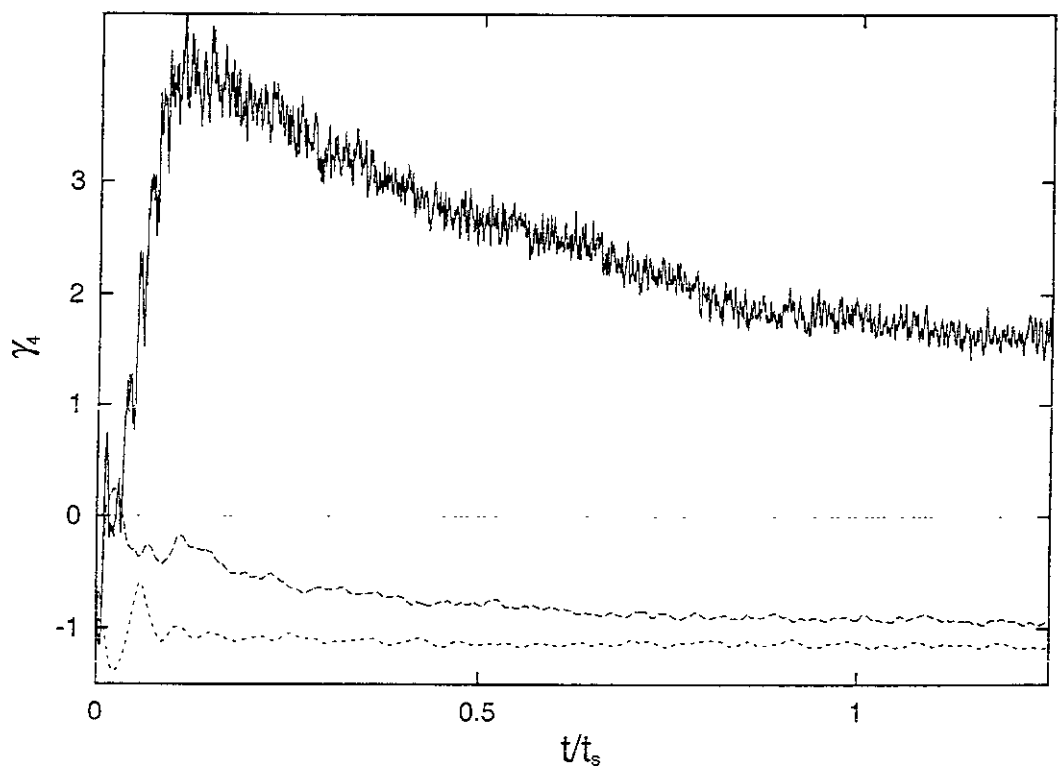

Fig.7

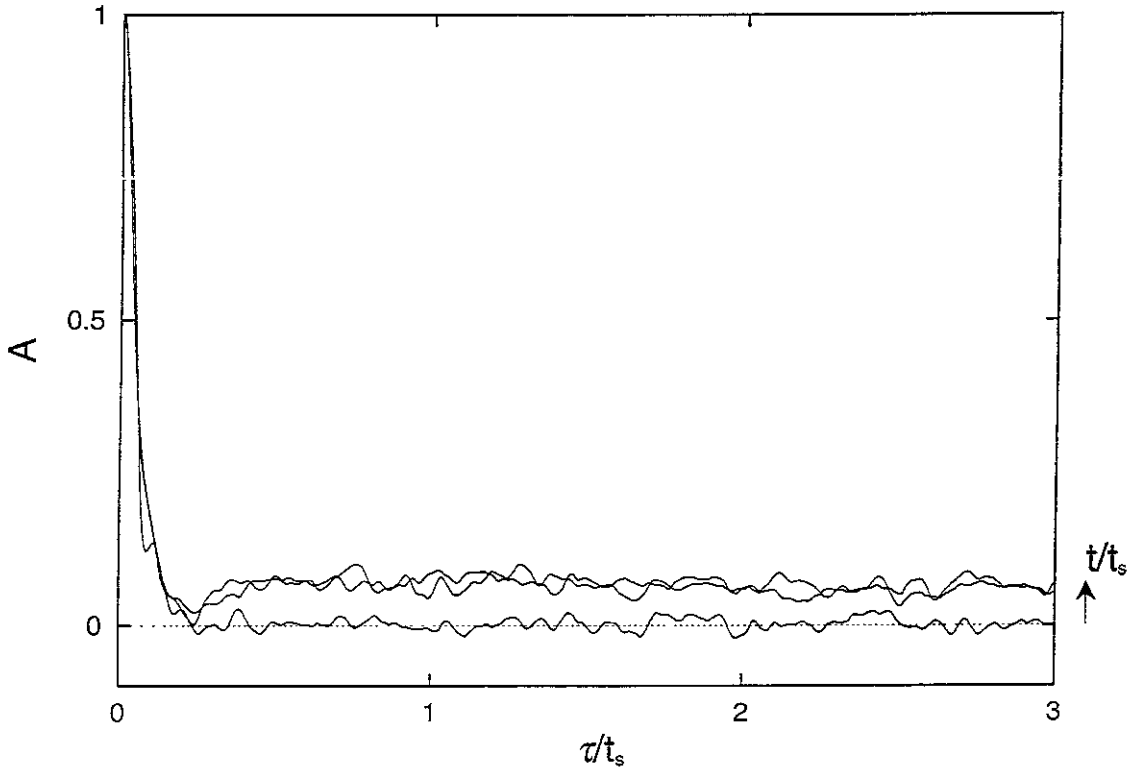

Fig.8

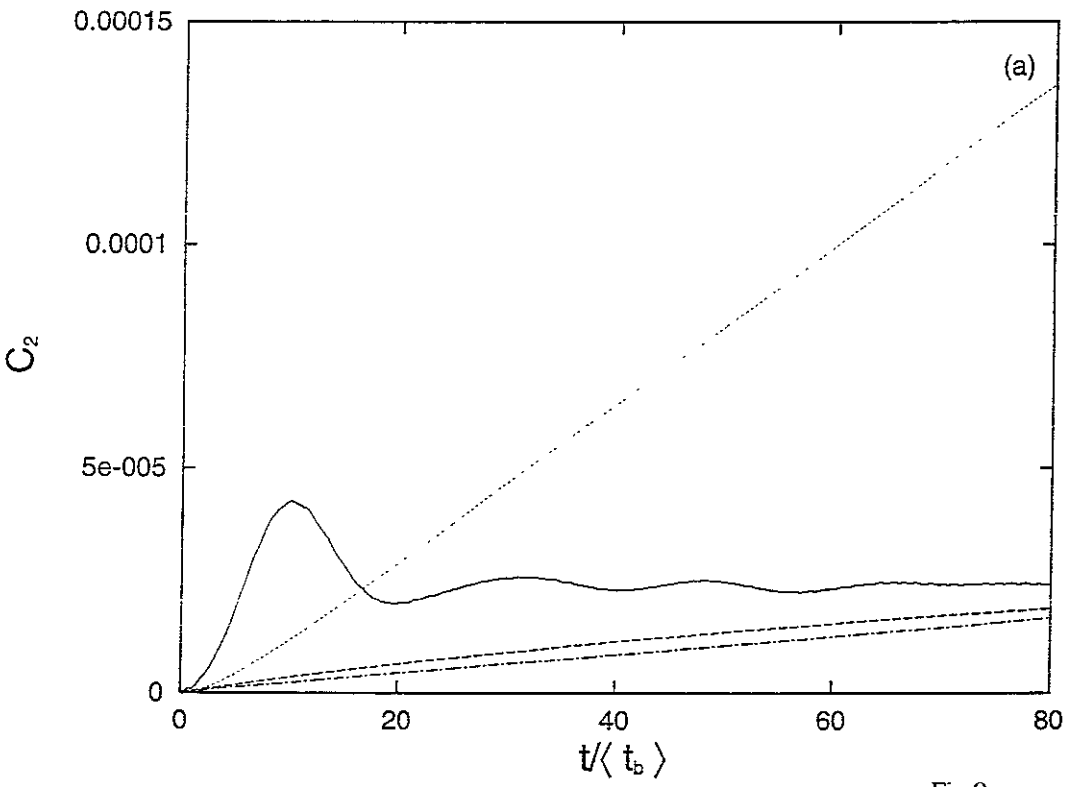

Fig.9a

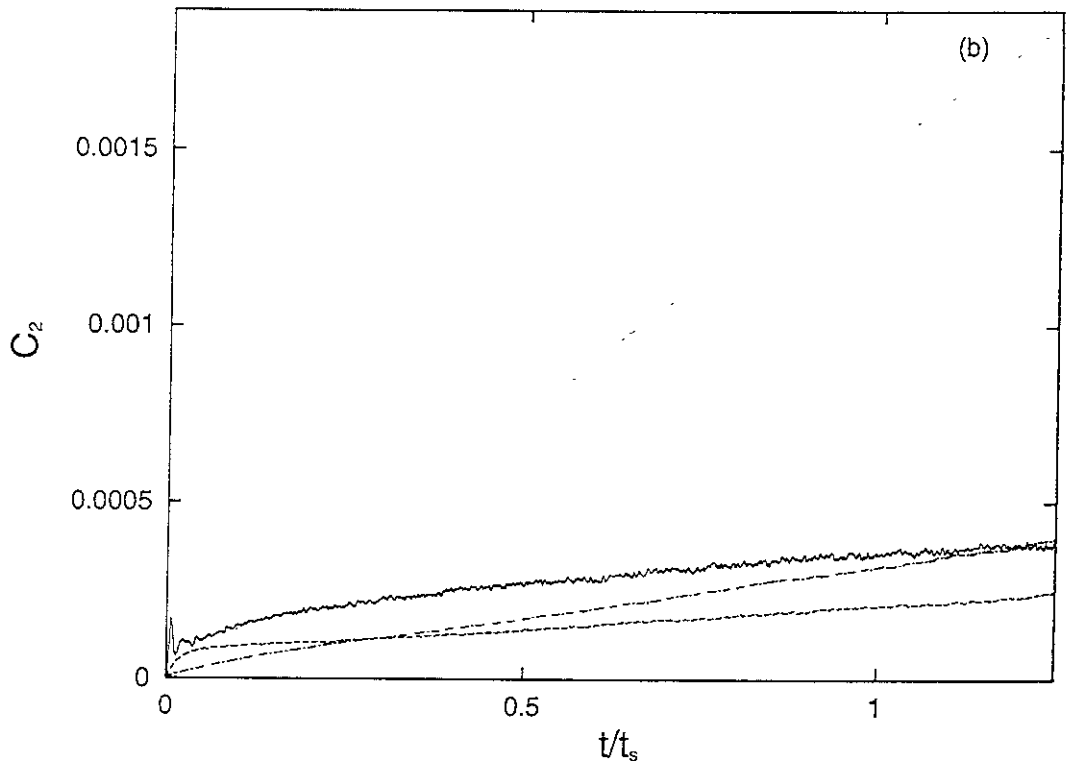
(b)
0.0015
0.001
0.0005
0
C_2
0
0.5
1
t/t_s

Fig.9b

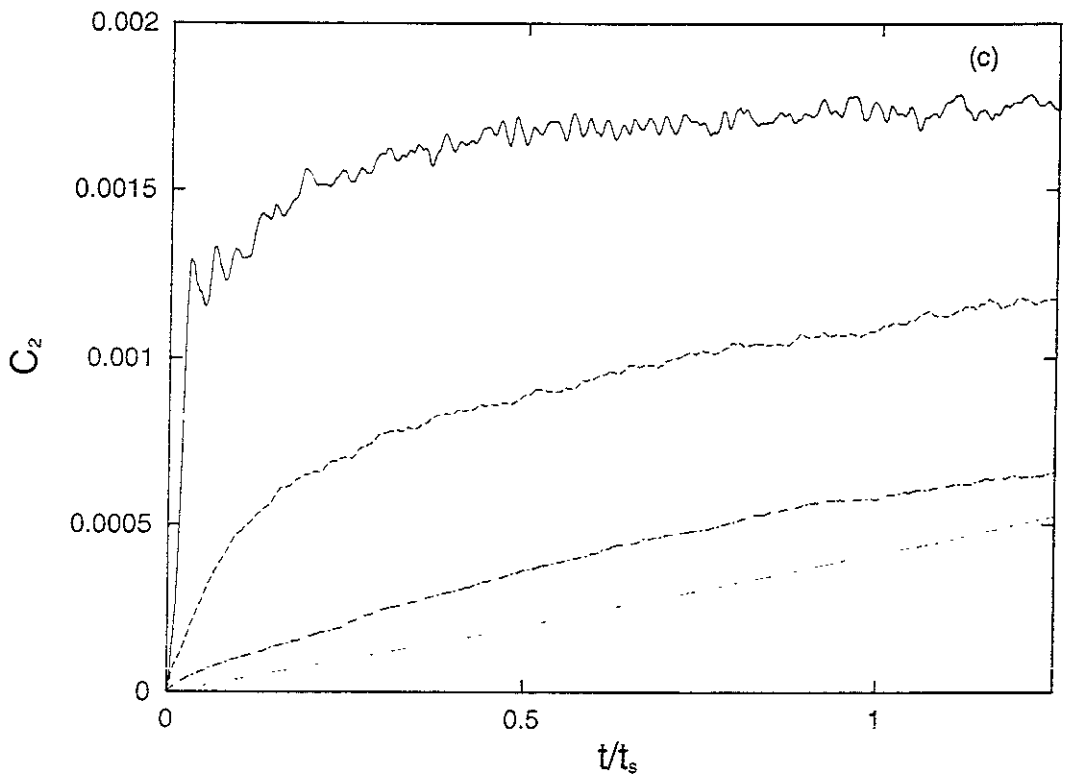
(c)
0.002
0.0015
0.001
0.0005
0
C_2
0
0.5
1
t/t_s

Fig.9c

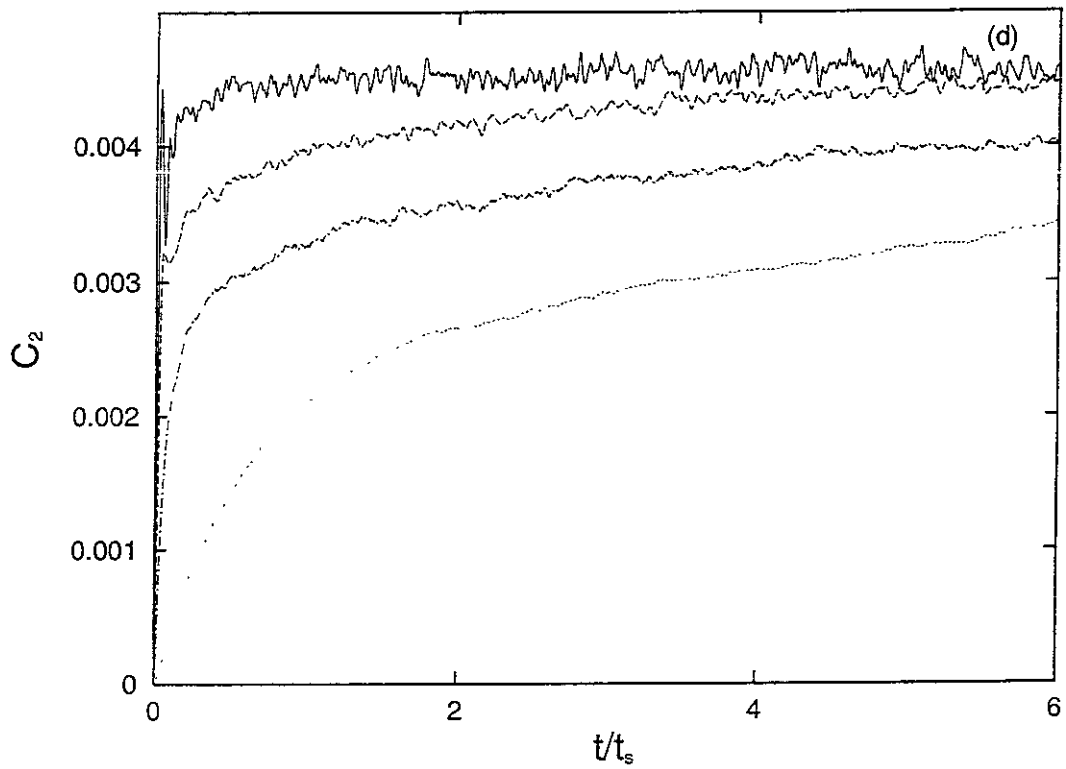

Fig.9d

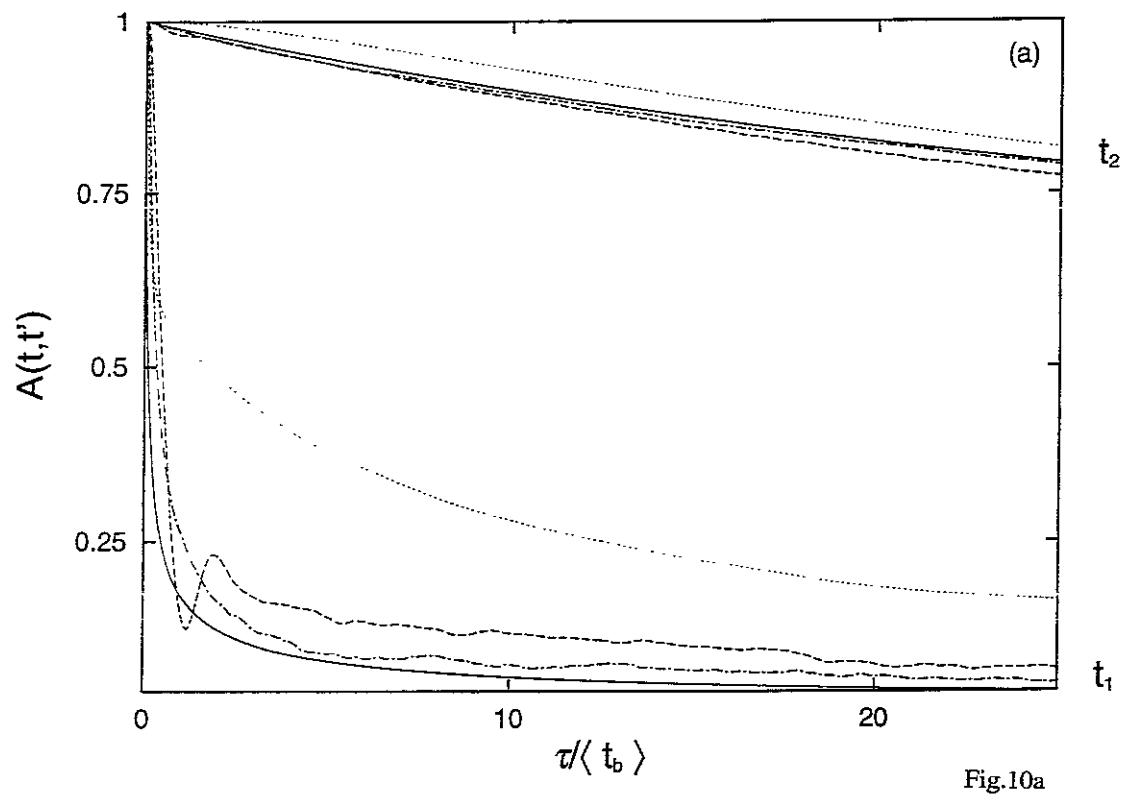

Fig.10a

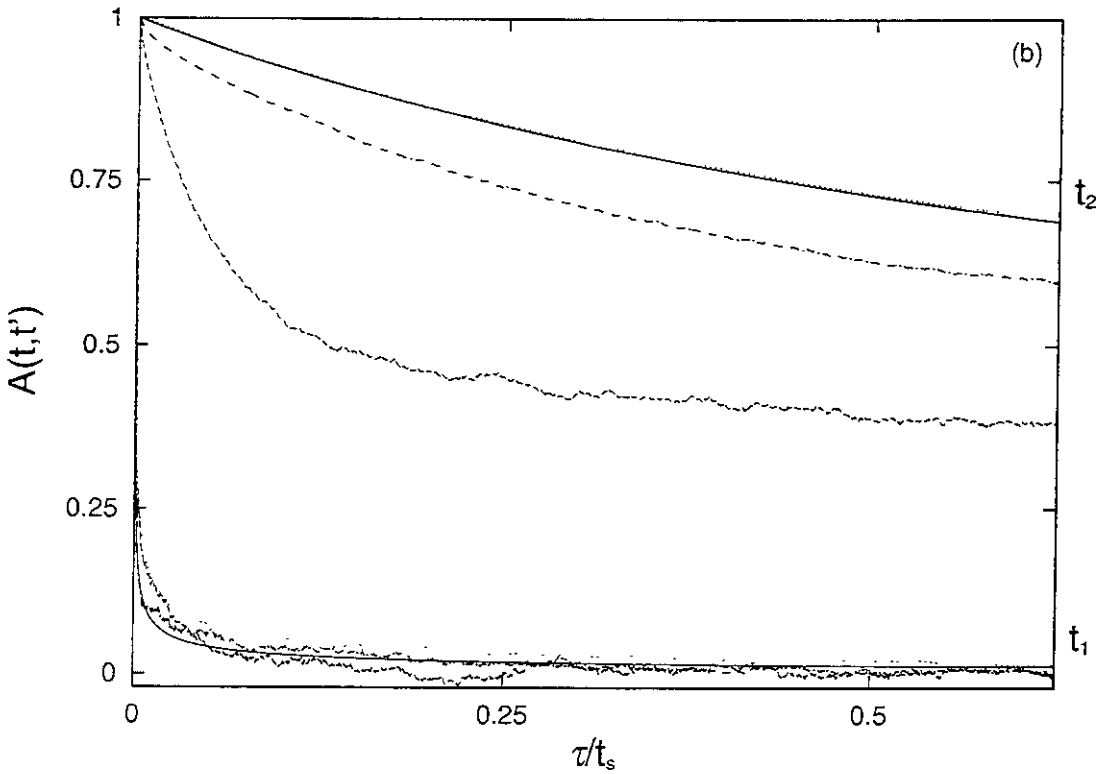

Fig.10b

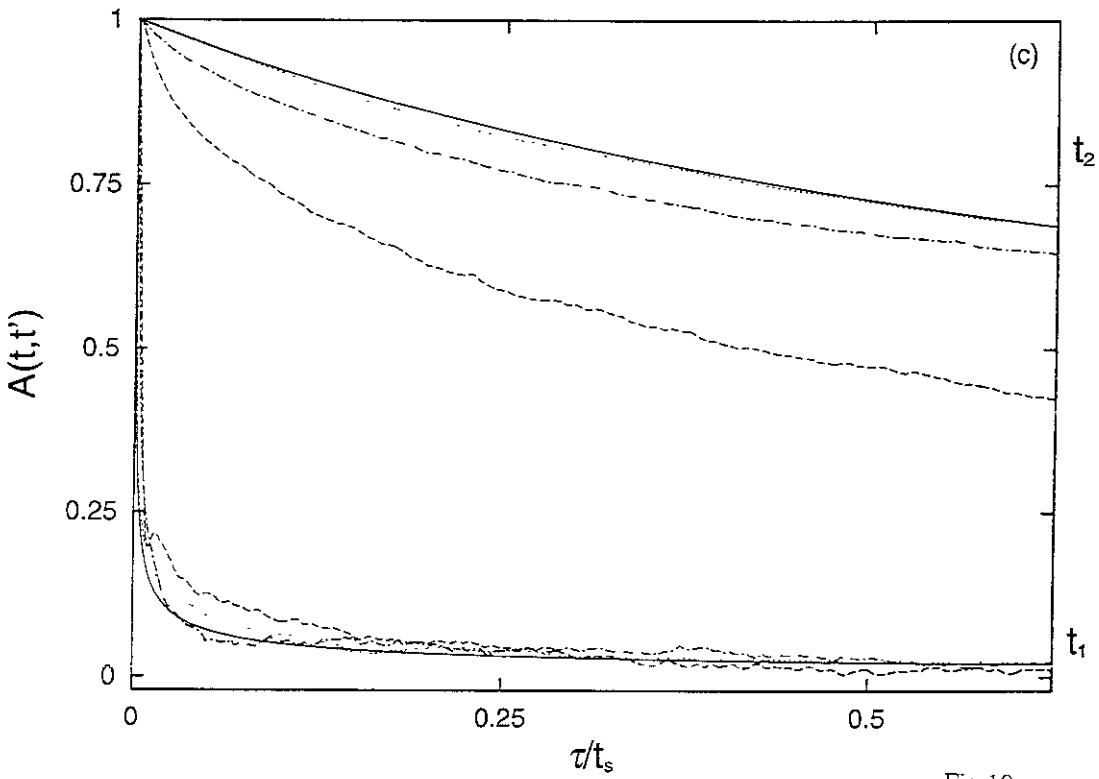

Fig.10c

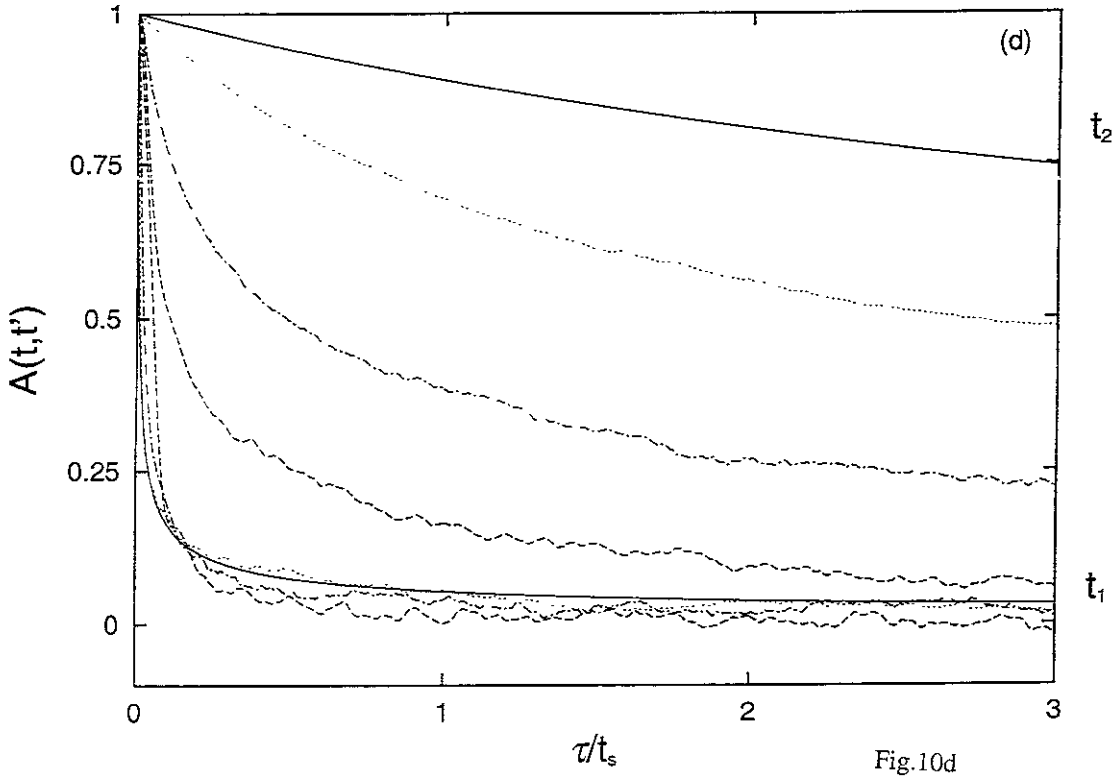

Fig.10d

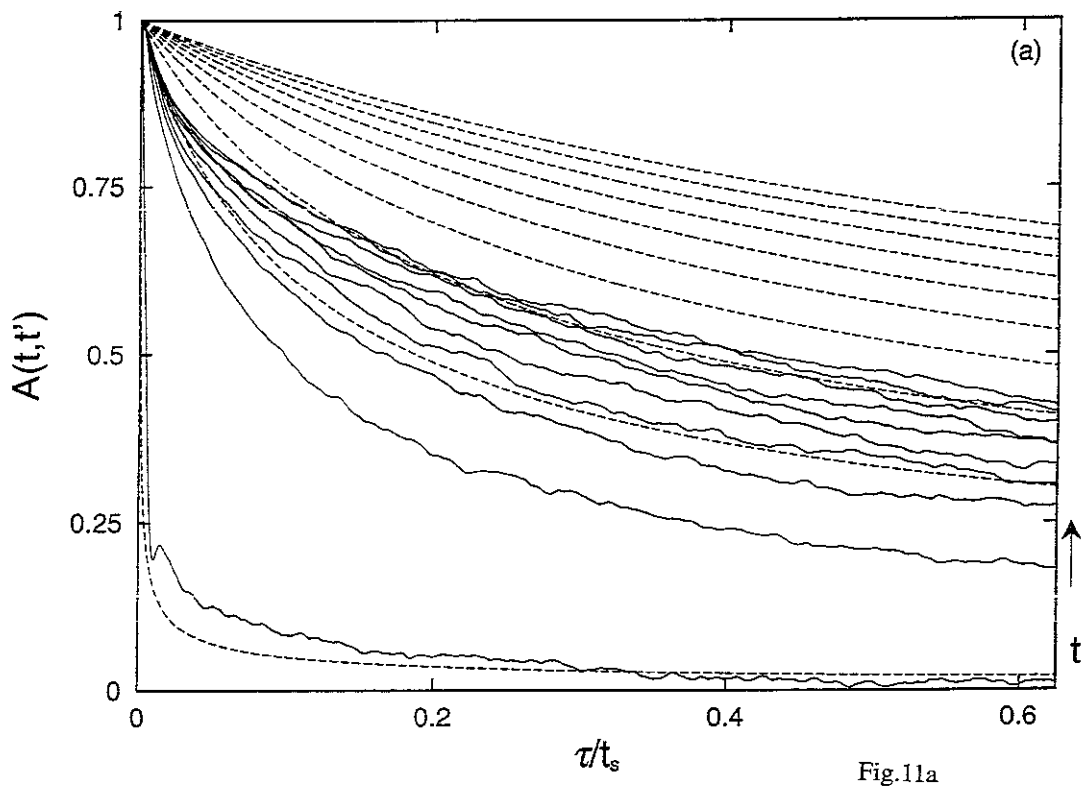

Fig.11a

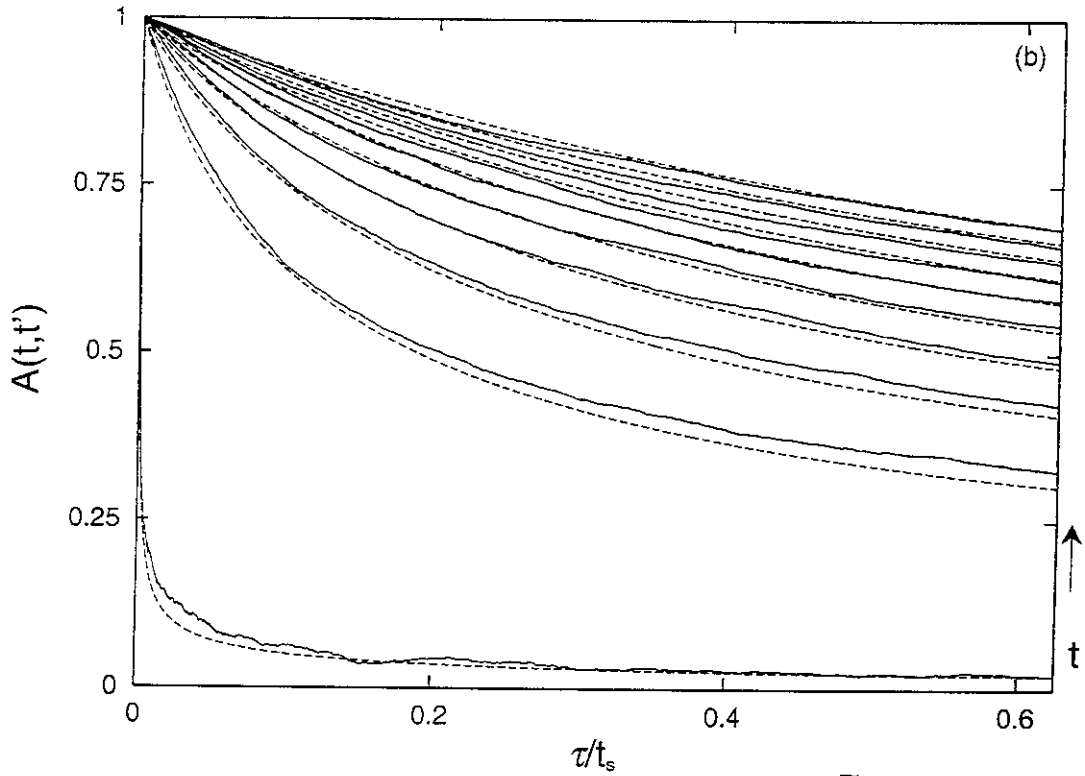

Fig.11b

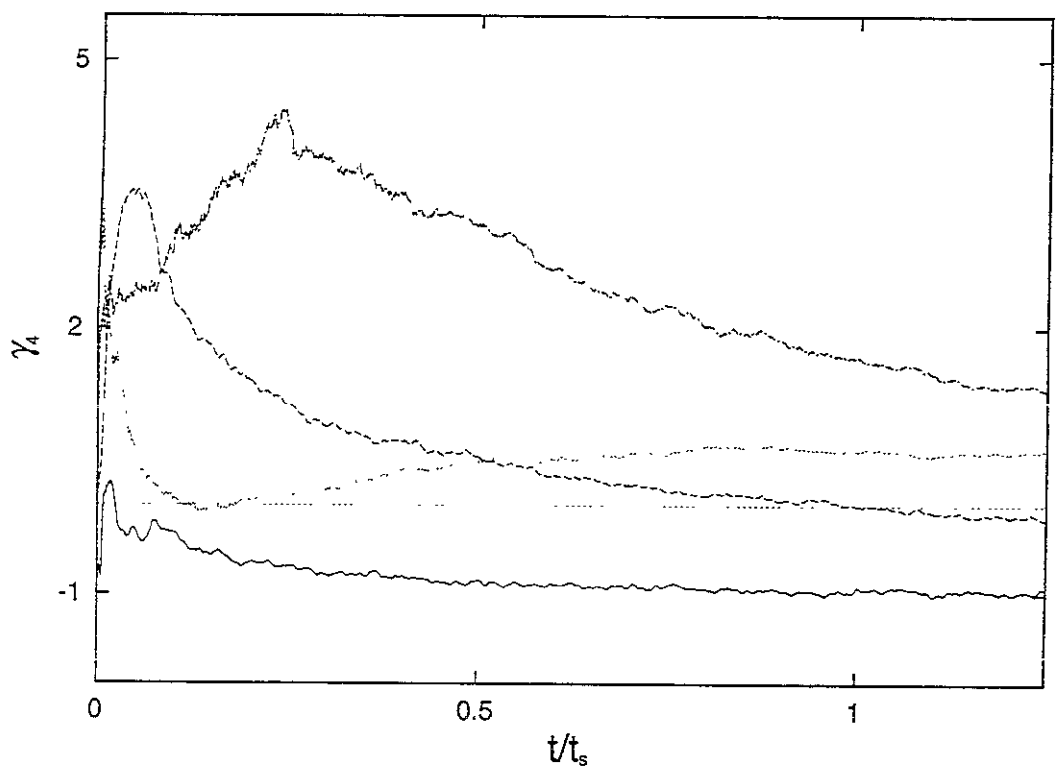

Fig.12

Recent Issues of NIFS Series

NIFS-690 Y Matsumoto, T Nagaura, Y Itoh, S-I Oikawa and T Watanabe
LHD Type Proton-Boron Reactor and the Control of its Peripheral Potential Structure Apr 2001

NIFS-691 A Yoshizawa, S -I Itoh, K Itoh and N Yokoi
Turbulence Theories and Modelling of Fluids and Plasmas Apr 2001

NIFS-692 K Ichiguchi, T Nishimura, N Nakajima, M Okamoto S -i Oikawa, M Itagaki,
Effects of Net Toroidal Current Profile on Mercier Criterion in Heliotron Plasma Apr 2001

NIFS-693 W Pei, R Horiuchi and T Sato,
Long Time Scale Evolution of Collisionless Driven Reconnection in a Two-Dimensional Open System Apr 2001

NIFS-694 L N Vyacheslavov, K Tanaka, K Kawahata,
CO2 Laser Diagnostics for Measurements of the Plasma Density Profile and Plasma Density Fluctuations on LHD Apr 2001

NIFS-695 T Ohkawa,
Spin Dependent Transport in Magnetically Confined Plasma May 2001

NIFS-696 M Yokoyama, K Ida, H Sanuki, K Itoh, K Narihara, K Tanaka, K Kawahata, N Ohyabu and LHD experimental group
Analysis of Radial Electric Field in LHD towards Improved Confinement May 2001

NIFS-697 M Yokoyama, K. Itoh, S Okamura, K Matsuoka, S -I Itoh,
Maximum-J Capability in a Quasi-Axisymmetric Stellarator May 2001

NIFS-698 S-I Itoh and K Itoh,
Transition in Multiple-scale-lengths Turbulence in Plasmas. May 2001

NIFS-699 K Ohi, H Naitou, Y Tauchi, O Fukumasa,
Bifurcation in Asymmetric Plasma Divided by a Magnetic Filter May 2001

NIFS-700 H Miura, T Hayashi and T. Sato,
Nonlinear Simulation of Resistive Ballooning Modes in Large Helical Device: June 2001

NIFS-701 G Kawahara and S. Kida,
A Periodic Motion Embedded in Plane Couette Turbulence June 2001

NIFS-702 K Ohkubo,
Hybrid Modes in a Square Corrugated Waveguide June 2001

NIFS-703 S -I Itoh and K Itoh,
Statistical Theory and Transition in Multiple-scale-lengths Turbulence in Plasmas June 2001

NIFS-704 S. Toda and K Itoh,
Theoretical Study of Structure of Electric Field in Helical Toroidal Plasmas June 2001

NIFS-705 K Itoh and S-I Itoh,
Geometry Changes Transient Transport in Plasmas June 2001

NIFS-706 M Tanaka and A Yu. Grosberg
Electrophoresis of Charge Inverted Macroion Complex Molecular Dynamics Study July 2001

NIFS-707 T-H Watanave, H Sugama and T Sato
A Nondissipative Simulation Method for the Drift Kinetic Equation. July 2001

NIFS-708 N. Ishihara and S Kida.
Dynamo Mechanism in a Rotating Spherical Shell Competition between Magnetic Field and Convection Vortices July 2001

NIFS-709 LHD Experimental Group,
Contributions to 28th European Physical Society Conference on Controlled Fusion and Plasma Physics (Madeira Tecnopolo, Funchal, Portugal, 18-22 June 2001) from LHD Experiment July 2001

NIFS-710 V.Yu Sergeev, R K Janev, M J Rakovic, S Zou, N Tamura, K.V Khlopenkov and S Sudo
Optimization of the Visible CXRS Measurements of TESPEL Diagnostics in LHD; Aug 2001

NIFS-711 M Bacal, M Nishiura, M Sasao, M Wada, M Hamabe, H Yamaoka,
Effect of Argon Additive in Negative Hydrogen Ion Sources, Aug 2001

NIFS-712 K. Saito, R Kumazawa, T. Mutoh, T. Seki, T Watari, T. Yamamoto, Y Torii, N Takeuchi C Zhang, Y Zhao, A Fukuyama, F Shimpo, G. Nomura, M. Yokota, A. Kato, M Sasao, M. Isobe, A V. Krasilnikov, T. Ozaki, M Osakabe, K Narihara, Y Nagayama, S Inagaki, K. Itoh, T Ido, S Morita, K Ohkubo, M. Sato, S Kubo, T Shimozuma, H Idei, Y Yoshimura, T Notake, O Kaneko, Y Takeiri, Y Oka, K. Tsumori, K Ikeda, A. Komori, H Yamada, H Funaba, K Y. Watanabe, S Sakakibara, R. Sakamoto, J Miyazawa, K Tanaka, B J Peterson, N. Ashikawa, S. Murakami, T Minami, M Shoji, S. Ohdachi, S Yamamoto, H. Suzuki, K. Kawahata, M Emoto, H Nakanishi, N. Inoue, N Ohyabu, Y Nakamura, S Masuzaki, S Muto, K Sato, T Morisaki, M Yokoyama, T. Watanabe, M Goto, I Yamada, K. Ida, T Tokuzawa, N Noda, K Toi, S Yamaguchi, K Akaishi, A Sagara, K. Nishimura, K Yamazaki, S Sudo, Y Hamada, O Motojima, M Fujiwara,
A Study of High-Energy Ions Produced by ICRF Heating in LHD Sep 2001

NIFS-713 Y. Matsumoto, S.-I Oikawa and T. Watanabe,
Field Line and Particle Orbit Analysis in the Periphery of the Large Helical Device. Sep. 2001

NIFS-714 S Toda, M Kawasaki, N Kasuya, K Itoh, Y Takase, A Furuya, M Yagi and S. -I Itoh,
Contributions to the 8th IAEA Technical Committee Meeting on H-Mode Physics and Transport Barriers (5-7 September 2001, Toki, Japan) Oct. 2001

NIFS-715 A. Maluckov, N Nakajima, M Okamoto, S Murakami and R Kanno,
Statistical Properties of the Particle Radial Diffusion in a Radially Bounded Irregular Magnetic Field; Oct 2001